Demonstrating a Refinery-adapted cluster-integrated strategy
to enable full-chain CCUS implementation - REALISE

D2.4. HS-3 Campaign at Tiller plant.

Thor Mejdell, Andreas Grimstvedt, Lars Hovdahl, Merete Wiig, Actor Chikukwa, Kai Hjarbo (SINTEF); Fredrik Gjertsen, Vemund Tjessem Svein Olav Hauger (Cybernetica)

2023-02-20

Dissemination Level (Public)

@realise-ccus | www.realiseccus.eu

Document History

Revision History

This document has been through the following revisions:

Version No.	Revision Date	Brief Summary of Changes	Name
0.1	2023-02-28	A draft document sent out for internal review	Thor Mejdell
1.0	2023-03-08	Revised version for submission	Thor Mejdell

Authorisation

This document requires the following approvals:

AUTHORISATION	Name	Signature	Date
WP Leader or QA	Peter van Os		20-3-2023
Project Coordinator	Inna Kim		2023-03-20

This project has received funding from the European Union's Horizon 2020 research and innovation programme under grant agreement No 884266

Executive summary

The present Deliverable D2.4, is a part of the REALISE project, and shows the results from a demonstration campaign which has been performed at the SINTEF CO_2Lab pilot plant, in Trondheim, Norway.

The objective of the campaign has been to demonstrate the benefits of the solvent HS-3 – a blend of two amines that has been optimised earlier during the project. A 12-week long campaign was conducted from 22nd of August to the 9th of December 2022. 91% of this period the plant was up and running, giving a total of 1802 hours' time on stream, implying that the solvent was robust and easy to run.

Altogether, 55 steady state runs were taken, and in each case, four independent measurements of the CO_2 transfer were measured: 1) The amount of CO_2 taken from the exhaust gas, 2) the amount of CO_2 absorbed in the absorber liquid, 3) the amount of CO_2 desorbed from the liquid in the stripper and 4) the amount of CO_2 leaving the top of the desorber. The deviation between these measurements was in average only 1.5%, meaning that the CO_2 mass balance was very good.

The first part of the campaign was dedicated to experimental optimization and the provision of data for modelling. The optimal L/G was found for 90% and 95% capture rates for both 5.5% and 12% CO_2 in the flue gas. These two flue gas concentrations are typical in the oil refinery industry. The results of steady state modelling validation are written in Deliverable D1.4 and shows high quality experimental as well as modelling results.

Dynamic step response tests were also conducted to give experimental basis for validation of dynamic models. The steps were in liquid rate, reboiler duty, flow gas rate and flue gas concentration. The dynamic models were used later in the campaign for testing nonlinear model predictive control.

After five weeks of the campaign, 20 litres of used and degraded solvent from another partner in the REALISE project was mixed in. The solvent was from TNO's mobile pilot onsite at Irving Oil Whitegate refinery in Ireland. See Deliverable D2.3.

An important part of the campaign was to measure solvent degradation both before and after the mixing of used solvent from Ireland.

Another task was to measure the degree of emissions of solvent and solvent degradation products to the air using varying number of water wash sections (up to 4 sections).

Finally, a unique part of the campaign was to use the newly installed CO_2 Compressor and Liquefaction Unit (CCLU) that was built in the project at Tiller. The results from the emission measurements and the analysis of impurities of the CO_2 gas are described and documented in Deliverable D2.4.

The main conclusions from the campaign are:

- Operationally the REALISE HS-3 solvent was easy to run in the pilot plant. The plant was up running more than 90% of the time. No precipitation was observed and no other major operational problems.

- The CO_2 mass balance was very good with a standard deviation from 4 independent measurements of only 1.5%.

- For 11% CO_2 gas the SRD was observed to be almost constant for various capture rates up to 98%. The optimal point is close to 2.0 in L/G and an SRD of about 3.35 MJ/kg CO_2 was measured for a fresh solvent.

- For 5.5% CO_2 the optimal L/G was around 1.0 for 90% capture rate and slightly higher for 95% capture rate. The SRD was around 3.72 MJ/kg CO_2 for 90% capture rate and only slightly higher for 95% capturer rate.

- Assuming no heat loss from the plant the SRD was estimated to be around 3.1 MJ/kg CO_2 for 11 mol% CO_2 in the flue gas, and 3.5 MJ/kg CO_2, for 5.5 mol% CO_2.

- Degraded solvent shows a higher need for energy. In the campaign the increase in SRD was about 0.1 - 0.2 MJ/kg CO_2.

- Runs with 15m absorber packing instead of 20m showed a substantially increase in SRD.

- All the dynamic closed loop tests with NMPC showed satisfactory results including the very fast "stripper stop scenario" with limitation in the reboiler duty.

- The degradation rate appears to be nearly constant during the campaign, where pyrrolidine and AP-Urea where the two largest degradation products in the solvent.

- Two nitrosamines (Nitroso-N-Methyl-AP during and NPYR) was observed in the solvent during the campaign, both showing an increasing trend with time.

- The solvent seems to be little corrosive as the determined metal concentration (Fe, Cr, Ni, Cu, Zn and Mn) where low (<2.5 mg/l).

- The campaign created a multitude of data for further scientific analysis, both regarding steady state and dynamic model development.

Table of Contents

1 Introduction

The present work is a part of Work Package 2 in REALISE, dealing with technology demonstration. Task 2.3 is dedicated to a 12 week long demonstration campaign at the pilot plant at SINTEF CO_2Lab, in Trondheim, Norway.

1.1 Campaign objective

The main objective has been to demonstrate the benefits of the solvent HS-3 – a blend of two amines (40 wt.% 1-(2HE)PRLD and15wt.% 3A1P) that has been optimised within the project. The campaign should:

- Find the optimal L/G giving the minimum specific thermal reboiler duty in terms of MJ/kg CO_2 captured.
- Measure solvent degradation during the campaign.
- Measure the degree of emissions of solvent and solvent degradation products to the air using varying number of water wash sections (up to 4 sections).
- Generate dynamic step response data for validation of the dynamic model.
- Test the Nonlinear Model Predictive Controller (NMPC) online in closed loop and provide valuable data for WP3.
- Measure impurities in liquefied CO_2 product by using the CO_2 Compressor and Liquefaction Unit (CCLU) commissioned and built in the project. These data are of high importance for the assessment and de-risking of CO_2-utilisation and CO_2-transport in WP3.

1.2 Activities

The 12-week long campaign was conducted from 22nd of August to the 9th of December 2022. 91% of this period the plant was up and running, giving a total of 1802 hours time-on-stream.

The first week was used for various start-up activities including mixing in the fresh solvent into the plant. The next four weeks was used to provide useful data to create baselines for verification of steady state and dynamic simulation tools. The optimal liquid/gas ratio was found for 90% and 95% capture rates for both concentrations of 5.5% and 12% CO_2 in the flue gas. These two flue gas concentrations are common in the oil refinery industry. Runs using only three of the four packing section was also tested.

After five weeks of the campaign, 20 litres of used and degraded solvent from another partner in the REALISE project was mixed in. The solvent was from TNO's mobile pilot onsite at Irving Oil Whitegate refinery in Ireland. The assumption, in this case, is that the solvent would then have a composition close to a partly reclaimed solvent from a refinery, and therefore of value for performance testing.

Important activities in the last seven weeks were:

- Closed loop testing of the NMPC for various disturbances scenarios.

- Solvent degradation measurements.
- Measurements of emissions in the flue gas leaving the absorber.
- Measurements of impurities in the compressed CO_2 gas.

The main results from the two last activities are described in the REALISE deliverable D2.5 "Quantification of emissions and CO_2 quality".

2 Description of the Tiller pilot

A process flow diagram of the total Tiller plant is shown in Figure 2.1. The pilot plant consists of three main parts: The flue gas pre-treatment, the CO_2 absorption part, and the solvent regeneration part. In addition, there is a propane burner and a coal/bio burner providing different types of flue gas to the plant. The absorber and desorber diameters are dimensioned according to the amount of flue gas available, giving quite small diameters. However, the design philosophy has been to otherwise design the plant as similar as possible to a full-scale post-combustion CO_2 capture plant, i.e., with an absorber packing height capable of absorbing CO_2 to a degree close to chemical and phase equilibrium for most solvents. The gas flow rate (m/s), the liquid load (m3/h*m2), the packing material and the total packing heights are similar, such that the conditions for mass and heat transfer from gas to liquid will be the same as in an industrial sized plant. Assuming evenly distributed gas and liquid flows in the towers and disregarding any wall effects, the scaling will be just a question of diameter. The most important wall effect is the heat loss to the surroundings, which is negligible for large full-scale columns because of very small surface to volume ratios. The heat loss might be significant for small plants. At the Tiller plant, this effect is minimized by insulation and heat tracing around most of the hot parts of the plant.

2.1 Burner and flue gas pretreatment

At Tiller there are two different burners that can provide the pilot with flue gas. It can either come from a 250 kW combined bio and coal burner which was installed in 2017 or from a 350 kW propane burner which has been an integrated part of the heating system of the surrounding building mass. In this campaign the propane burner was used. The burner load will vary depending on the heating system demand but will have a fixed minimum load of 90 kW heat to always provide sufficient exhaust gas to the pilot plant. The flue gas will contain 10-11% CO_2.

The pilot plant is provided with exhaust gas from the burner via a connection in the gas burner chimney. The CO_2-content in the flue gas entering the conditioning column can be set by either diluting the exhaust gas by fresh air or by adding CO_2 (see Figure 2.1) re-circulated from the top of the stripper.

The flue gas from the propane burner is pre-treated by a direct contact cooler/conditioner (DCC1) to get well defined humidity and temperature of the feed gas to the absorber. The DCC is an absorption column with 2.5 m height Mellapak 2X structured packing (inner diameter 26 cm). The liquid sump of the conditioning column is level controlled; water can be withdrawn, or de-ionized water can be added to the sump.

A high-capacity fan (500 m3/h) is positioned downstream the DCC. An electric heater is installed upstream the blower/fan to avoid droplet or condensate transferred to the blower/fan inlet. The blower/fan will liberate heat to the gas; the heat is removed in a cooler upstream the absorber. Both the degree of saturation and the feed gas temperature can therefore be controlled under a wide range of operational conditions.
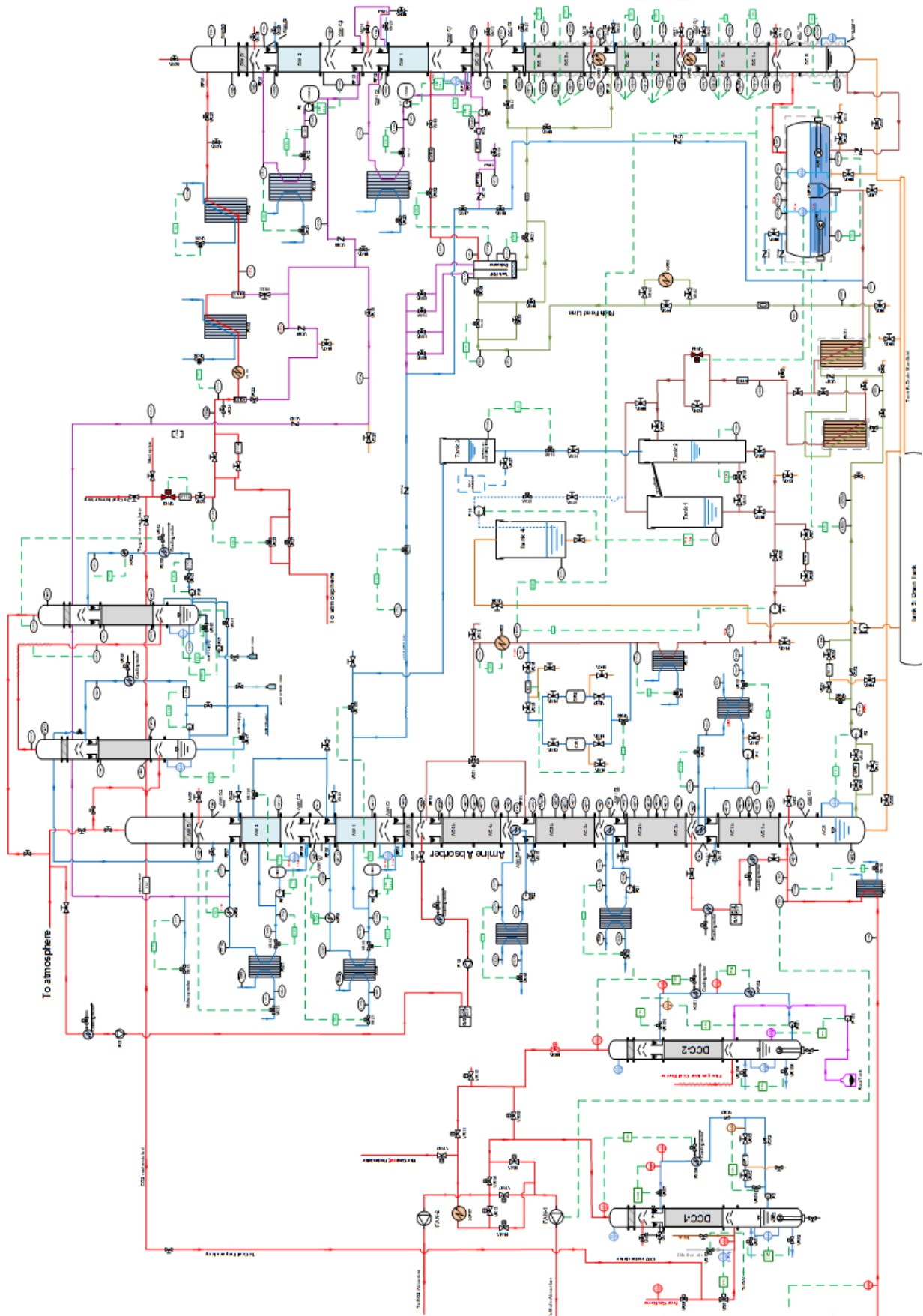
Figure 2-1: Flow sheet of the Tiller plant.

2.2 Absorption system

The absorber column has 20 cm inner diameter and is equipped with 19.5 meter structured packing (Mellapak 2X) divided into four sections. Liquid collector and redistributor sections (in-house SINTEF design) are installed between each section and facilitate sampling of both gas and liquid. The liquid collected may also be cooled down in an external loop before it is redistributed. These inter-coolers may give more optimal temperature conditions in the absorber. Note that during the campaign no intercooling was used, but the insulation was removed from the lower part of the column to detect a possible leakage. This extra cooling could have a similar effect. The column is instrumented with temperature sensors every meter, and pressure sensors below each packed column sections. Lean amine can alternatively be fed to section no. 3 to reduce the packing height to 14.9 m and the solvent residence time.

In the upper part of the column (above the 4th absorption section) two water-wash sections with 1.8 and 1.6 m height structured Mellapak 2X packing are used to remove amine vapor in the flue gas. It is also possible to redirect the flue gas to two additional water wash sections to get improved control of the emissions. The last section is equipped with pH control and may be used as an acid wash. Demisters are placed above the upper lean solvent distributor and above the upper water section as well as in the top of the two additional water wash sections.

The exhaust gas fan has the capacity to reach a gas velocity of above 4 m/s ($\approx$ 450 m3/h) in the absorber inlet, which is calculated to be around the column flooding point. The solvent flow rate must be adjusted to the CO_2 capture requirement. The maximum solvent flow rate is 10-20 l/min depending on the viscosity of the liquid and the pressure in the desorber.

2.3 Solvent regeneration system

The solvent regeneration system consists of a desorption column, a reboiler, and two condensers to separate stripped CO_2 from water/amine vapour. Recovered CO_2 is discharged to the atmosphere or recirculated to the feed gas system upstream the DCC in order to increase the CO_2-concentration to meet "coal exhaust case" conditions. Lean solvent from the reboiler is heat-exchanged with rich solvent from the absorber before the lean solvent temperature is adjusted by a watercooler, and the solvent is recirculated to the top of the absorber.

The reboiler is of kettle type with electrical elements and a maximum duty of 60 kW. It has a liquid holdup of 270 litres (gross volume of 500 litres). A correlation between solvent CO_2 concentration and solvent density and temperature can often be established for a given solvent such that the CO_2 concentration can be estimated by online density and temperature measurements. The reboiler duty can then be used to control the CO_2 loading of lean amine and thus also the CO_2 recovery in the absorber (and capture rate).

The stripper column has an inner diameter of 16.2 cm, and a total packing height of 13.6 meters structured Mellapak 2X packing consisting of 3 sections with solvent collector and redistribution between each section. The liquid may be heated up at two inter-heaters (see Figure 2.2) before redistributed to a lower section.

The two inter-heaters have a capacity of 10 kW each. The collector and the redistributor are of similar design as in the absorber. The stripper column is equipped with temperature measurement every meter and pressure measurement below each section and above the upper section.
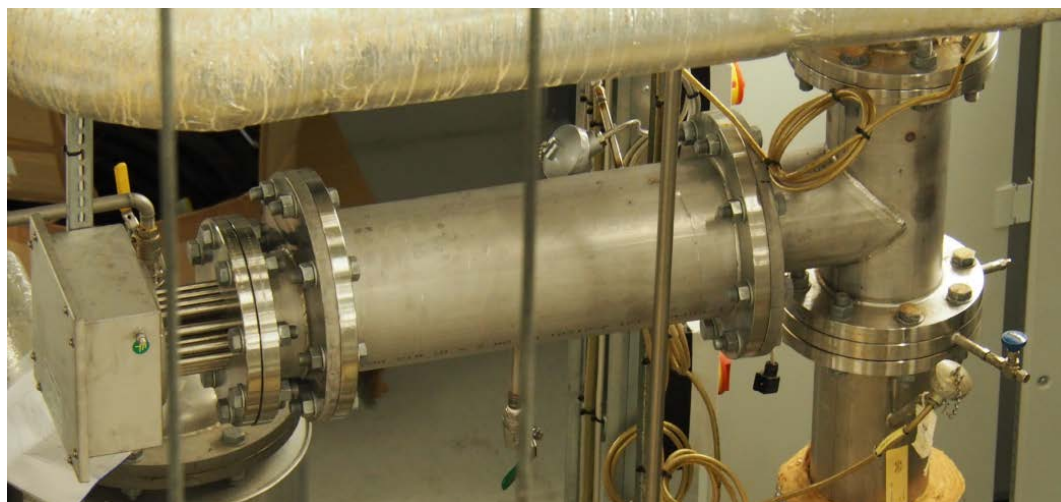
Figure 2-2: Photo of an inter-heating section before it was insulated

The stripper and the reboiler are equipped with a heat tracing system to minimize the heat loss in this warm part of the plant. The heat tracing system consists of two layers with 5 cm of insulation with an aluminium shield and heating tapes in between (see Figure 2.3). Control loops adjust the temperature at the shield to be the same as inside the column. With almost no driving forces, the heat transport from the column wall to the shield becomes negligible. The desorber and reboiler system is divided into 8 different zones (two for each desorber section, + reboiler + sump and pipes) to take care of the temperature gradients along the column.
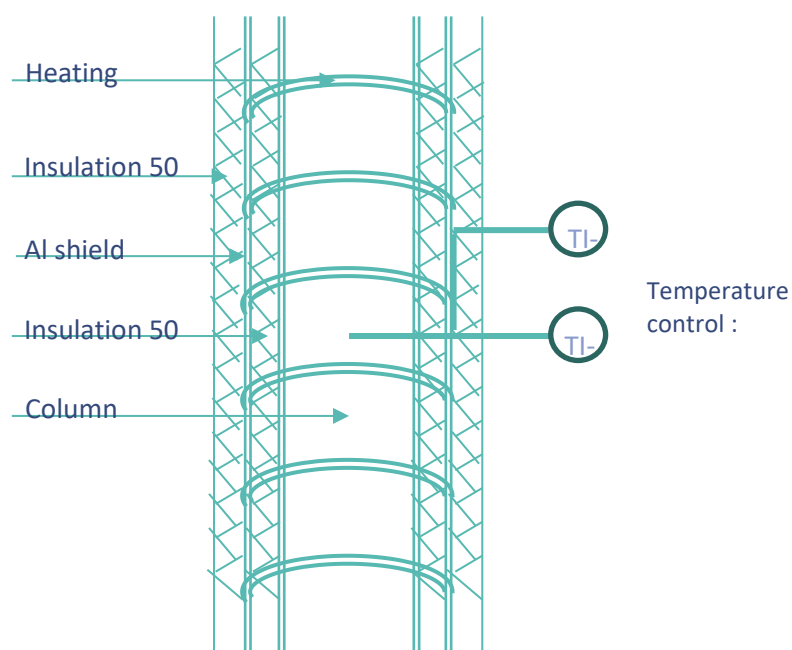
Figure 2-3 Heat tracing system for the desorber column

The upper part of the stripper column has two water-wash sections similar to the water wash in the absorber. Feed water is provided entirely as condensate from the condensers. The condensate outlet from the wash section can either be returned to the top of the desorber column, to the lean solvent downstream the reboiler, or as feed water to the wash sections in the absorber. Demisters are fitted above the upper (rich) solvent distributor and above the upper water distributor to remove entrained droplets.

2.4 Solvent lines

From the absorber bottom the rich solvent is heated up by the lean solvent from the reboiler. The heat exchanger between the rich and lean solvent consists of two separate units each of 20 m2. The two was used in series with total area of 40 m2.

After the rich solvent is heated up in the heat exchanger it can be additionally heated by a preheater with a total power capacity of 5 kW.

To prevent heavy CO_2 flashing in the rich amine flow that gives disturbing gas-liquid slug flow into the desorber, a flash tank is installed close to the desorber liquid inlet. The pressure in the flash tank is controlled by a gas stream valve and the liquid level by a liquid valve. Together with a control valve also before the flash tank, the system gives great flexibility for controlling the pressure in the upcoming stream from the rich-lean heat exchanger. Visual observations of the gas and liquid streams are accessible through local inspection glasses.

After the lean stream is cooled down in the rich/lean heat exchanger, it flows into the buffer Tank2. The level in this tank is not controlled but measured and is used for supervision of the overall water balance. Another buffer Tank1 with higher volume is used to increase the buffer capacity, if needed.

A liquid pump P1 pumps the lean liquid from the Tank2 into the absorber. On this line there is both a trim cooler and a liquid heater to control the liquid temperature. The liquid may also go through a carbon filter for cleaning.

2.5 CO_2 Compression and Liquefaction Unit

In REALISE, the CO_2Lab pilot has been equipped with a compact CO_2 compression and liquefaction unit (CCLU), enabling liquefying the CO_2 produced in the desorber. The main objective of these units is to identify and quantify expected impurities in the CO_2 product when using HS-3 solvent in the refinery industry.

In the design of the CCLU it has been an important issue to be as close to a large scale standard unit as possible such that the results at Tiller are relevant for industrial cases.

The compressor train consists of three compression stages using Haskel gasboosters from Proserv. After each stage the gas is cooled downt to 20 - 25 °C and the water is separated after each stage. Typical pressures after each stage are 5, 14, and 40 bars. The PI&D of the compression train is shown in the Figure 2-4.
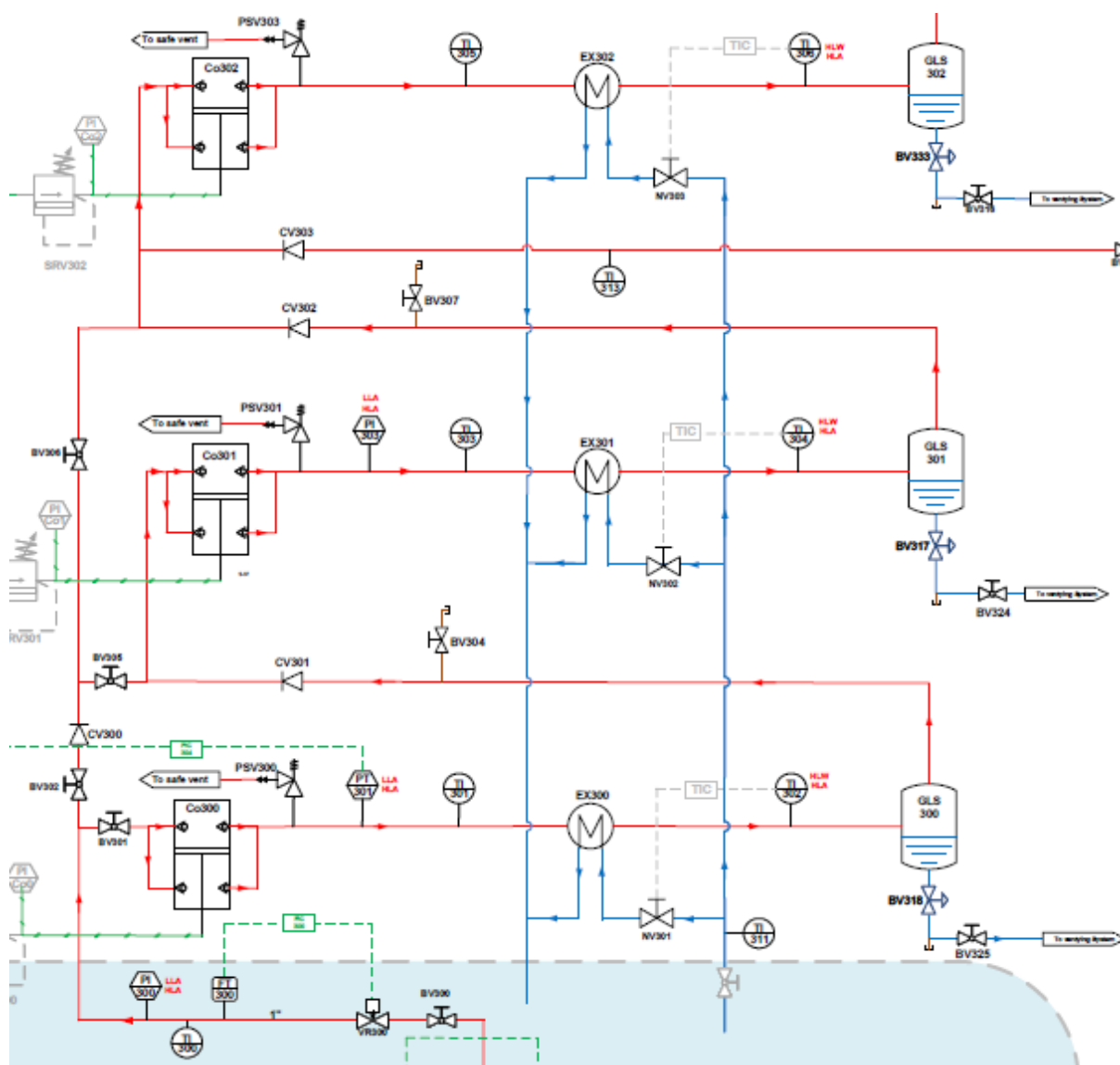
Figure 2-4. PI&D Compression part of the CCLU. The CO₂ from the stripper enters the figure at the bottom and leaves at the top.

After the third knock out drum the compressed CO_2 gas is at 35 - 40 bar and 15 - 25 °C. The gas at this stage will have 400 – 600 ppm of water. To reduce the amount of water to 20 – 30 ppm that often is required, the gas is dried in a cylinder filled with molecular sieve beads. Two such cylinders are mounted in parallel to increase the flexibility of the system.

An external Lauda Integral IN 250XTW cooler provides a cooling medium (ethanol) at typically -5 to -20 °C. The CO_2 gas is liquified with this ethanol by a plate-and-frame heat exchanger. The temperature of the liquid CO_2 will then typically be -5 to -15 °C.

Afterwards the liquid is expanded through an expansion valve to the desired pressure (15-16 bar). This expansion will produce a two-phase stream at about –26 °C The stream then enters a Carbo-Max CO_2 storage tank. The liquid will be accumulated in the tank while the gas phase will leave the tank to ventilation or sent back to the last compression stage. The desired

pressure is set by control valve on the gas out of the storage tank. The tank is well insulated, and any heat loss will be compensated by evaporation of liquid CO_2, which is then released through this control valve.

For safety reasons the CCLU is built inside a cabinet with ventilation and CO_2 level alarm see Figure 2-5.

Figure 2-5 Cabinet housing the CCLU. The Lauda cooler is the white unit in the middle, and the Carbo-Max storage tank to the right.

More information and details of the CCLU is found in the REALISE report D2.2 "Tiller plant modification".

3 Campaign steady state results

The steady state results from the 16 weeks long campaign are presented in this chapter. This includes averaged data from the Siemens PC7 and the Gasmet FTIR analyser, and liquid analyses of CO_2 and amine (titration)

3.1 Campaign overview

The solvent (40 wt% 1-(2HE)PRLD, 15 wt. % 3A1P and 45 wt.% H_2O) was loaded into the plant the 20th of September 2022. The plant started to operate 22nd of September and ended the 9th of December 2022. 91% of the period the plant was up running. All together the plant operated in 1802 hours. The largest stop was due to a two-day meeting that was compulsory for all SINTEF employees.
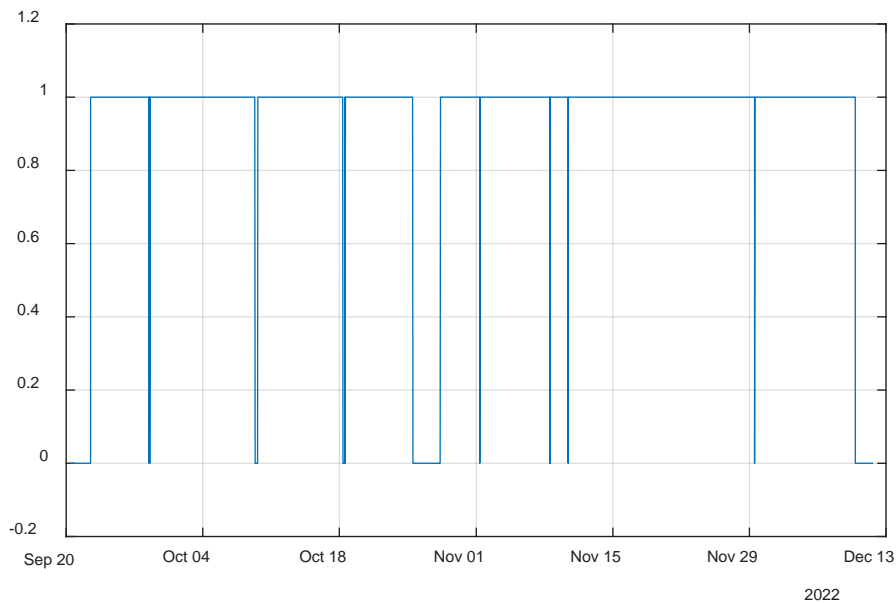
Figure 3-1Time periods when the plant was running.

During the campaign 55 steady state runs were taken. The results of a run will typically consist of analysed liquid samples and the average of process variables over the last hour before the sampling.

3.2 Experimental plan

The first part of the campaign was dedicated for solvent circulation rate optimization. Together with dynamic step response data described in Chapter 4, the data was going to be used for model validation. The solvent was fresh such that it would be compatible with equilibrium and physical data for the solvent from the lab.

Table 3-1 Experimental plan

	Run nr	Activity description	Gas rate FT03 m3/h	CO2in GA1_1 % dry	CapRat CR %	CO2out GA3_2 % dry	Liq Rate FMD1_1 kg/min	Humidity TI03 C	Lean flow T TT07 C	Des press PT11 mbarg
22 Sep		Startup								
23 Sep										
24 Sep	1	Liquid sirc optim No1, 11% CO2, CR=90%	160.0	11.0 %	90 %	1.22 %	10.0	35	40	800
25 Sep										
26 Sep	2	Liquid sirc optim No2, 11% CO2, CR=90%	160.0	11.0 %	90 %	1.22 %	9.0	35	40	800
27 Sep	3	Liquid sirc optim No3, 11% CO2, CR=90%	160.0	11.0 %	90 %	1.22 %	8.0	35	40	800
28 Sep	4	Liquid sirc optim No4, 11% CO2, CR=90%	160.0	11.0 %	90 %	1.22 %	5.3	35	40	800
29 Sep	5	Liquid sirc optim No5, 11% CO2, CR=90%	160.0	11.0 %	90 %	1.22 %	6.5	35	40	800
30 Sep	6	Liquid sirc optim No1, 11% CO2, CR=95%	160.0	11.0 %	95 %	0.61 %	7.3	35	40	800
1 Oct										
2 Oct										
3 Oct	7	Liquid sirc optim No2, 11% CO2, CR=95%	160.0	11.0 %	95 %	0.61 %	8.7	35	40	800
4 Oct	8	Liquid sirc optim No3, 11% CO2, CR=95%	160.0	11.0 %	95 %	0.61 %	5.9	35	40	800
5 Oct	9+10	Liquid sirc optim No1, 11% CO2, CR=98%	160.0	11.0 %	98 %	0.25 %	6.2	35	40	800
6 Oct	11	Liquid sirc optim No1, 11% CO2, CR=85%	160.0	11.0 %	85 %	1.82 %	7.0	35	40	800
7 Oct	12	Liquid sirc optim No1, 5% CO2, CR=90%	250.0	5.0 %	90 %	0.52 %	6.0	35	40	800
8 Oct										
9 Oct										
10 Oct	13	Liquid sirc optim No1, 5% CO2, CR=95%	250.0	5.0 %	95 %	0.26 %	5.0	35	40	800
11 Oct	14	Liquid sirc optim No2, 5% CO2, CR=90%	250.0	5.0 %	90 %	0.52 %	4.2	35	40	800
12 Oct	15	Liquid sirc optim No3, 5% CO2, CR=90%	250.0	5.0 %	90 %	0.52 %	4.6	35	40	800
13 Oct	16	Liquid sirc optim No4, 5% CO2, CR=90%	250.0	5.0 %	90 %	0.52 %	5.0	35	40	800
14 Oct	17	Liquid sirc optim No2, 5% CO2, CR=95%	250.0	5.0 %	95 %	0.26 %	4.9	35	40	800
15 Oct										
16 Oct										
17 Oct	18	Liquid sirc optim No3, 5% CO2, CR=95%	250.0	5.0 %	95 %	0.26 %	6.0	35	40	800
18 Oct	19	Liquid sirc optim No3, 5% CO2, CR=95%	250.0	5.0 %	95 %	0.26 %	5.5	35	40	800
19 Oct	20	3 packing absorber 5% CO2, CR=90%	250.0	5.0 %	90 %	0.52 %	4.8	35	40	800
20 Oct	21	3 packing absorber 5% CO2, CR=90%	250.0	5.0 %	90 %	0.52 %	5.3	35	40	800
21 Oct	22	3 packing absorber 5% CO2, CR=90%	250.0	5.0 %	90 %	0.52 %	4.7	35	40	800
22 Oct										
23 Oct										
24 Oct	23	Liquid sirc optim No1, 5% CO2, CR=85%	250.0	5.0 %	85 %	0.78 %	4.7	35	40	800
25 Oct	24	Liquid sirc optim No1, 5% CO2, CR=98%	250.0	5.0 %	98 %	0.11 %	5.2	35	40	800
26 Oct										
27 Oct										
28 Oct										
29 Oct										
30 Oct										
31 Oct	25	Liquid sirc optim No1, 5% CO2, CR=90%	250.0	5.0 %	90 %	0.52 %	4.9	35	40	800
1 Nov	26	Liquid sirc optim No2, 5% CO2, CR=90%	250.0	5.0 %	90 %	0.52 %	4.3	35	40	800
2 Nov	27	Liquid sirc optim No3, 5% CO2, CR=90%	250.0	5.0 %	90 %	0.52 %	4.5	35	40	800
3 Nov	28	Liquid sirc optim No4, 5% CO2, CR=90%	250.0	5.0 %	90 %	0.52 %	5.4	35	40	800
4 Nov	29	Liquid sirc optim No4, 5% CO2, CR=90%	250.0	5.0 %	90 %	0.52 %	6.0	35	40	800
5 Nov										
6 Nov										
7 Nov	30	Liquid sirc optim No4, 5% CO2, CR=90%	250.0	5.0 %	90 %	0.52 %	6.0	35	40	800
8 Nov	31	Liquid sirc optim No5, 11% CO2, CR=90%	160.0	11.0 %	90 %	1.22 %	6.5	35	40	800
9 Nov	32	Liquid sirc optim No3, 11% CO2, CR=90%	160.0	11.0 %	90 %	1.22 %	8.0	35	40	800
10 Nov	33	Liquid sirc optim No4, 5% CO2, CR=90%	250.0	5.0 %	90 %	0.52 %	5.7	35	40	800
11 Nov	34	Liquid sirc optim No3, 11% CO2, CR=90%	160.0	11.0 %	90 %	1.22 %	7.0	35	40	800
12 Nov										
13 Nov										
14 Nov	35	Liquid sirc optim No3, 11% CO2, CR=90%	160.0	11.0 %	90 %	1.22 %	8.0	35	40	800
15 Nov	36	Liquid sirc optim No3, 11% CO2, CR=90%	160.0	11.0 %	90 %	1.22 %	9.0	35	40	PT11
16 Nov	37	Liquid sirc optim No3, 11% CO2, CR=90%	160.0	11.0 %	90 %	1.22 %	5.3	35	40	mbarg
17 Nov	38	Liquid sirc optim No3, 11% CO2, CR=90%	160.0	11.0 %	90 %	1.22 %	6.5	35	40	800
18 Nov	39+40									
19 Nov										
20 Nov										
21 Nov	41	Step in capture rate setpoint, min SRD	160.0	11.0 %	90 %			35	40	800
22 Nov	42	Step in capture rate setpoint, min SRD	160.0	11.0 %	95 %			35	40	800
23 Nov	43	Step in gas rate, min SRD, no steam limit	Various	11.0 %	90 %			35	40	800
24 Nov	44	Step in gas rate, min SRD, no steam limit ("predi	Various	11.0 %	90 %			35	40	800
25 Nov	45	Contingency	160.0	11.0 %	85 %			35	40	800
26 Nov										
27 Nov										
28 Nov	46	Step in gas rate and CO2, min SRD, no steam lim	Various	Various	90 %			35	40	800
29 Nov	47	Step in gas rate, min SRD, steam limitations	Various	11.0 %	90 %			35	40	800
30 Nov	48	Step in gas rate, min SRD, steam limitations	Various	11.0 %	90 %			35	40	800
1 Des	49	Gas rate following scenario	Various	11.0 %	90 %			35	40	800
2 Des	50	Liquid sirc optim No3, 11% CO2, CR=95%	160.0	11.0 %	95 %	0.61 %	6.5	35	40	800
3 Des										
4 Des										
5 Des	51	Liquid sirc optim No2, 11% CO2, CR=95%	160.0	11.0 %	95 %	0.61 %	7.0	35	40	800
6 Des	52	Liquid sirc optim No2, 11% CO2, CR=95%	160.0	11.0 %	95 %	0.61 %	7.5	35	40	800
7 Des	53	Liquid sirc optim No4, 5% CO2, CR=90%	250.0	5.0 %	90 %	0.52 %	5.0	35	40	800
8 Des	54	Liquid sirc optim No4, 5% CO2, CR=90%	250.0	5.0 %	90 %	0.52 %	5.0	35	40	800
9 Des	55	Liquid sirc optim No4, 5% CO2, CR=90%	250.0	5.0 %	90 %	0.52 %	5.0	35	40	800

3.3 Operational issues

In general, the solvent mixture was easy to operate. As shown in Figure 3-1 this resulted in a high percentage on-stream time. However, there was an issue that gave some stability problems.

The problem can be illustrated by Figure 3-2 where the flows into and out from the desorber is shown. The flow out of the desorber has much higher variation than the flow into.
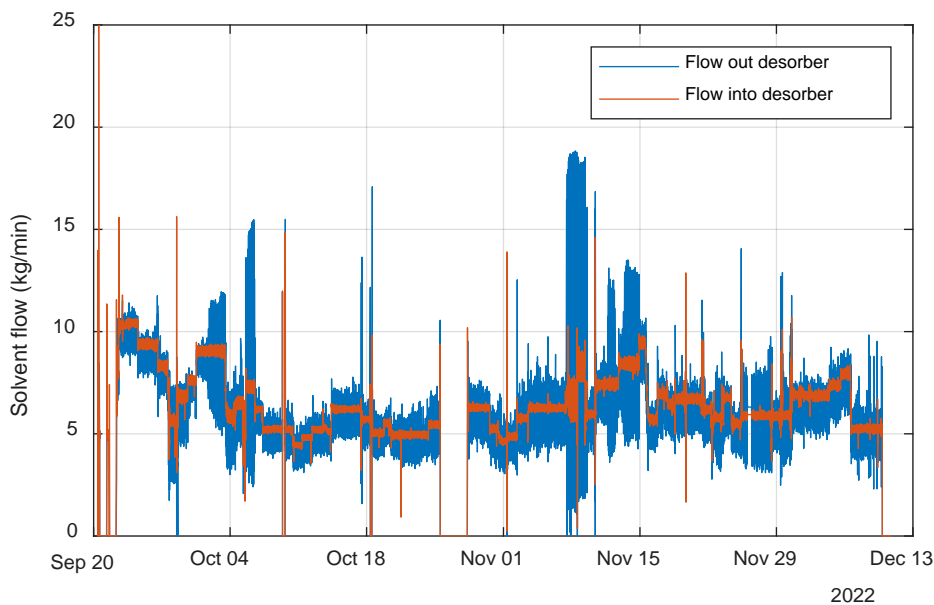
Figure 3-2: Flow into (FMD2_1) and out (FMD3_1). of the desorber

Especially the plant was difficult to operate during the 7 to 10th of November. It was noticed that it was correlated to the flue gas concentration of CO_2 which again is correlated with the rich loading. The pressure sensor PT14 turned out to be erroneous and the control loop with the valve VR32 was consequently not working properly. Without a working flash tank the we got slug-flow into the desorber and poor performance. Since it was impossible to get a new pressure sensor quickly the valve was set in manual on 30% opening the rest of the campaign. Although not perfect, this reduced the oscillating flow from the desorber to an acceptable level.
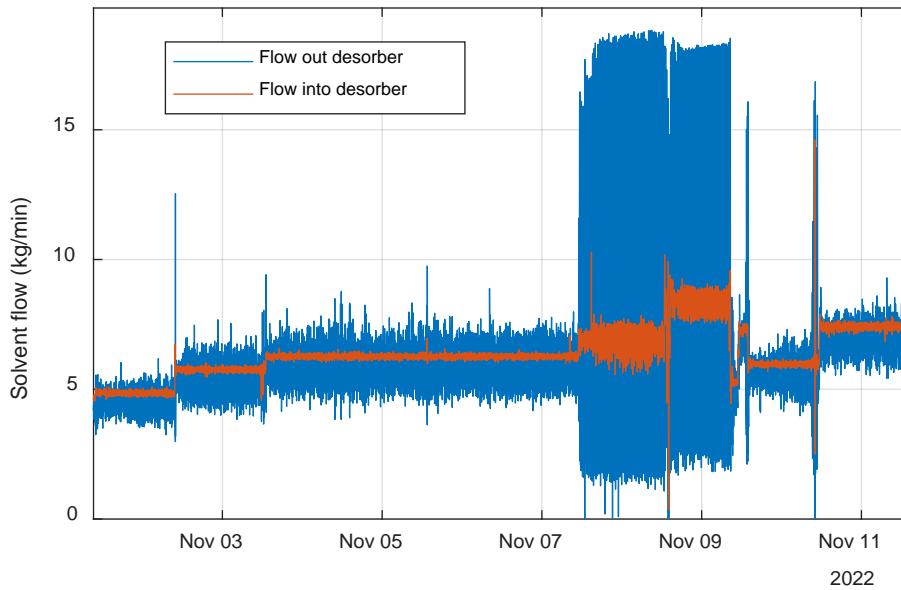
Figure 3-3: Flow into (FMD2_1) and out (FMD3_1). of the desorber in the beginning of NovemberT

3.4 Evaluation of experimental quality

3.4.1 Steady state stability

In order to compare different runs with each other it was important to do some qualification checks of the runs. The different runs should be at steady state conditions and data with serious oscillations should be detected.

The following process parameters were examined based on importance and sensitivity:

- Lean flow rate

- Rich flow rate

- Lean solvent density (lean loading)

- Rich solvent density (rich loading)

- Reboiler duty

- Reboiler temperature

- Temperature (TDp2) in the stripper

- Rich flow temperature from lean/rich heat exchanger

- Total pressure drop in the desorber

The standard deviation and the averaged gradient (slope) during the one hour averaging period were calculated for each of the variables and then compared with the other runs. The standard deviation reveals if the process has serious oscillations and the gradient if the process is drifting and not at steady state conditions. For example, a high positive or negative gradient means that the variable has increased or decreased significantly during the averaging period.

The result of the tests is shown in Table 3-2. For each variable we have set a threshold based on experience from earlier campaigns. If a variable is close to this threshold, it is marked yellow. If it is above, it is marked red and dark red if it is far above the threshold. In the last column an overall assessment for each run is shown. The runs are divided into three groups:

-        Good   marked with green colour   69%   (38 runs)

-        Medium   marked with yellow colour   15%   (8 runs)

-        Not so good   marked with red colour   9%   (5 runs)

-        Bad   marked with dark red colour 7%   (4 run)

The table shows that the data was in steady state most of the time. The runs that were not in steady state was due to the oscillations described in the previous section.

Table 3-2 Evaluation of steady state conditions

RUN	Gas flow	Liq flow	CO2 in	CO2 out	KW rebo	alfaLean	alfaRich	avg dP	std KW eff	slope KW eff	std LeanFlo	slope LeanFlo	std RichFlo	slope RichFlo	std LeanDer	slope LeanDer	std RichDer	slope RichDer	std Reb T	slope Reb T	std TDp2	slope TDp2	std TrichEx	slope TrichEx
RUN1_240922	160.0	10.00	11.83	1.17	28.11	0.16	0.344	39.4	0.01	0.00	0.01	0.00	0.04	-0.01	0.05	-0.13	0.09	-0.38	0.04	0.00	0.09	-0.11	0.09	0.0
RUN2_280922	160.0	9.00	11.42	1.14	27.23	0.15	0.379	44.0	0.01	-0.01	0.01	0.00	0.05	0.00	0.08	-0.15	0.10	-0.24	0.05	0.04	0.27	0.18	0.25	0.0
RUN3_270922	160.0	8.00	11.99	1.21	27.32	0.13	0.385	48.5	0.01	0.00	0.01	0.00	0.09	-0.05	0.07	-0.05	0.09	-0.10	0.04	0.05	0.28	0.12	0.15	0.1
RUN4_280922	160.0	5.27	11.90	1.13	30.04	0.04	0.438	36.9	0.01	0.01	0.02	-0.04	0.09	-0.09	0.29	-0.28	0.11	-0.30	0.29	0.10	0.24	0.07	0.98	0.4
RUN5_290922	160.0	6.50	11.76	1.14	25.70	0.10	0.407	38.0	0.01	0.01	0.05	0.03	0.08	-0.01	0.33	-0.13	0.13	-0.06	0.14	-0.17	1.90	0.95	0.61	0.3
RUN6_300922	160.0	7.30	11.89	0.64	27.71	0.10	0.379	42.2	0.01	0.00	0.05	0.01	0.08	-0.05	0.02	0.02	0.17	-0.06	0.02	-0.03	0.11	0.13	0.07	0.1
RUN7_031022	160.0	8.69	11.92	0.67	29.33	0.12	0.362	67.1	0.00	0.00	0.06	0.01	0.11	-0.04	0.33	-0.03	0.17	-0.18	0.32	0.06	1.84	-0.22	1.87	-0.1
RUN8_041022	160.0	5.55	11.99	0.61	31.04	0.04	0.412	43.6	0.01	0.01	0.05	0.02	0.11	0.01	0.29	-0.01	0.14	-0.01	0.29	0.01	0.22	0.00	0.31	-0.4
RUN9_051022	160.0	4.59	11.84	1.88	28.42	0.03	0.438	36.2	0.01	0.00	0.03	-0.01	0.05	-0.04	0.30	0.02	0.07	-0.08	0.04	0.01	0.04	-0.04	0.13	0.1
RUN10_051022	160.0	6.20	11.83	0.21	28.41	0.05	0.404	51.6	0.01	0.00	0.03	-0.03	0.10	-0.04	0.27	0.06	0.09	-0.12	0.05	0.00	0.10	-0.07	0.41	0.4
RUN11_061022	160.0	7.00	11.73	1.89	24.59	0.14	0.406	61.6	0.01	0.02	0.06	0.05	0.10	0.02	0.43	0.50	0.16	0.05	0.31	-0.10	3.41	0.65	2.02	-0.6
RUN12_070922	250.0	6.00	5.45	0.62	20.65	0.12	0.352	23.6	0.01	0.01	0.02	-0.01	0.06	-0.06	0.25	0.03	0.09	0.02	0.04	-0.06	0.17	0.03	0.14	-0.01
RUN13_101022	250.0	5.00	5.45	0.26	21.96	0.06	0.372	20.5	0.01	0.01	0.01	-0.01	0.05	-0.04	0.30	0.05	0.05	0.09	0.03	-0.04	0.02	-0.03	0.15	0.1
RUN14_111022	250.0	4.25	5.45	0.58	22.37	0.04	0.381	13.4	0.01	0.00	0.01	0.00	0.06	-0.04	0.29	0.00	0.04	-0.08	0.02	0.01	0.04	-0.02	0.16	0.1
RUN15_121022	250.0	4.60	5.46	0.62	20.14	0.07	0.379	23.2	0.01	0.00	0.01	-0.01	0.04	-0.04	0.30	-0.03	0.09	0.16	0.02	-0.03	0.07	0.08	0.13	0.1
RUN16_131022	250.0	5.00	5.45	0.58	20.44	0.08	0.372	24.8	0.00	0.00	0.02	0.00	0.05	-0.02	0.30	-0.08	0.08	-0.20	0.03	0.01	0.13	-0.01	0.18	0.0
RUN17_141022	250.0	4.90	5.45	0.25	22.97	0.05	0.360	17.6	0.01	0.01	0.01	-0.01	0.05	0.01	0.31	-0.14	0.05	-0.09	0.03	-0.06	0.04	-0.08	0.14	0.0
RUN18_171022	250.0	6.00	5.46	0.29	22.68	0.09	0.354	31.5	0.01	0.00	0.01	-0.02	0.05	-0.05	0.27	-0.13	0.14	-0.37	0.03	0.04	0.14	0.22	0.14	0.0
RUN19_181022	250.0	5.50	5.46	0.28	22.37	0.07	0.362	29.6	0.01	0.01	0.01	0.00	0.05	-0.01	0.28	-0.13	0.11	-0.25	0.02	-0.01	0.13	0.08	0.18	-0.1
RUN20_191022	250.0	4.80	5.45	0.55	22.27	0.05	0.343	21.6	0.01	0.01	0.02	-0.02	0.03	-0.02	0.03	-0.04	0.07	0.00	0.01	-0.06	0.03	-0.01	0.27	-0.3
RUN21_201022	250.0	5.30	5.44	0.68	21.66	0.08	0.344	23.2	0.01	0.00	0.01	0.01	0.07	-0.03	0.02	0.04	0.12	0.25	0.02	-0.04	0.08	0.07	0.13	0.0
RUN22_211022	250.0	4.69	5.46	0.56	22.78	0.05	0.345	19.7	0.01	0.00	0.01	-0.01	0.04	-0.04	0.28	-0.13	0.10	-0.08	0.03	-0.01	0.03	-0.02	0.15	-0.1
RUN23_241022	250.0	4.70	5.46	0.82	19.96	0.08	0.372	35.7	0.01	0.02	0.01	0.00	0.03	0.01	0.26	0.08	0.13	-0.17	0.03	0.01	0.17	0.02	0.23	0.1
RUN24_251022	250.0	5.20	5.45	0.15	23.99	0.05	0.342	38.5	0.00	0.00	0.02	-0.01	0.05	-0.02	0.30	-0.02	0.15	-0.29	0.02	-0.03	0.06	0.00	0.25	0.3
RUN25_311022	250.0	5.00	5.44	0.58	21.06	0.08	0.366	38.7	0.01	0.00	0.02	0.00	0.05	-0.01	0.30	0.01	0.13	-0.17	0.06	0.01	0.18	0.00	0.21	0.0
RUN26_011122	250.0	4.38	5.45	0.52	21.98	0.04	0.354	19.9	0.01	0.00	0.01	0.00	0.05	0.00	0.24	-0.12	0.12	0.06	0.03	0.02	0.03	-0.03	0.20	0.0
RUN27_021122	250.0	4.60	5.46	0.63	21.26	0.06	0.375	35.9	0.01	0.00	0.02	0.01	0.05	-0.03	0.37	0.04	0.12	0.21	0.07	0.05	0.18	0.02	0.25	0.0
RUN28_031122	250.0	5.50	5.46	0.68	21.58	0.10	0.363	40.4	0.01	0.01	0.03	0.01	0.06	0.00	0.32	-0.08	0.15	-0.10	0.07	0.03	0.55	-0.21	0.28	0.0
RUN29_041122	250.0	6.00	5.45	0.74	20.80	0.12	0.350	46.7	0.02	0.00	0.02	0.00	0.05	0.01	0.31	-0.10	0.11	-0.02	0.06	-0.02	0.49	-0.01	0.25	0.1
RUN30_071122	250.0	6.00	5.45	0.76	21.00	0.12	0.356	46.9	0.02	-0.01	0.03	0.00	0.04	0.00	0.30	0.01	0.06	-0.02	0.04	0.02	0.71	0.10	0.32	0.1
RUN31_081122	160.0	6.52	11.87	1.46	28.00	0.10	0.414	119.5	0.03	0.00	0.25	-0.18	0.36	-0.35	0.84	-0.60	0.84	0.30	0.95	-0.95	4.10	0.85	8.17	1.47
RUN32_091122	160.0	7.99	11.82	1.35	29.50	0.12	0.388	121.5	0.03	0.02	0.24	0.17	0.29	0.10	1.15	0.64	0.56	0.43	1.18	0.80	5.75	0.38	9.86	-5.85
RUN33_101122	250.0	5.70	5.45	0.65	21.50	0.10	0.357	42.0	0.03	0.00	0.02	-0.02	0.06	-0.02	0.36	0.19	0.12	0.28	0.04	-0.02	0.65	0.13	0.27	-0.1
RUN34_111122	160.0	7.00	11.95	1.49	26.70	0.11	0.406	60.0	0.03	0.00	0.02	-0.01	0.08	-0.04	0.10	0.08	0.12	0.16	0.07	0.08	0.39	0.14	0.17	0.0
RUN35_141122	160.0	8.00	12.11	1.31	28.00	0.12	0.379	68.4	0.02	0.00	0.03	0.00	0.13	-0.06	0.02	-0.27	0.11	0.05	0.07	-0.01	2.78	0.18	0.78	0.1
RUN36_151122	160.0	9.00	11.87	1.35	28.50	0.14	0.367	65.8	0.03	-0.01	0.04	-0.03	0.06	-0.02	0.37	-0.02	0.11	0.36	0.03	0.01	0.49	-0.15	0.13	0.1
RUN37_161122	160.0	5.32	11.89	1.27	28.50	0.04	0.422	39.7	0.02	0.00	0.04	-0.01	0.05	-0.05	0.31	-0.16	0.11	0.09	0.06	0.02	0.23	-0.03	0.14	0.0
RUN38_171122	160.0	6.52	11.73	1.56	25.60	0.10	0.402	54.8	0.03	-0.01	0.02	0.00	0.06	0.01	0.32	0.03	0.08	0.01	0.05	0.03	0.18	0.00	0.16	-0.1
RUN39_181122	160.0	6.02	11.81	1.26	26.00	0.07	0.383	56.1	0.03	0.00	0.03	-0.01	0.07	-0.03	0.31	-0.11	0.06	0.14	0.05	0.07	0.19	-0.02	0.19	0.1
RUN40_181122	160.0	5.52	11.75	1.25	26.50	0.05	0.392	56.4	0.02	0.00	0.15	-0.40	0.16	-0.33	0.43	-0.78	0.43	1.22	0.04	0.07	0.19	0.58	0.23	-0.1
RUN41_211122	160.0	6.30	11.57	1.32	25.50	0.09	0.380	53.2	0.03	0.01	0.01	0.00	0.06	-0.03	0.32	-0.20	0.09	0.03	0.06	0.00	0.21	0.15	0.17	0.0
RUN42_221122	160.0	5.80	11.63	0.53	28.85	0.04	0.395	43.5	0.03	0.02	0.02	0.00	0.05	-0.01	0.36	0.06	0.09	-0.10	0.05	-0.02	0.04	0.01	0.12	0.1
RUN43_231122	160.0	5.40	11.83	1.21	26.22	0.04	0.391	59.0	0.03	0.00	0.02	-0.01	0.08	-0.03	0.34	-0.08	0.08	-0.05	0.06	-0.04	0.10	-0.02	0.61	0.0
RUN44_241122	195.0	6.39	11.83	1.35	33.01	0.03	0.385	52.9	0.03	-0.01	0.02	0.00	0.04	0.01	0.33	-0.05	0.09	-0.05	0.05	0.04	0.06	0.02	0.16	0.0
RUN45_251122	160.0	5.10	11.97	1.53	26.30	0.04	0.403	35.1	0.03	0.00	0.02	-0.01	0.06	-0.01	0.32	-0.04	0.08	0.01	0.05	-0.05	0.05	0.04	0.20	0.0
RUN46_281122	160.0	5.50	11.92	1.25	26.35	0.04	0.394	69.8	0.02	0.00	0.02	0.00	0.06	-0.01	0.32	0.02	0.08	0.01	0.05	0.00	0.11	-0.01	0.96	-0.1
RUN47_291122	160.0	5.47	11.91	1.17	27.39	0.04	0.403	40.7	0.03	0.02	0.02	0.00	0.07	-0.02	0.31	0.08	0.05	0.01	0.07	0.06	0.07	0.03	0.18	0.1
RUN48_301122	160.0	5.52	11.54	0.98	26.00	0.04	0.385	67.4	0.02	0.03	0.02	-0.01	0.06	0.01	0.31	0.00	0.06	-0.19	0.05	-0.03	0.07	0.01	0.30	0.1
RUN49_011222	200.0	6.56	11.49	1.20	32.70	0.03	0.375	54.5	0.03	0.02	0.03	0.00	0.08	-0.04	0.30	-0.02	0.07	-0.03	0.07	-0.01	0.08	0.02	0.20	-0.1
RUN50_021222	160.0	6.46	11.60	0.47	27.99	0.06	0.351	57.8	0.03	-0.02	0.02	-0.01	0.06	0.02	0.30	0.00	0.09	0.08	0.07	0.01	0.12	0.04	0.20	0.0
RUN51_051222	160.0	6.96	11.75	0.72	28.50	0.08	0.370	60.7	0.02	0.00	0.02	0.00	0.05	0.00	0.29	0.07	0.11	0.01	0.06	-0.07	0.26	-0.12	0.13	0.0
RUN52_061222	160.0	7.50	11.37	0.60	28.50	0.09	0.365	62.8	0.02	0.00	0.02	0.00	0.06	0.02	0.32	-0.47	0.09	-0.09	0.07	0.00	0.37	0.00	0.13	0.0
RUN53_071222	250.0	5.00	5.44	0.57	21.60	0.06	0.351	22.5	0.02	0.00	0.01	0.02	0.05	0.01	0.34	-0.29	0.12	-0.24	0.05	0.13	0.21	0.07	0.27	-0.1
RUN54_081222	250.0	5.00	5.45	0.58	21.50	0.06	0.353	21.3	0.02	0.00	0.02	0.02	0.05	0.05	0.37	-0.07	0.09	-0.02	0.07	0.04	0.19	0.04	0.44	0.1
RUN55_091222	250.0	5.00	5.45	0.60	21.50	0.06	0.350	22.2	0.02	0.00	0.02	0.00	0.19	0.02	0.06	-0.12	0.25	-0.26	0.07	-0.03	0.25	-0.15	0.39	0.2
Mean								44.88	0.02	0.01	0.03	0.02	0.07	0.04	0.30	0.13	0.13	0.16	0.10	0.07	0.52	0.12	0.65	0.23
Treshold								50	0.20	0.3	0.06	0.04	0.15	0.07	0.3	0.6	0.4	0.6	0.15	0.2	0.4	0.25	1	0.5

3.4.2 CO_2 mass balance

In Figure 3-4 the mass transfer of CO_2 in the plant is plotted. Four values are shown for each run:

1) Gas_{abs} : The amount of CO_2 taken from the exhaust gas, calculated from gas CO_2 analyses and temperatures in the gas.
2) Liq_{abs} : The amount of CO_2 absorbed in the liquid calculated from liquid measurements before and after the absorber.
3) Liq_{des} : The amount of CO_2 desorbed from the liquid calculated from liquid measurements before and after the desorber.
4) CO_2prod : The amount of CO_2 leaving the desorber, measured by the gas flow sensor FT14. 0.51 kg/h is added due to a zero point deviation and the estimated water content is subtracted.
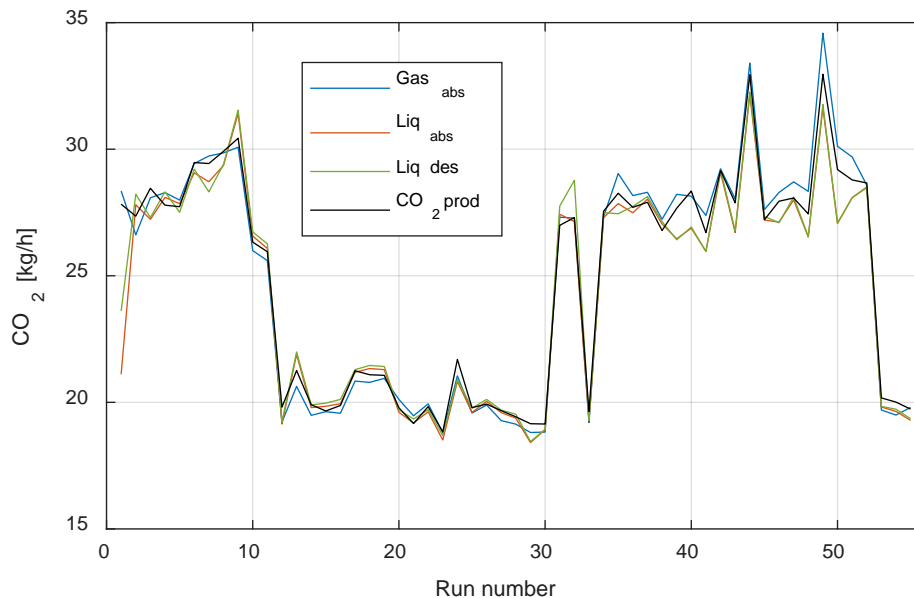
Figure 3-4 Mass transfer rates for CO_2

Except for the first run a very good accordance between the four independent measurements is shown. The standard deviation between the four values is for run 2 to 55 is on average 0.39 kg/h or 1.5%.

One may calculate the specific reboiler duty (SRD) based on each of these four mass transfer values. This is shown in Figure 3-5.
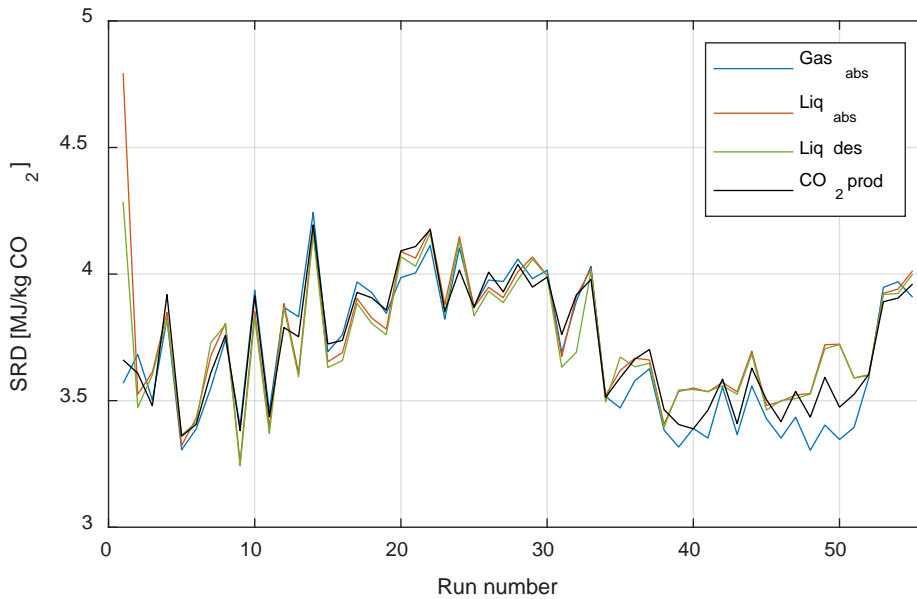
Figure 3-5 The specific reboiler duty (SRD) based on the individual mass transfer rates in Figure 3-4.

The standard deviation is in average only 0.06 MJ/kg CO_2. The CO_2 production rate (CO_2prod) is considered to be the most consistent measurement since it involves only the "FT14" flowmeter sensor with a small correction for the water content (typically 1%). In the present report, we will use this value further on in tables and figures when we compare the different runs internally.

3.4.3 Total amine balance

There are three liquid sampling points for the amine concentration. VSL1 (lean stream from the desorber), VSL2 (lean stream to the absorber) and the rich stream VSR1. To better compare the different values, they are in Figure 3-6 shown on CO_2 free basis. This is done by using the following calculations:

$$Cam_{CO_2free} = \frac{Cam}{1 - w_{CO_2}}$$

$$w_{CO_2} = \frac{C_{CO_2} \cdot 44}{1000}$$

C_{am} and C_{CO2} are the analyzed concentrations in mol/kg solution and w_{CO2} is the weight fraction of CO_2.
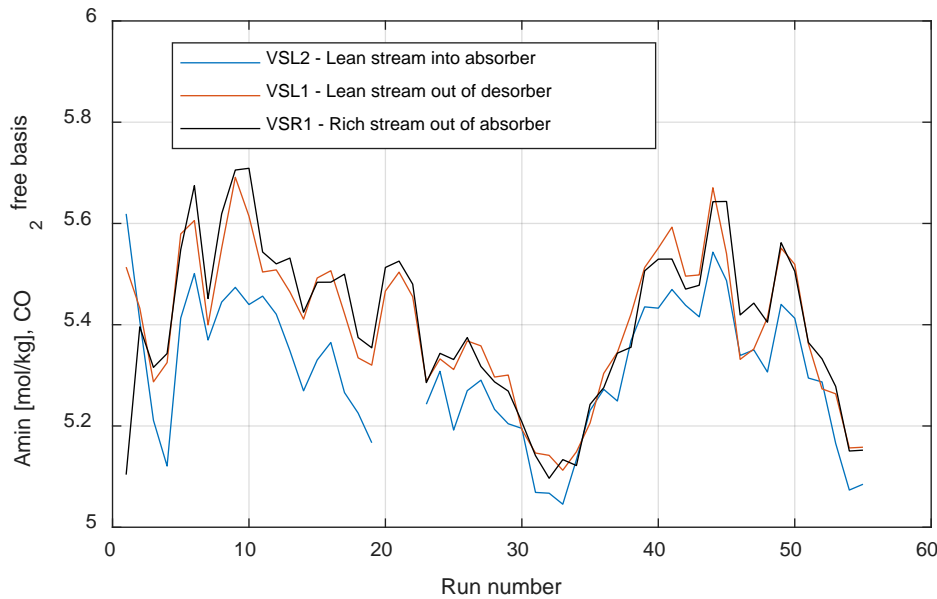
Figure 3-6 Amine concentration during the campaign in mol/kg CO₂ free solution

The CO_2 free amine concentration should be very similar for the sampling points VSL1 and VSR1 since the mass of water going out with the CO_2 product is very small (~0.15-0.30 kg/h), which is less than 0.1% of the overall liquid circulation flow. Except for the first run the measurements also show that mean difference between them is almost zero (-0.012 mol/kg). The standard deviation between the two (VSL1 and VSR1) is only 0.04 mol/kg for runs 2-45 and give confidence to the analysed results.

The difference between VSL1 and VSL2 is caused by the water coming from water wash sections into Tank 3 and further to Tank 2 (See Figure 2.1). The three runs 20-22 were run with only three sections and the sampling point VSL2 was bypassed for these runs.

3.5 Energy results with fresh solvent

The campaign started with fresh solvent 40 wt.% 1-(2HE)PRLD, 15 wt.% 3A1P and 45 wt.% H_2O). The results would then be compatible with equilibrium and physical data for the solvent from the bench lab, to which experimental property models and VLE are derived from.

3.5.1 Results with 11.5 – 12 % CO₂

The main parameters for the first 11 runs are shown Table 3-3. The flue gas from the propane burner has typically a concentration between 11.5 -12 % CO_2 (dry) and in these runs the gas was used without any dilution with air.

Table 3-3 Main parameters for Run 1-11

		Run 1	Run 2	Run 3	Run 4	Run 5	Run 6
Year: 2022	Date	24 Sep	26 Sep	27 Sep	28 Sep	29 Sep	30 Sep
	Averaging time	11:55-12:55	07:10-08:10	07:10-08:10	07:15-08:15	07:08-08:08	07:10-08:10
Time on steam	Hours	48.9	92.2	116.2	140.3	163.6	187.6
No of absorber sections		4	4	4	4	4	4
Gas inlet ABS	m^3/h	160.0	160.0	160.0	160.0	160.0	160.0
CO_2 inlet ABS	vol% dry	11.83	11.42	11.99	11.90	11.76	11.89
CO_2 outlet WW	vol% dry	1.17	1.137	1.211	1.130	1.141	0.637
CO_2 recovery	%	91.2 %	91.1 %	91.0 %	91.5 %	91.3 %	95.2 %
Temp Gas outlet DCC	°C	34.7	34.7	34.7	34.7	34.7	34.7
Liquid inlet Absorber	kg/min	10.00	9.00	8.00	5.27	6.50	7.30
Temp Liquid inlet Absorber	°C	39.4	39.3	39.3	38.3	38.8	39.2
L/G ratio	kg/kg	3.16	2.92	2.58	1.69	2.07	2.33
VSL2 Amine	mole/kg	5.398	5.221	5.058	5.071	5.289	5.371
Lean2 Loading	mole/mole	0.166	0.150	0.132	0.043	0.099	0.100
Rich Loading	mole/mole	0.344	0.379	0.385	0.438	0.407	0.379
Temp Liq Reboiler	°C	117.7	117.6	118.5	120.4	119.8	119.9
Desorber press top	mBar (g)	827.55	827.75	827.74	827.45	827.64	827.77
Reboiler duty	kW	28.11	27.23	27.32	30.04	25.70	27.71
SRD (based on CO_2prod)	MJ/kg CO_2	3.64	3.58	3.46	3.89	3.34	3.38
		Run 7	Run 8	Run 9	Run 10	Run 11	
Year: 2022	Date	03 Oct	04 Oct	05 Oct	05 Oct	06 Oct	
	Averaging time	07:08-08:08	06:10-07:10	05:50-06:50	13:40-14:40	06:10-07:10	
Time on steam	Hours	259.6	282.6	306.3	314.1	330.6	
No of absorber sections		4	4	4	4	4	
Gas inlet ABS	m^3/h	160.0	160.0	160.0	160.0	160.0	
CO_2 inlet ABS	vol% dry	11.92	11.99	11.83	11.84	11.73	
CO_2 outlet WW	vol% dry	0.668	0.612	0.207	1.884	1.886	
CO_2 recovery	%	95.0 %	95.5 %	98.5 %	85.7 %	85.5 %	
Temp Gas outlet DCC	°C	34.7	34.7	34.6	34.7	34.7	
Liquid inlet Absorber	kg/min	8.69	5.55	6.20	4.59	7.00	
Temp Liquid inlet Absorber	°C	39.3	38.5	39.0	38.1	39.2	
L/G ratio	kg/kg	2.75	1.77	1.99	1.49	2.27	
VSL2 Amine	mole/kg	5.219	5.395	5.407	5.394	5.283	
Lean2 Loading	mole/mole	0.122	0.038	0.051	0.035	0.137	
Rich Loading	mole/mole	0.362	0.412	0.404	0.438	0.406	
Temp Liq Reboiler	°C	119.5	121.2	121.1	120.8	118.7	
Desorber press top	mBar (g)	827.53	828.04	827.88	827.70	827.41	
Reboiler duty	kW	29.33	31.04	28.41	28.42	24.59	
SRD (based on CO_2prod)	MJ/kg CO_2	3.59	3.73	3.36	3.89	3.41	

90% capture rate (Runs 1-5)

The purpose of the first five runs was to find the minimum SRD (specific reboiler duty) for 90% capture rate. Various liquid rates were used while the flue gas rate was held constant at 160 m3/h. For each run the reboiler duty was adjusted to obtain the desired capture rate. The result is shown in Figure 3-7 where the SRD is a function of L/G on mass basis (kg/kg).
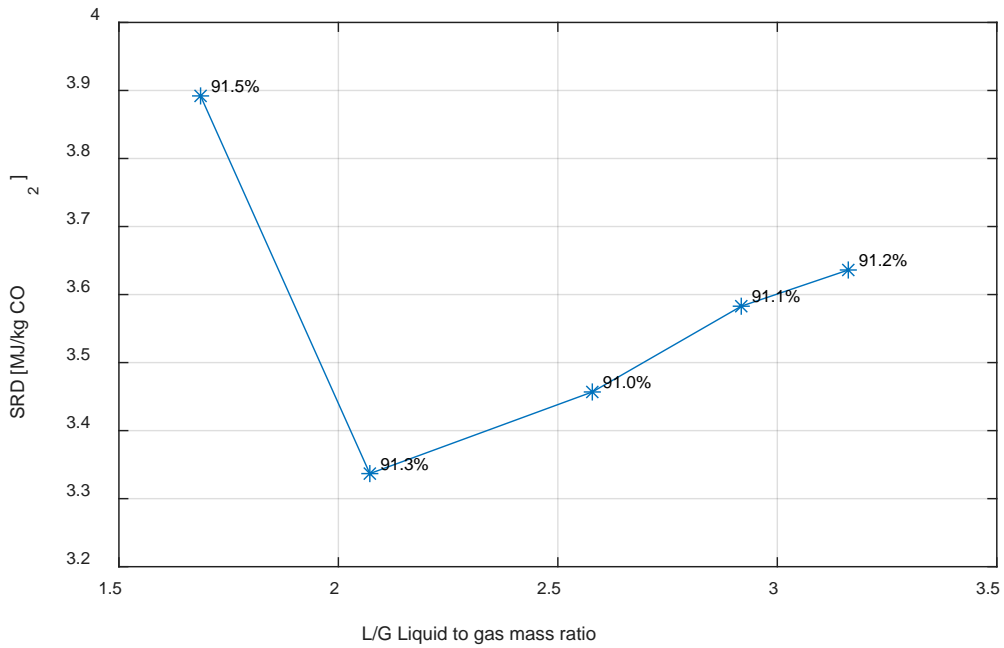
Figure 3-7 SRD as a function of L/G for 90% capture rate. The attached numbers are the measured capture rates.

The figure shows that the SRD is decreasing with L/G to about 2, and then increases quickly at 1.7. The minimum is about 2. The Capture rate was slightly higher than 90%.

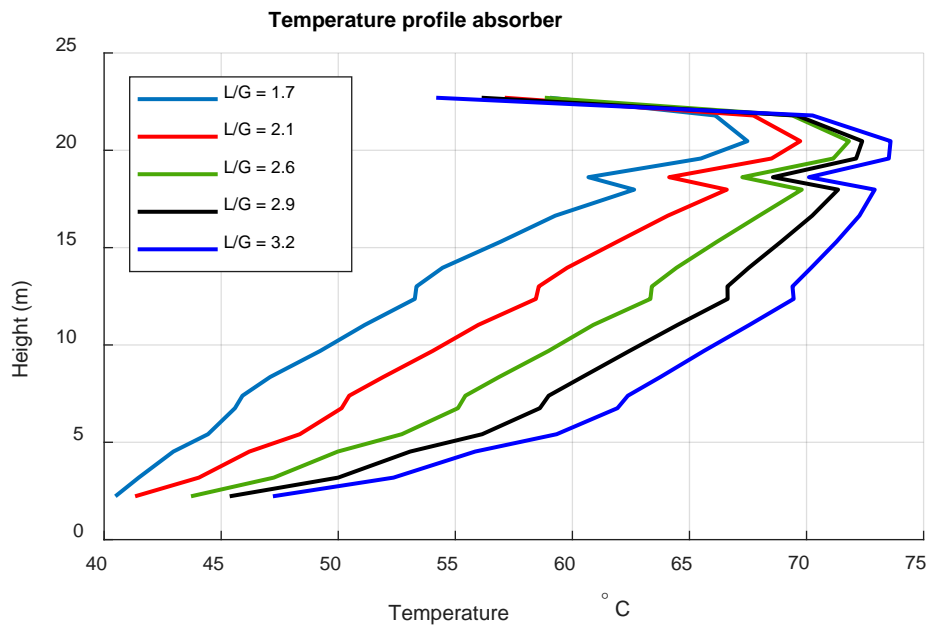The temperature profile in the absorber is shown in Figure 3-8.

Figure 3-8 Temperature profiles in the absorber for runs 1- 5

In shape the profiles are very similar to each other. A higher L/G correlates with higher temperatures in the column. This seems strange, because simulations shows that the temperatures do not change much for various L/G and rather has a small reduction. The effect we see is probably the removal of insulation before the campaign (see section 2.2), and this cooling has a larger effect on small L/G with lower heat capacity.

In Figure 3-9 the temperature profiles for the desorber are shown. The one that differs significantly from the other has an L/G of 1.7 and corresponds to the point with high SRD to the left in Figure 3-7. The most optimal point with an L/G of 2.1 has the lowest temperatures up in the column.
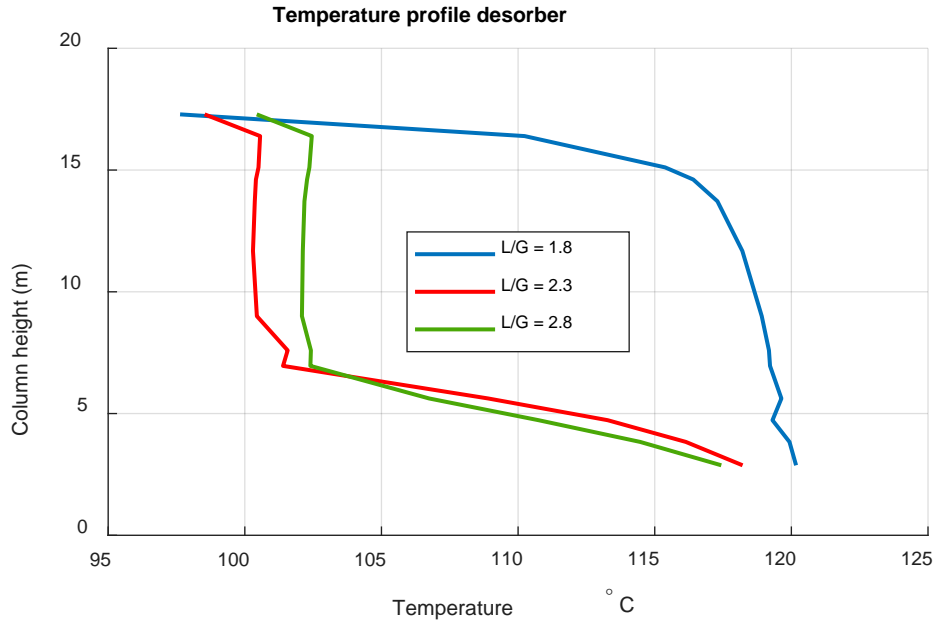

Temperature profile desorber
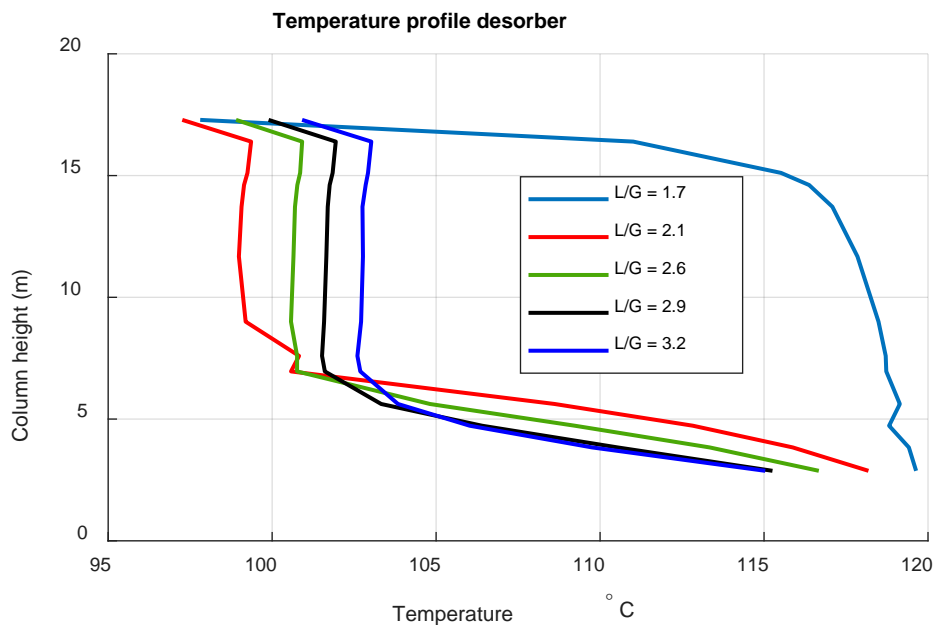
Figure 3-9 Temperature profiles in the desorber for runs 1- 5

95% capture rate (Runs 6-8)

The same procedure was used to find the optimal L/G for 95% capture rate. The result is shown in Figure 3-10 where the SRD is a function of L/G on mass basis.
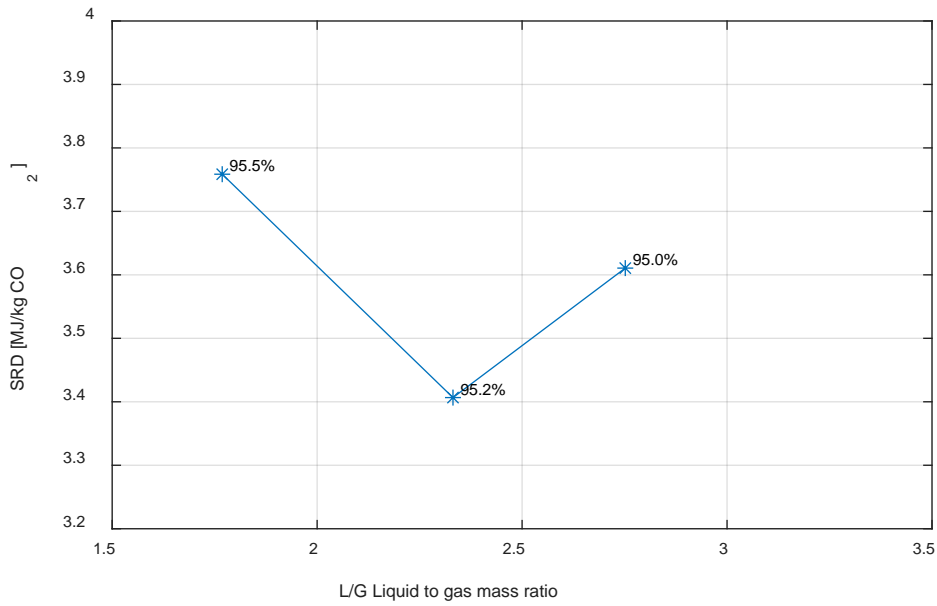
Figure 3-10 SRD as a function of L/G for 95% capture rate. The attached numbers are the measured CR.

Also, here the optimal L/G is close to 2.0. The temperature profiles in the absorber are shown in Figure 3-11.
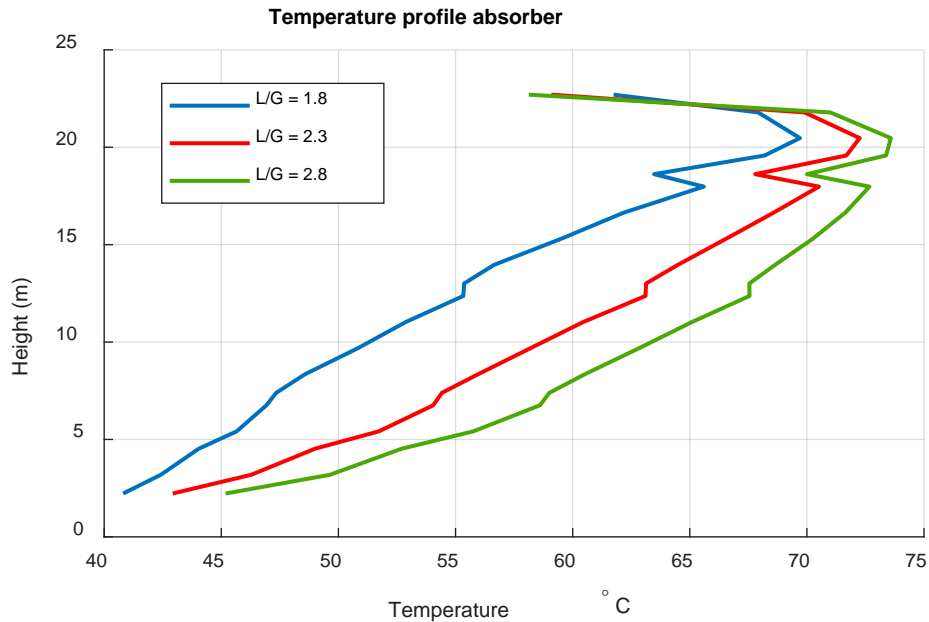
Figure 3-11 Temperature profile in the absorber Run 6-

Again, a higher L/G correlates with higher temperatures in the column.

In Figure 3-12 the temperature profiles for the desorber are shown. Again, the one that differs significantly from the other two has an L/G of 1.8 and corresponds to the point

with high SRD to the left in Figure 3-7. The optimal point with an L/G of 2.1 has the lowest temperature profile in up in the column.

Figure 3-12 Temperature profile in the desorber Run 6-8

Data including capture rates with 85% and 98% (Runs 9 - 11)
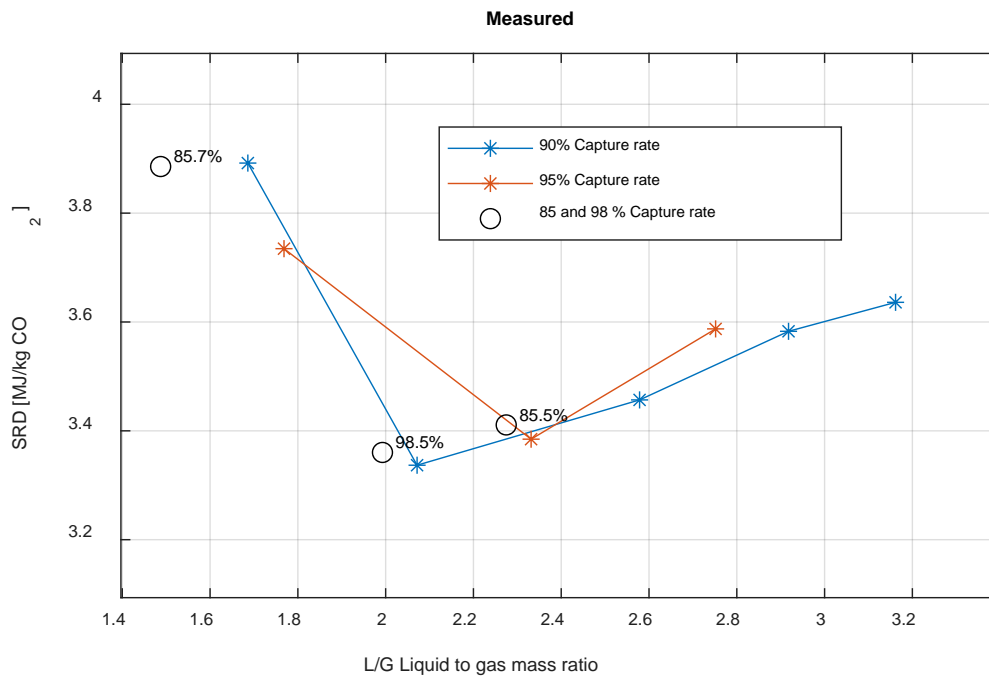
Figure 3-13 SRD for runs with 85 and 98% capture rate together with the 90 and 95 % capture rate runs.

In Figure 3-13 the curves for 90% and 95 % capture rate are plotted together. In addition, two points at 85% capture rate and one point at 98% are shown. The figure shows that there are very small differences between the capture rates. The optimal point is close to 2.0 in L/G and the SRD is then about 3.35 MJ/kg CO_2.

3.5.2 Energy results with 5.5 % CO_2

During the runs 12 to 24 similar test were done with 5.5% CO_2. The main parameters are shown in Table 3-4

Table 3-4 Main parameters for Run 12-24

		Run 12	Run 13	Run 14	Run 15	Run 16	Run 17	Run 18
Year: 2022	Date	07 Oct	10 Oct	11 Oct	12 Oct	13 Oct	14 Oct	17 Oct
	Averaging time	06:05-07:05	05:55-06:55	06:05-07:05	06:00-07:00	06:10-07:10	06:10-07:10	06:15-07:15
Time on steam	Hours	354.6	419.8	444.0	467.9	492.0	516.0	588.1
No of absorber sections		4	4	4	4	4	4	4
Gas inlet ABS	m^3/h	250.0	250.0	250.0	250.0	250.0	250.0	250.0
CO_2 inlet ABS	vol% dry	5.45	5.45	5.45	5.46	5.45	5.45	5.46
CO_2 outlet WW	vol% dry	0.624	0.256	0.580	0.619	0.580	0.250	0.293
CO_2 recovery	%	89.1 %	95.6 %	89.9 %	89.2 %	89.9 %	95.7 %	94.9 %
Temp Gas outlet DCC	°C	34.7	34.7	34.7	34.7	34.7	34.7	34.7
Liquid inlet Absorber	kg/min	6.00	5.00	4.25	4.60	5.00	4.90	6.00
Temp Liquid inlet Absorber	°C	38.56	38.2	38.1	38.0	38.2	38.1	38.4
L/G ratio	kg/kg	1.26	1.05	0.89	0.95	1.04	1.02	1.24
VSL2 Amine	mole/kg	5.267	5.277	5.219	5.248	5.263	5.207	5.118
Lean2 Loading	mole/mole	0.122	0.058	0.042	0.067	0.082	0.049	0.091
Rich Loading	mole/mole	0.352	0.372	0.381	0.379	0.372	0.360	0.354
Temp Liq Reboiler	°C	118.69	120.3	120.3	120.3	119.9	120.4	119.8
Desorber press top	mBar (g)	827.79	827.78	827.73	827.77	827.79	827.74	827.71
Reboiler duty	kW	20.65	21.96	22.97	20.14	20.44	22.97	22.68
SRD (based on CO_2prod)	MJ/kg CO_2	3.75	3.72	4.15	3.69	3.70	3.89	3.87
		Run 19	Run 20	Run 21	Run 22	Run 23	Run 24	
Year: 2022	Date	18 Oct	19 Oct	20 Oct	21 Oct	24 Oct	25 Oct	
	Averaging time	06:05-07:05	06:05-07:05	06:05-07:05	06:10-07:10	06:10-07:10	06:10-07:10	
Time on steam	Hours	612.0	631.2	655.2	679.3	751.3	775.3	
No of absorber sections		4	3	3	3	4	4	
Gas inlet ABS	m^3/h	250.0	250.0	250.0	250.0	250.0	250.0	
CO_2 inlet ABS	vol% dry	5.46	5.45	5.44	5.46	5.46	5.45	
CO_2 outlet WW	vol% dry	0.279	0.549	0.684	0.563	0.815	0.151	
CO_2 recovery	%	95.2 %	90.4 %	88.0 %	90.2 %	85.8 %	97.4 %	
Temp Gas outlet DCC	°C	34.7	34.7	34.7	34.7	34.7	34.7	
Liquid inlet Absorber	kg/min	5.50	4.80	5.30	4.69	4.70	5.20	
Temp Liquid inlet Absorber	°C	38.2	40.3	40.6	38.3	38.3	38.2	
L/G ratio	kg/kg	1.13	0.98	1.08	0.96	0.97	1.09	
VSL2 Amine	mole/kg	5.080				5.15	5.25	
Lean2 Loading	mole/mole	0.075				0.080	0.049	
Rich Loading	mole/mole	0.362	0.343	0.344	0.345	0.372	0.342	
Temp Liq Reboiler	°C	120.2	120.7	120.1	120.6	119.9	120.4	
Desorber press top	mBar (g)	827.73	827.72	827.72	827.73	827.76	827.77	
Reboiler duty	kW	22.37	22.27	21.66	22.78	19.96	23.99	
SRD (based on CO_2prod)	MJ/kg CO_2	3.82	4.05	4.07	4.14	3.81	3.98	

90% capture rate (Runs

The purpose of the first five runs was to find the minimum SRD (specific reboiler duty) for 90% capture rate. Various liquid rates were used while the flue gas rate was held constant at 160 m3/h. For each run the reboiler duty were adjusted to obtain the desired

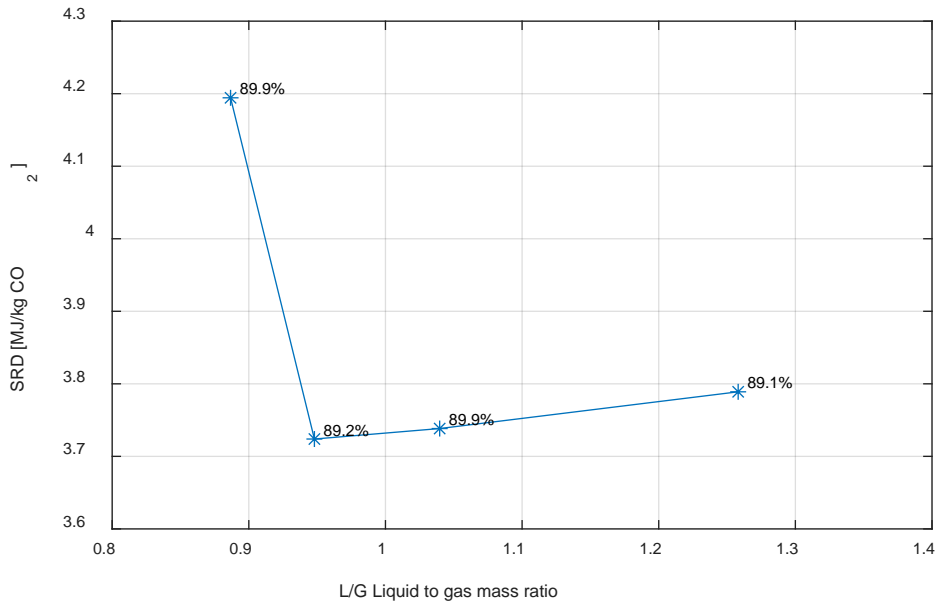capture rate. The result is shown in Figure 3-14 where the SRD is a function of L/G on mass basis.

Figure 3-14 SRD as a function of L/G for 90% capture rate and 5%. The attached numbers are the measured CR.

The figure shows that the SRD is decreasing with L/G to about 2, and then increases quickly at 1.7. The minimum is about 2.

The temperature profile in the absorber is shown in Figure 3-15.
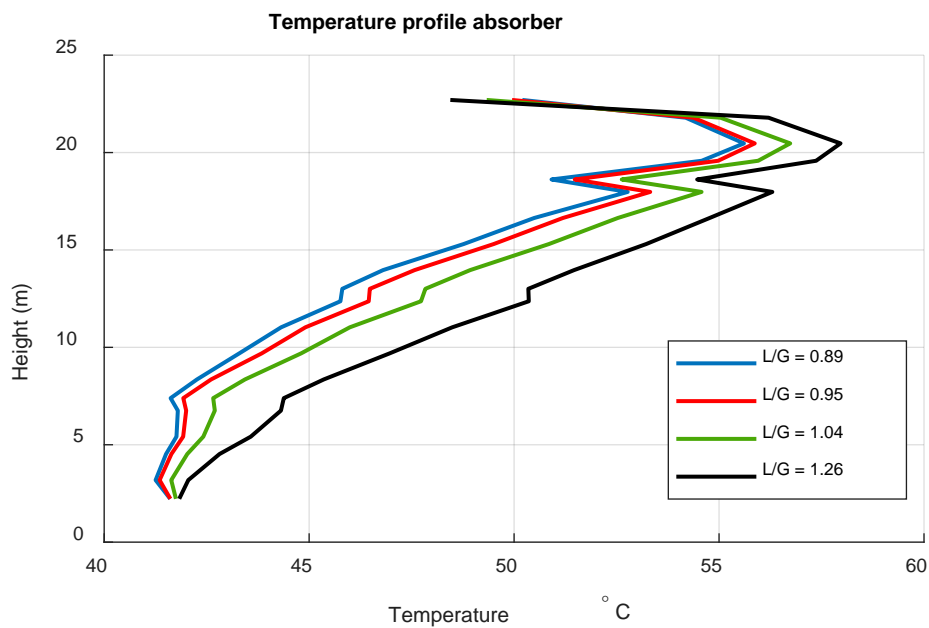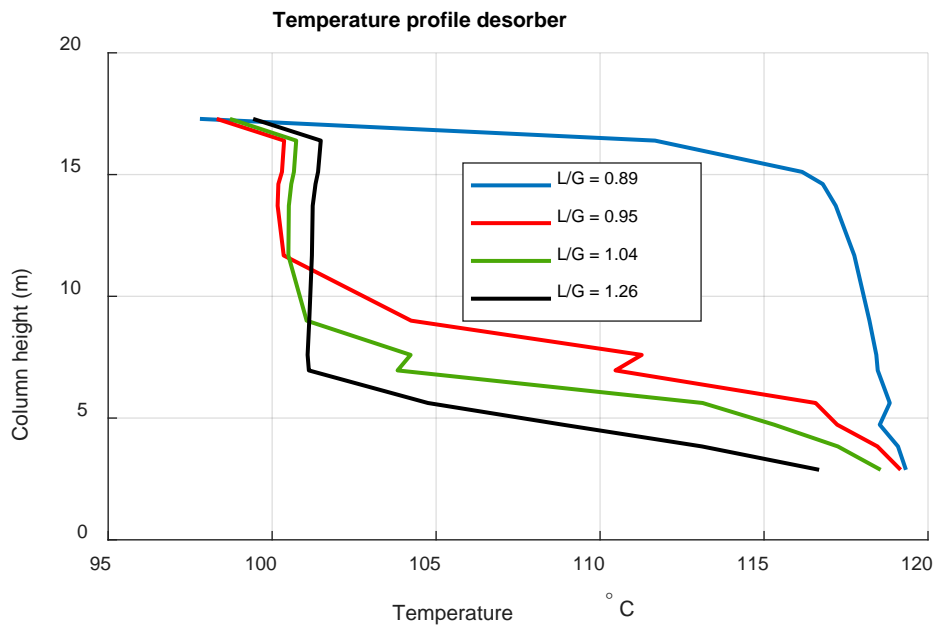

Figure 3-15 Temperature profile in the absorber runs 12, 14-16.

In shape the profiles are very similar to each other. A higher L/G correlates with higher temperatures in the column as shown and discussed in the 11% CO_2 case.

In Figure 3-9 the temperature profiles for the desorber are shown. The one that differs significantly from the other has an L/G of 1.7 and corresponds to the point with high SRD to the left in Figure 3-16. The optimal point with an L/G of 2.1 has th lowest temperature profile in up in the column.
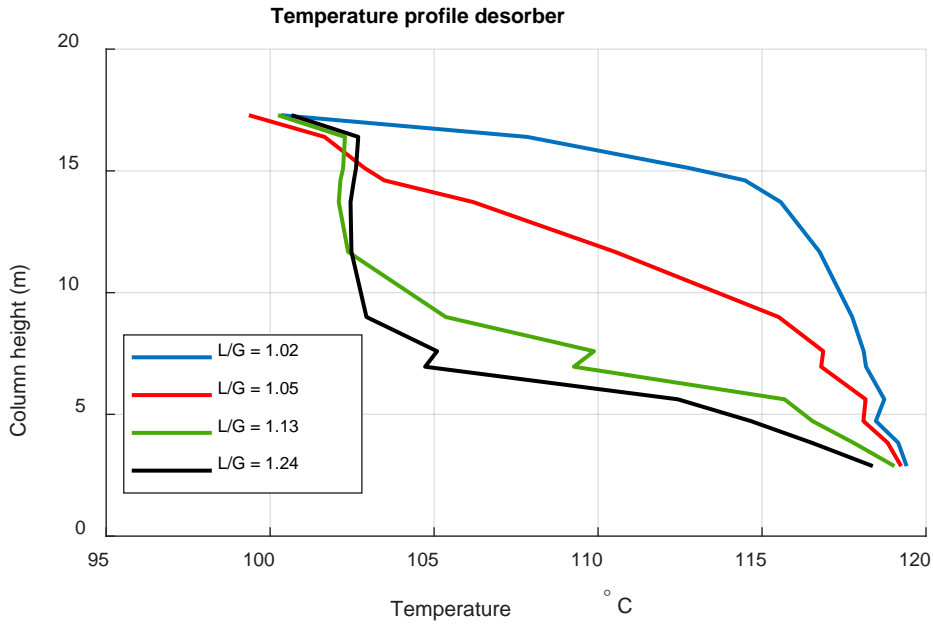

Figure 3-16 Temperature profile in the desorber for runs 12, 14-16

95% capture rate

The same procedure was used for the 95% capture rate. The result is shown in Figure 3-17 where the SRD is a function of L/G on mass basis.
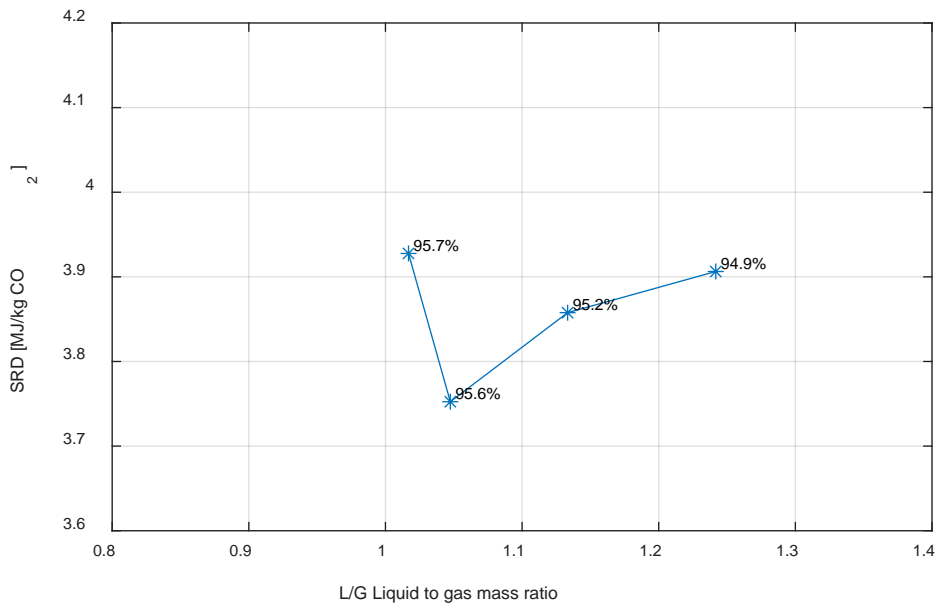
Figure 3-17 SRD as a function of L/G for 95% capture rate. The attached numbers are the measured CR.

The temperature profile in the absorber is shown in Figure 3-18.
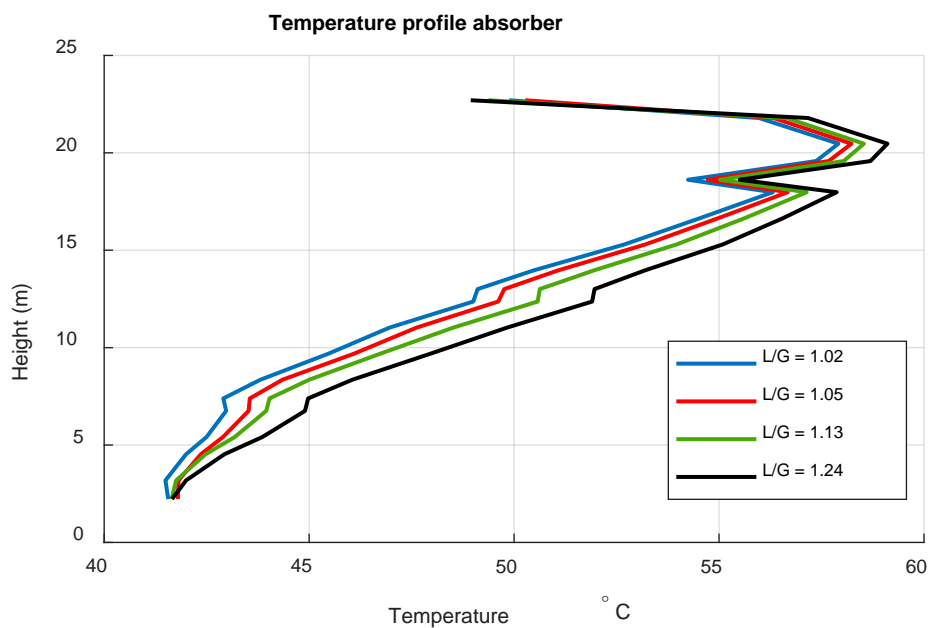
Figure 3-18 Temperature profile in the absorber Run 6- 8

Since the span in L/G is smaller, also the difference in temperature profile is less.

In Figure 3-19 the temperature profiles for the desorber are shown. The one that differs significantly from the other has an L/G of 1.7 and corresponds to the point with high SRD to the left in Figure 3-7. The optimal point with an L/G of 2.1 has the lowest temperature profile in up in the column.

Figure 3-19 Temperature profile in the desorber Run 6-8

Capture rates 85 and 98 included.
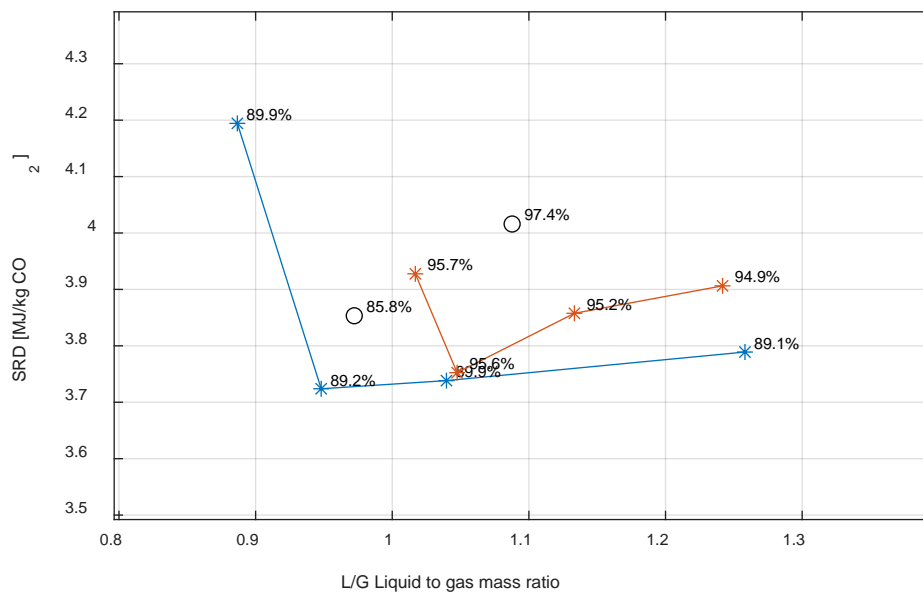
Figure 3-20 Temperature profile in the desorber Run 1- 5

90% capture rate with shorter absorber column (Runs 20-22)

To evaluate the importance of packing height three runs were done where the liquid solvent went to the top of the 3rd section instead of the 4th section. In Figure 3-21 these runs are compared with the four-section absorber. The fourth section was then a dry bed.
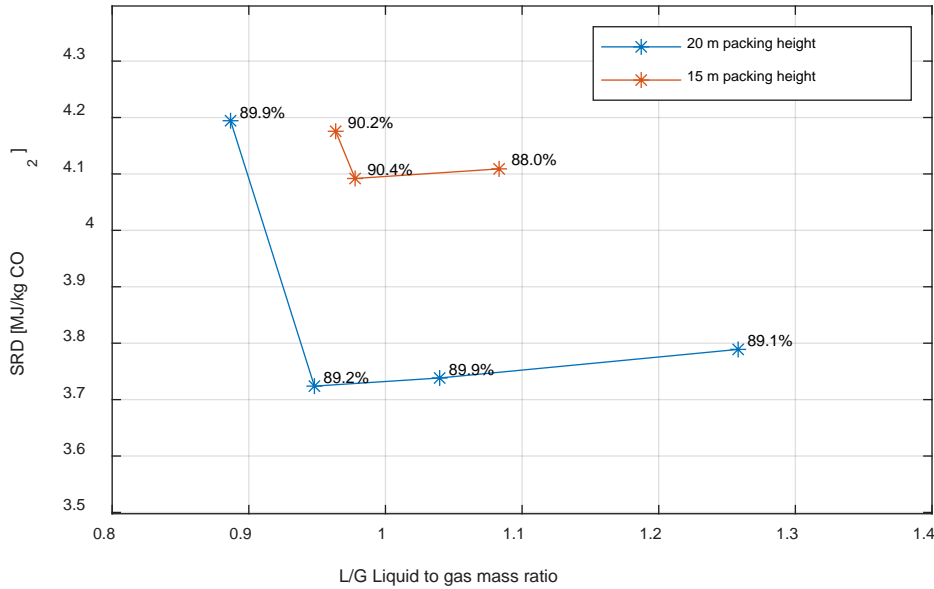

Figure 3-21 SRD for runs using only three sections of the absorber (15m) compared to the runs with four section 20m)

The increase in SRD is substantial, almost 0.35 MJ/kg CO_2.

3.5.3 Step responses

Five step response tests were conducted during the campaign. They are summarized in Table 3-5. The use of these data together with responses from the modelling part is shown in Chapter 4.

Table 3-5 Step response experiments

	From	To	
Test B - Step i liquid rate	10	9	kg/min
Test A - Step in reboiler duty	27.23	24.25	kW
Test C - Step in gas flow	160	180	m3/h
Test B - Step i liquid rate	7.3	8.7	kg/min
Test D - Step in CO2 concentration	11	9	%

3.6 Energy results with degraded solvent

During the campaign several samples was analysed for degradation products. The results of these analysis are described in Chapter.5. The conclusion is basically that the solvents degrade constantly with time. In addition, twenty litres of degraded solvent from Cork were added to the plant 28th of October. In the following section we compare runs taken late in the campaign with the ones that were taken early in the campaign. In Table 3-6 and Table 3-7, the main results for the runs done after the addition are shown.

Table 3-6 Main parameters for Run 25-40

		Run 25	Run 26	Run 27	Run 28	Run 29	Run 30	Run 31	Run 32
Year: 2022	Date	31 Oct	01 Nov	02 Nov	03 Nov	04 Nov	07 Nov	08 Nov	09 Nov
	Averaging time	06:05-07:05	06:10-07:10	06:05-07:05	06:10-07:10	06:05-07:05	06:05-07:05	06:05-07:05	06:05-07:05
Time on steam	Hours	852.4	876.5	900.3	924.4	948.3	1020.3	1044.3	1068.3
No of absorber sections		4	4	4	4	4	4	4	4
Gas inlet ABS	m^3/h	250.0	250.0	250.0	250.0	250.0	250.0	160.0	160.0
CO_2 inlet ABS	vol% dry	5.44	5.45	5.46	5.46	5.45	5.45	11.87	11.82
CO_2 outlet WW	vol% dry	0.576	0.525	0.628	0.677	0.741	0.757	1.459	1.350
CO_2 recovery	%	89.9 %	90.8 %	89.1 %	88.2 %	87.0 %	86.8 %	89.0 %	89.8 %
Temp Gas outlet DCC	°C	34.7	34.7	34.7	34.7	34.7	34.7	34.7	34.7
Liquid inlet Absorber	kg/min	5.00	4.38	4.60	5.50	6.00	6.00	6.52	7.99
Temp Liquid inlet Absorber	°C	38.1	38.4	38.1	38.3	38.6	38.4	39.0	39.4
L/G ratio	kg/kg	1.04	0.91	0.96	1.15	1.26	1.25	2.09	2.58
VSL2 Amine	mole/kg	5.10	5.22	5.21	5.11	5.06	5.06	4.96	4.93
Lean2 Loading	mole/mole	0.079	0.045	0.062	0.102	0.122	0.118	0.095	0.128
Rich Loading	mole/mole	0.366	0.377	0.375	0.363	0.350	0.356	0.414	0.388
Temp Liq Reboiler	°C	119.8	120.3	120.3	119.4	118.8	118.8	120.7	119.5
Desorber press top	mBar (g)	827.73	827.72	827.62	827.83	827.62	827.69	826.99	827.01
Reboiler duty	kW	21.06	21.98	21.26	21.58	20.80	21.00	28.00	29.50
SRD (based on CO_2prod)	MJ/kg CO_2	3.83	3.97	3.89	4.00	3.91	3.95	3.73	3.89
		Run 33	**Run 34**	**Run 35**	**Run 36**	**Run 37**	**Run 38**	**Run 39**	**Run 40**
Year: 2022	Date	10 Nov	11 Nov	14 Nov	15 Nov	16.11.2022	17.11.2022	18.11.2022	18.11.2022
	Averaging time	06:05-07:05	06:10-07:10	06:10-07:10	06:10-07:10	06:10-07:10	06:10-07:10	06:10-07:10	13:30-14:30
Time on steam	Hours	1092.3	1116.3	1188.3	1212.3	1236.3	1260.3	1284.3	1291.6
No of absorber sections		4	4	4	4	4	4	4	4
Gas inlet ABS	m^3/h	250.0	160.0	160.0	160.0	160.0	160.0	160.0	160.0
CO_2 inlet ABS	vol% dry	5.45	11.95	12.11	11.87	11.89	11.73	11.81	11.75
CO_2 outlet WW	vol% dry	0.647	1.490	1.312	1.348	1.270	1.562	1.262	1.250
CO_2 recovery	%	88.7 %	88.9 %	90.4 %	89.9 %	90.5 %	88.1 %	90.5 %	90.5 %
Temp Gas outlet DCC	°C	34.7	34.7	34.7	34.7	34.7	34.7	34.7	34.7
Liquid inlet Absorber	kg/min	5.70	7.00	8.00	9.00	5.32	6.52	6.02	5.52
Temp Liquid inlet Absorber	°C	38.2	39.2	39.3	39.4	38.1	38.6	38.3	38.2
L/G ratio	kg/kg	1.19	2.26	2.51	2.83	1.68	2.06	1.89	1.73
VSL2 Amine	mole/kg	4.94	5.01	5.09	5.11	5.20	5.25	5.34	5.37
Lean2 Loading	mole/mole	0.100	0.107	0.119	0.140	0.040	0.098	0.073	0.052
Rich Loading	mole/mole	0.357	0.406	0.379	0.367	0.422	0.402	0.383	0.392
Temp Liq Reboiler	°C	119.2	119.3	119.4	118.6	120.9	120.0	120.8	121.3
Desorber press top	mBar (g)	827.62	827.72	827.80	827.83	827.58	827.84	827.81	827.71
Reboiler duty	kW	21.50	26.70	28.00	28.00	28.50	25.60	26.00	26.50
SRD (based on CO_2prod)	MJ/kg CO_2	3.94	3.49	3.57	3.64	3.68	3.44	3.38	3.37

Table 3-7 Main parameters for Run 41-55

		Run 41	Run 42	Run 43	Run 44	Run 45	Run 46	Run 47	Run 48
Year: 2022	**Date**	21.11.2022	22.11.2022	23.11.2022	24.11.2022	25.11.2022	28.11.2022	29.11.2022	30.11.2022
	Averaging time	06:05-07:05	06:05-07:05	06:05-07:05	06:05-07:05	06:05-07:05	06:10-07:10	06:10-07:10	06:05-07:05
Time on steam	**Hours**	1356.2	1380.2	1404.2	1428.2	1452.2	1524.3	1548.3	1572.2
No of absorber sections		4	4	4	4	4	4	4	4
Gas inlet ABS	m^3/h	160.0	160.0	160.0	195.0	160.0	160.0	160.0	160.0
CO$_2$ inlet ABS	vol% dry	11.57	11.63	11.83	11.83	11.97	11.92	11.91	11.54
CO$_2$ outlet WW	vol% dry	1.315	0.525	1.209	1.346	1.534	1.249	1.166	0.984
CO$_2$ recovery	%	89.8 %	96.0 %	90.9 %	89.8 %	88.5 %	90.7 %	91.3 %	92.4 %
Temp Gas outlet DCC	°C	34.7	34.7	34.7	34.7	34.7	34.7	34.7	34.7
Liquid inlet Absorber	kg/min	6.30	5.80	5.40	6.39	5.10	5.50	5.47	5.52
Temp Liquid inlet Absorber	°C	38.3	38.2	38.2	38.9	38.3	38.4	38.4	38.4
L/G ratio	kg/kg	1.98	1.84	1.72	1.69	1.63	1.74	1.72	1.73
VSL2 Amine	mole/kg	5.35	5.39	5.36	5.50	5.44	5.29	5.30	5.25
Lean2 Loading	mole/mole	0.090	0.040	0.041	0.034	0.037	0.042	0.039	0.042
Rich Loading	mole/mole	0.380	0.395	0.391	0.385	0.403	0.394	0.403	0.385
Temp Liq Reboiler	°C	120.3	121.1	121.3	121.5	121.1	121.4	121.1	121.6
Desorber press top	mBar (g)	827.88	827.58	827.76	827.86	827.62	827.56	827.94	827.69
Reboiler duty	kW	25.50	28.85	26.22	33.01	26.30	26.35	27.39	26.00
SRD (based on CO$_2$prod)	MJ/kg CO$_2$	3.44	3.56	3.39	3.61	3.48	3.39	3.51	3.41

		Run 49	Run 50	Run 51	Run 52	Run 53	Run 54	Run 55	
Year: 2022	**Date**	01 Dec	02 Dec	05 Dec	06 Dec	07 Dec	08 Dec	09 Dec	
	Averaging time	06:05-07:05	06:05-07:05	06:25-07:25	10:20-11:20	08:35-09:35	06:15-07:15	09:00-10:00	
Time on steam	**Hours**	1596.2	1620.2	1692.6	1720.5	1742.7	1764.4	1791.1	
No of absorber sections		4	4	4	4	4	4	4	
Gas inlet ABS	m^3/h	200.0	160.0	160.0	160.0	250.0	250.0	250.0	
CO$_2$ inlet ABS	vol% dry	11.49	11.60	11.75	11.37	5.44	5.45	5.45	
CO$_2$ outlet WW	vol% dry	1.199	0.465	0.724	0.597	0.569	0.577	0.604	
CO$_2$ recovery	%	90.7 %	96.4 %	94.5 %	95.3 %	90.0 %	89.9 %	89.5 %	
Temp Gas outlet DCC	°C	34.7	34.7	34.7	34.7	34.7	34.7	34.7	
Liquid inlet Absorber	kg/min	6.56	6.46	6.96	7.50	5.00	5.00	5.00	
Temp Liquid inlet Absorber	°C	38.8	38.5	38.5	39.2	38.0	38.0	38.9	
L/G ratio	kg/kg	1.64	2.00	2.16	2.36	1.03	1.04	1.02	
VSL2 Amine	mole/kg	5.40	5.34	5.20	5.18	5.10	5.01	5.02	
Lean2 Loading	mole/mole	0.035	0.056	0.078	0.087	0.059	0.057	0.058	
Rich Loading	mole/mole	0.375	0.351	0.370	0.365	0.351	0.353	0.350	
Temp Liq Reboiler	°C	121.9	121.5	120.8	120.3	120.1	119.9	120.0	
Desorber press top	mBar (g)	827.49	827.75	827.77	827.69	827.83	827.93	827.51	
Reboiler duty	kW	32.70	27.99	28.00	28.50	21.60	21.50	21.50	
SRD (based on CO$_2$prod)	MJ/kg CO$_2$	3.57	3.45	3.50	3.58	3.85	3.87	3.92	

3.6.1 Results with 11% CO$_2$

A new set of experiments with 11% CO$_2$ in the flue gas and 90% capture rate was done from 11th to 17th of November. A comparison with the first set is shown in Figure 3-22.

The second curve that was taken approximately 7 weeks later shows an increase in SRD if about 0.1 MJ/kg CO$_2$.
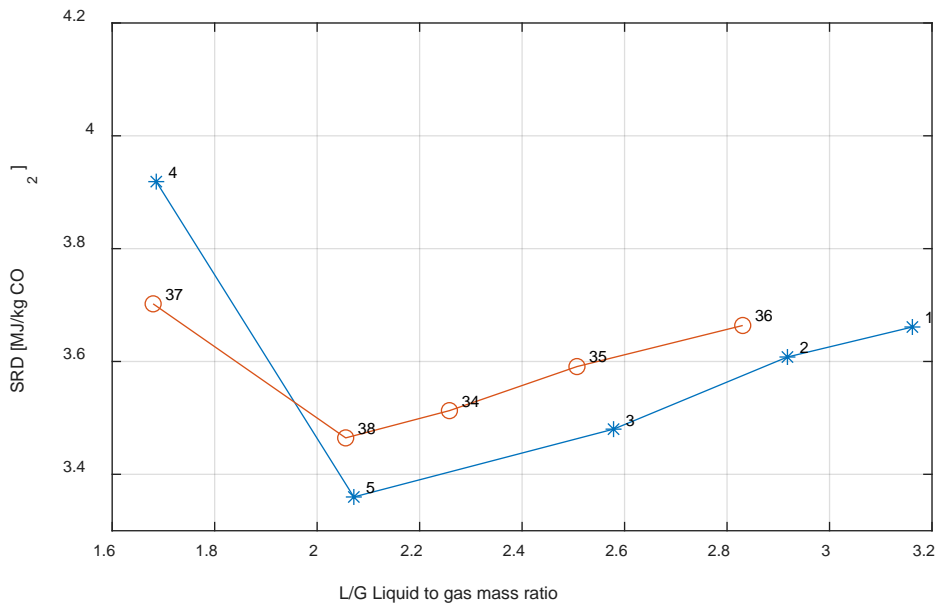
Figure 3-22 Comparison of U-curves at the beginning and later on in the campaign.

A similar test was done with the 95% capture rate and shown in Figure 3-23. With only three points in each curve it is difficult to conclude. But since we know that the minimum SRD vs LG rate is around 2.0, we can extrapolate the line from run 7 and 6 down to L/G of 2, and then it seems to be in a similar range, i.e about 0.1-0.2 MJ/kg CO_2. This is just an approximation, but it suggests that the blue line representing fresh solvent has a lover SRD also at 95% capture.
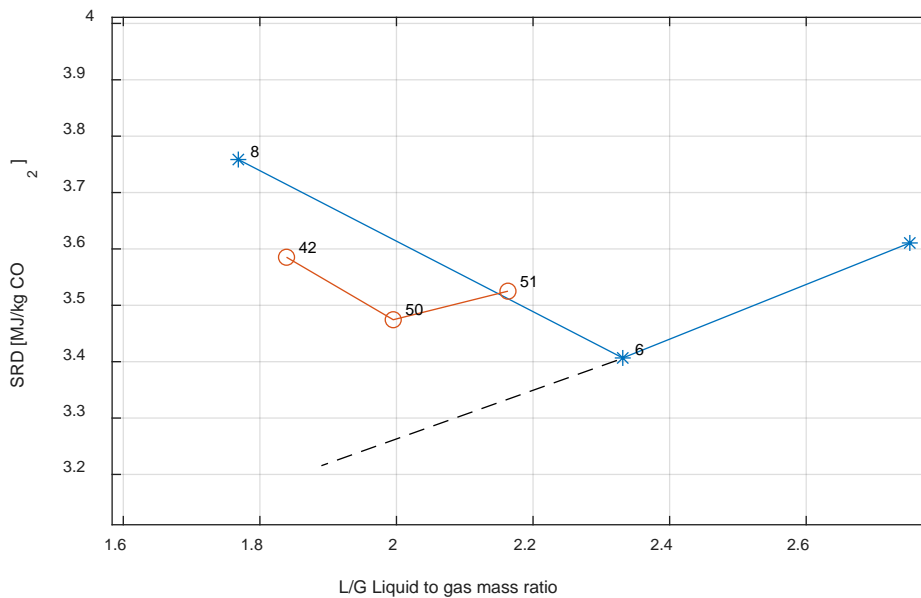
Figure 3-23 Comparison of U-curves at the beginning and later on in the campaign.

3.6.2 Results with 5% CO$_2$

In Figure 3-24 the results for runs 26 -33 is shown together with the data 12-16. Again, we see a higher SRD with time (showing that the fresh amine performs better). The average time between these two series is 26 days, and the difference in SRD is about 0.2 MJ/kg CO$_2$.
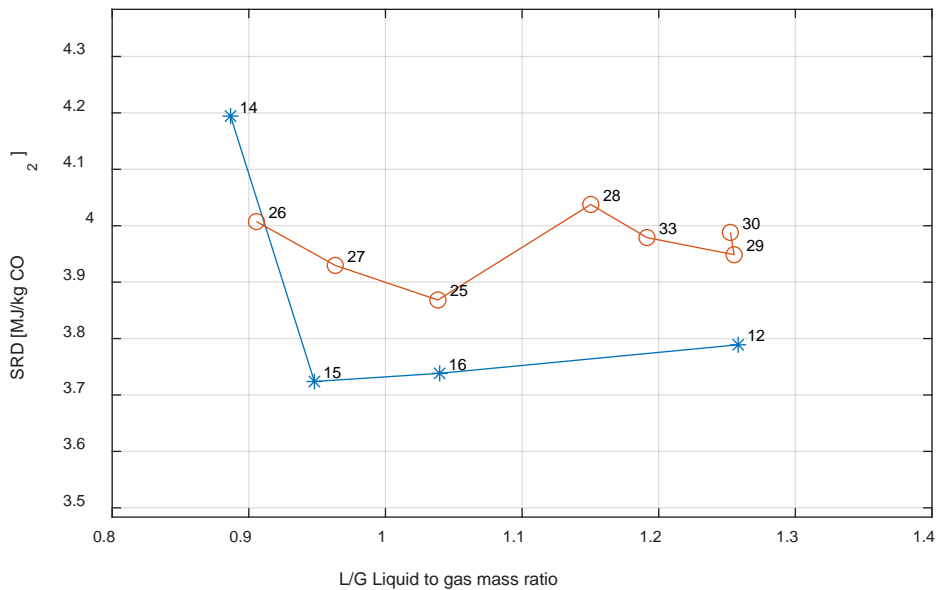
Figure 3-24 Comparison of U-curves at the beginning and later on in the campaign.

4 Process dynamics and control

4.1 Description of the Cybernetica CENIT software

The Cybernetica CENIT software was selected for demonstration of advanced control of the capture plant, namely non-linear model-predictive control (NMPC). Model-predictive control (MPC) is a widespread and acknowledged technology within several industries [1], for example oil refineries, where *linear* MPCs are popular [2]. The linear MPCs are typically based on empirical models, discovered by step-response experiments in the plant of deployment. Linear MPC will typically fall short in many real-life processes, since, due to many processes having inherently non-linear behaviour, the linear empirical models will be insufficient or even invalid under certain operating conditions. Non-linear MPC is an attractive alternative in many cases because the use of mechanistic models, built from first principles and adapted to fit real-life plant data, rather than empirical models saves the intrusive step-response testing. Additionally, the mechanistic models are less prone to deterioration over time since they are built from first principles. Cybernetica has deployed NMPC for a variety of processes within industries such as polymer production [3][4], chemical, oil & gas and metallurgical [5].[1] In addition, Cybernetica has successfully demonstrated NMPC for amine-based CO_2 capture on both the TCM and Tiller pilot plants, through R&D collaborations. [6][7][8]

To comply with the Cybernetica CENIT software suite, the models are formulated as *Cybernetica Model and Application Components*. A block diagram is shown in Figure 4.1 to illustrate the components of the CENIT software and how they interact with each other. In the following conversation, the term model is often used widely to include the features and functionality of the *application* too, in addition to the mechanistic process model itself.

---

[1] At the time of writing, the accumulated time of real-time operation for Cybernetica CENIT is almost 3000 years, across a large *family* of applications with world-wide deployment!
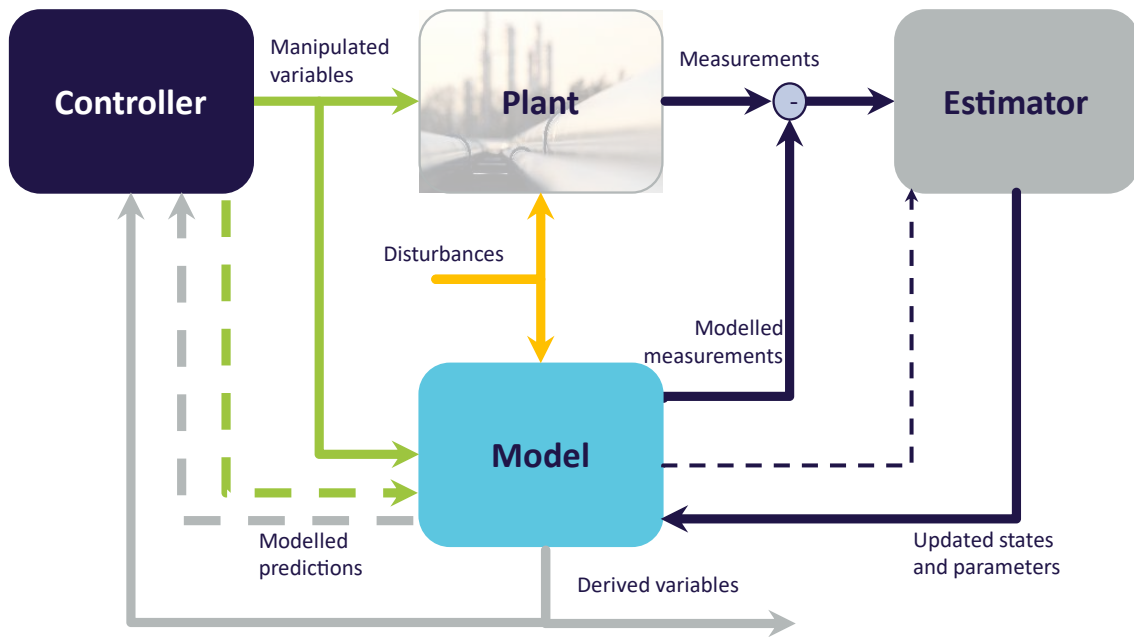
Figure 4.1 Block diagram showing the components of the Cybernetica CENIT software, and how they interact.

The controller stands on the shoulders of the estimator, metaphorically, in the sense that the controller uses the states and parameters that are calculated by the estimator. Also, the controller performance will be better if the state and parameters estimates match reality (represented by the plant measurements) well, in real time. The combination of estimation and control is sketched for a hypothetical variable of key interest, in Figure 4.2. The estimator is concerned with aligning the model with the history and the current state of the plant, while the controller performs optimal control by planning ahead.

In many cases, the quantity of interest to control is not directly measurable (such as the capture rate of CO_2, for example). For this purpose, the model (through the on-line estimator) is a useful soft-sensor to monitor plant variables.
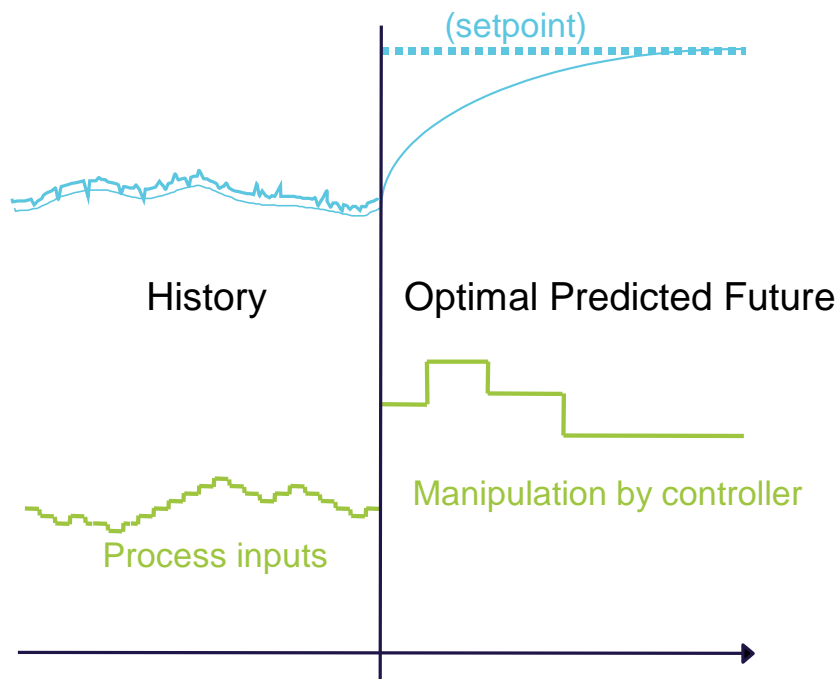
Figure 4.2 Illustration of how the CENIT NMPC controls a quantity of interest to a target value (dashed, blue line) by predicting the optimal sequence of future controller moves (green lines). Along the history, CENIT runs an estimator to ensure that the model calculations (thin, blue line) align with what the measurements (thick, blue line) suggest.

For amine-based CO_2 capture in particular, the building blocks of the model can be categorised in different modules, as illustrated in Figure 4.3. The modular approach was chosen at an early stage, to promote reuse and deployment across different capture plants where there are large similarities but certain key differences (Tiller Pilot vs. TCM, for instance). Some parts of the code base are generic, meaning that they apply for every single application of CENIT for CO_2 capture. Other parts of the application are solvent specific, dependent on a solvent library where each solvent has been implemented according to the model interface. Additionally, a separate plant-specific module is appointed to handle details that are specific to the target plant.
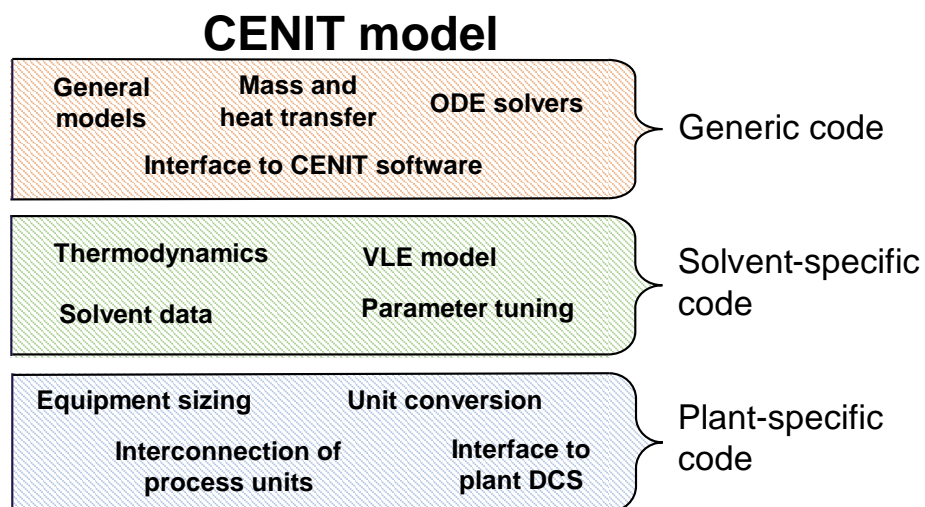
Figure 4.3 Main building blocks of the CENIT mechanistic process model.

4.2 Dynamic step response data

Dynamic step response tests were conducted at an early stage of the campaign, to validate the process models and prepare for the controller tests. Four different types of dynamic step response tests were performed, these were:

- Test A: Step in reboiler duty
- Test B: Step in liquid rate
- Test C: Step in gas flow
- Test D: Step in CO_2 concentrations

An overview of the conducted tests is given in Table 4-1. The table shows which test type was conducted and which values were stepped to and from. 5 dynamic step response tests were conducted in total, at least one of each type. Two tests of type B were conducted, one with a step up and one with a step down.

Table 4-1 Overview of dynamic step tests

Test number	Test type	From	To	Unit
1 (run #1)	B	10	9	kg/min
2 (run #2)	A	27.22	24.23	kW
3 (run #3)	C	160	180	m^3/h
4 (run #6)	B	7.3	8.7	kg/min
5 (run #11)	D	11	9	%

Problems with the solvent model, which was based on best guesses and some parameters from D1.1, were identified already before the dynamic step responses were conducted. It was quickly apparent that the reaction rate in the model was too slow, as the achieved capture rates were in the range of 5-10%. This was corrected by scaling up the reaction rate constant and using correction factors for the CO_2 transfer rates in the columns. Two measurements in particular were used to evaluate the model's performance, these were the CO_2 concentration in the gas outlet at the top of the absorber column and the flow of CO_2 from the condenser. By adjusting parameters and correction factors the model gave more accurate predictions.

Figure 4.4 shows the results from test 2, conducted on the 26th of September 2022. The first row of plots shows two important inputs to the plant, the reboiler duty and the solvent recirculation rate, these are the manipulated variables (MVs) in the NMPC. The second row shows output from the plant, both measured values and values calculated from the model. These plots show three different lines for model values. The lines labelled "Old parameters" are from the model when using the old parameters and correction factors (from before the Tiller campaign). The lines labelled "New parameters" are from the model when using the new parameters and correction factors, which were discovered during the first phases of the Tiller campaign. The lines labelled "New parameters w/ est" are from the model when using the new parameters and correction factors and with bias estimation. The new parameters make the model perform better, but some bias correction based on the measured CO_2 mass flow out of the condenser is still necessary.
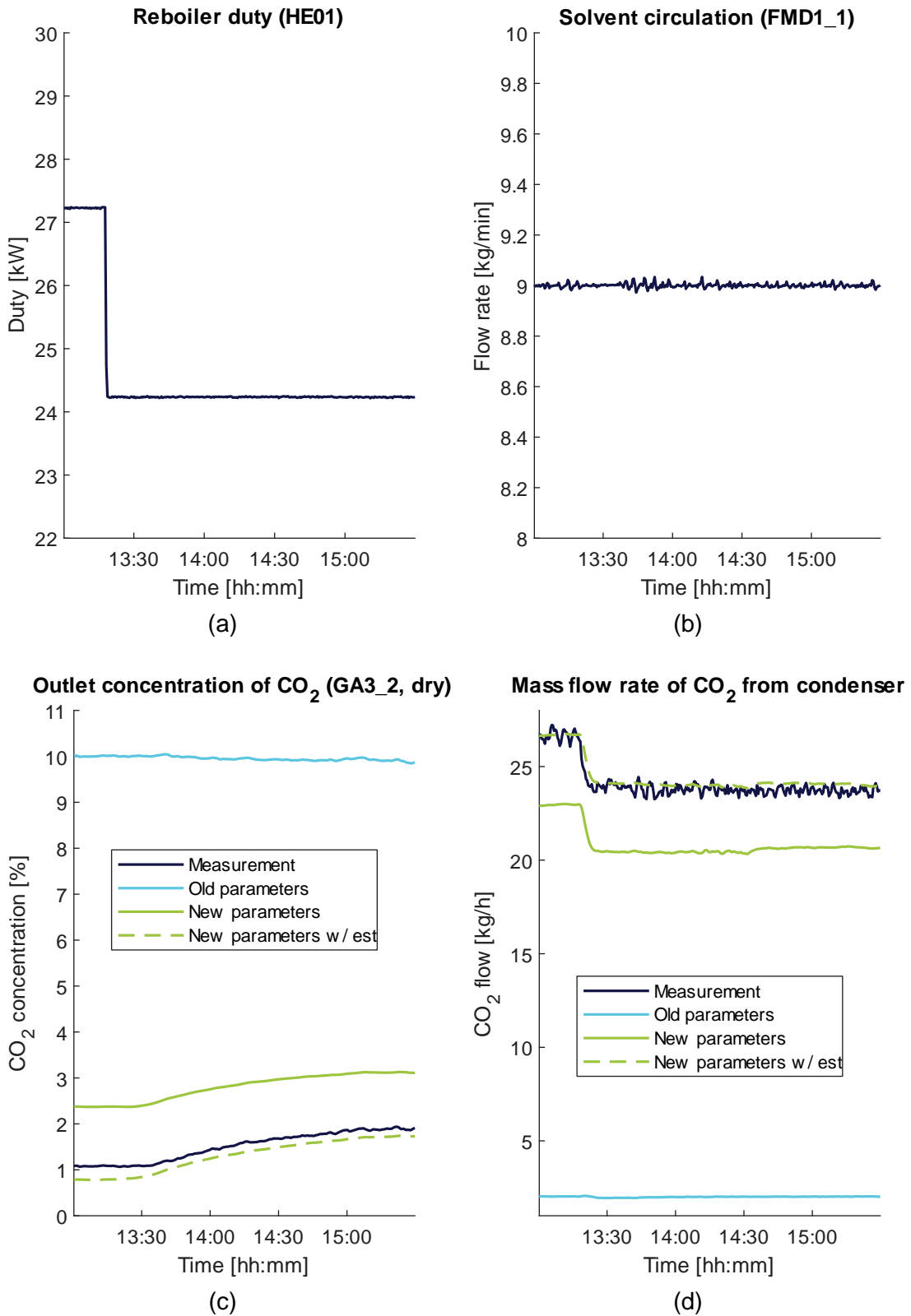
Figure 4.4 Dynamic step response test were the reboiler duty is stepped down from 27.2 kW to 24.2 kW, while the solvent circulation rate is kept constant. The first row of subfigures shows the reboiler duty (a) and the solvent circulation rate (b). The second row shows the CO_2 concentration out of the absorber top (c) and the mass flow rate of CO_2 from the condenser (d), both values from different model parameters and measurements from the Tiller plant.

The model calculations with "old parameters", i.e., from before the campaign, are included in the figures to highlight the importance of model validation with pilot data. These results will likely be revisited and elaborated in the upcoming REALISE delivery D1.3, as well.

4.3 Closed-loop CENIT tests: Setpoint changes

The CO_2 capture rate setpoint is decided by the plant operator, and the CENIT NMPC will automatically capture the prescribed rate[2] at the minimum energy usage, controlling the lean solvent flow rate and the reboiler duty. Typically, the capture rate setpoint is 90% during normal operation, but it is often desirable to capture 95% or even beyond that.

Figure 4.5 shows the first closed-loop control experiment of the campaign, which is run 41. The NMPC was activated close to 90% capture and made some adjustments to hit 90% capture while trying to reduce the specific reboiler duty (SRD), followed by an increase in capture rate setpoint from 90% to 95%. It is interesting to see how the solvent circulation rate is virtually the same for 90% and 95% capture (when comparing the "steady states"), even though it moves dynamically to match the capture rate setpoint instantaneously.

Figure 4.6 shows run 42, with a large step in capture rate setpoint from 97% (which was the approximate state of the plant the beginning of the day – CENIT was deactivated overnight) to 87%. After the large step, an investigation was made to see if CENIT had gone below the *real* optimum solvent circulation rate, by increasing the minimum allowed solvent circulation rate to force it slightly higher. Specifically, the min. constraint was changed from 3.5 kg/min to 5.3 kg/min, when CENIT resided around 5.0 kg/min. During this period, the SRD went slight down, indicating that the solvent circulation was a bit too low indeed.

---

[2] The capture ratio will be fulfilled as long as there is sufficient reboiler power available. The contrary will be explored in section 4.5.
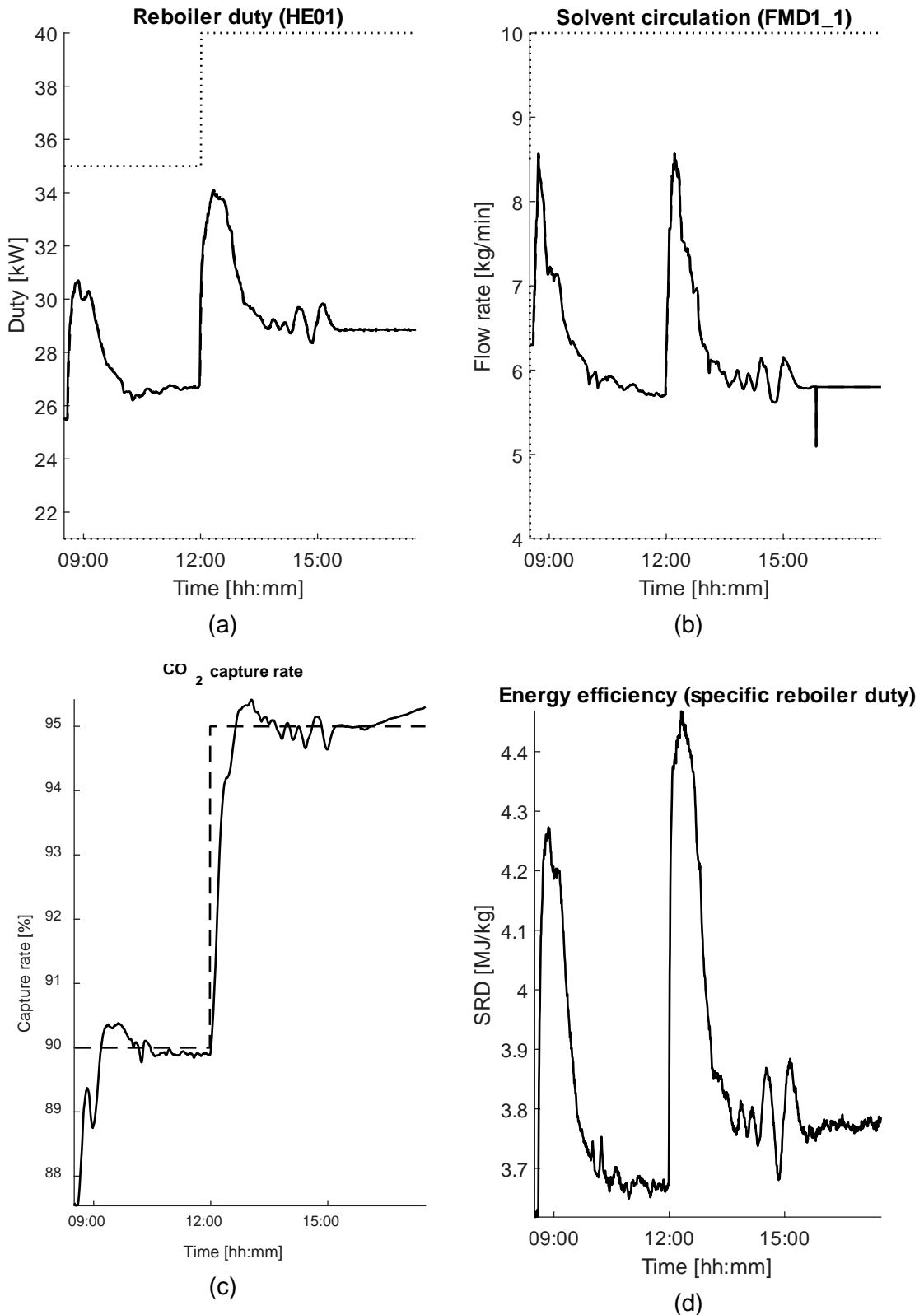
Figure 4.5 Control test (run 41) with NMPC activation close to a setpoint for CO₂ capture rate at 90%, followed by a setpoint increase from 90% to 95% capture. The subfigures show how the NMPC govern the reboiler duty (a) and the solvent circulation rate (b) to obey the capture rate setpoint (c) together with the SRD (d). Dashed lines are setpoints, while dotted lines are constraints.
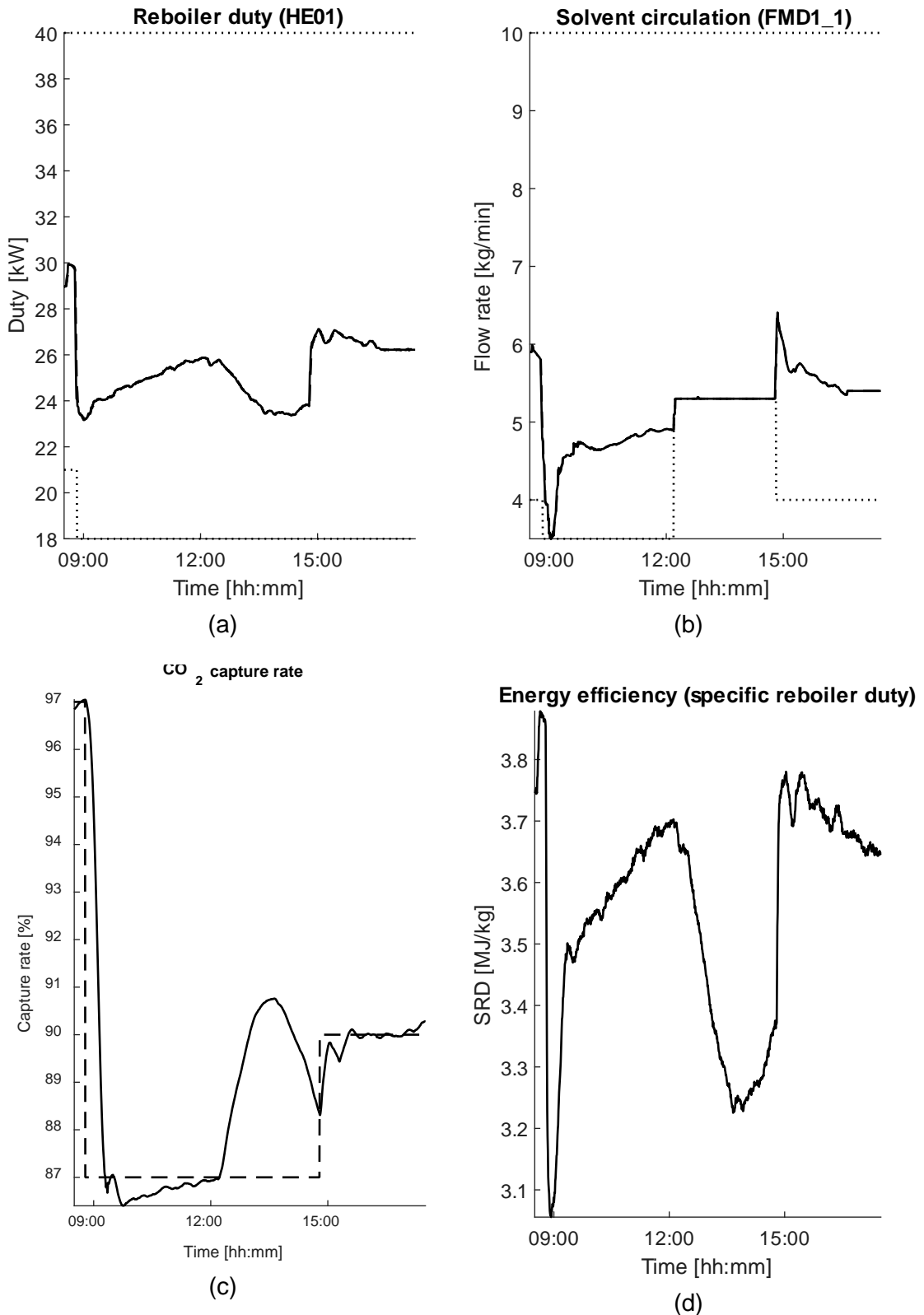
Figure 4.6 Control test (run 42) starting at 97% CO₂ capture rate setpoint, changing the setpoint from 97% to 87% capture, followed by a setpoint change from 87% to 90%. The subfigures show how the NMPC govern the reboiler duty (a) and the solvent circulation rate (b) to obey the capture rate setpoint (c) together with the SRD (d). Dashed lines are setpoints, while dotted lines are constraints.

4.4 Closed-loop CENIT tests: Disturbance rejection

A key feature of the CENIT NMPC is the ability to adapt to changes in the operating conditions. Amine-based CO_2 capture, for most solvents, has a delicately placed point of optimal operation, when trying to minimize the specific reboiler duty. Inability to reside at optimal operation means unnecessary use of energy over time. Approaching optimal operation manually by trial-and-error would typically be a time-consuming task, even with the attention of experienced plant personnel. Even for plants with seemingly steady flue gases, the help of an adaptive, optimal controller will be useful.

There are many process properties that affect the point of optimal operation, such as column pressures, liquid hold-ups, heat exchanger parameters, and solvent concentration to name a few, but this work tends to separate between internal properties of the capture plant (which are within control of the NMPC) and external properties, typically governed by an upstream process. Therefore, the experiments focus on the flue gas as the main process disturbance and show how the NMPC adapts to *significant* changes in the flue gas to the capture plant.

4.4.1 Unpredictable flue gas disturbances

The flue gas can change unexpectedly for a variety of reasons, typically originating from events in the upstream process. In those cases, the NMPC will still try to capture the prescribed *rate* of CO_2 from the flue gas, at the minimal use of energy.

In one experiment, specifically run 46, the flue gas flow rate was unexpectedly increased from 160 m^3/h to 195 m^3/h, while the CO_2 concentration of the flue gas increased from 11% to 14%, which constitutes a large increase in the CO_2 flow into the absorber column. After approximately 2 hours, the flue gas conditions went back to 160 m^3/h and 11% CO_2. The results are shown in Figure 4.7. It is observed that the NMPC is able to detect changing flue gas conditions and efficiently counteract them, by controlling the lean solvent circulation and reboiler duty, to maintain the desired capture rate.

In another set of experiments, the flue gas CO_2 concentration was kept constant while the flue gas flow rate was ramped from 160 m^3/h up to 195 m^3/h and then back to 160 m^3/h, eventually. These changes were made during run 43. The ramp rates were chosen to both constitute large (approximately 20% change), sudden disturbances, while at the same time giving long ramps where predictive knowledge about the ramps could prove useful (to be assessed in section 4.5, for run 44). During flue gas ramp-up, the ramp rate was 3.2 m^3/h/min, while the ramp rate was -4.8 m^3/h/min during flue gas ramp-down. That implies ramp durations of approximately 11 mins and 7 minutes, respectively.

The results from these tests are shown in Figure 4.8, where the NMPC was able to go through the ramps of run 43 without deviating significant from the capture rate setpoint. These tests will also constitute the basis for comparison with the tests in the next section, where the potential of enhanced predictions will be explored.
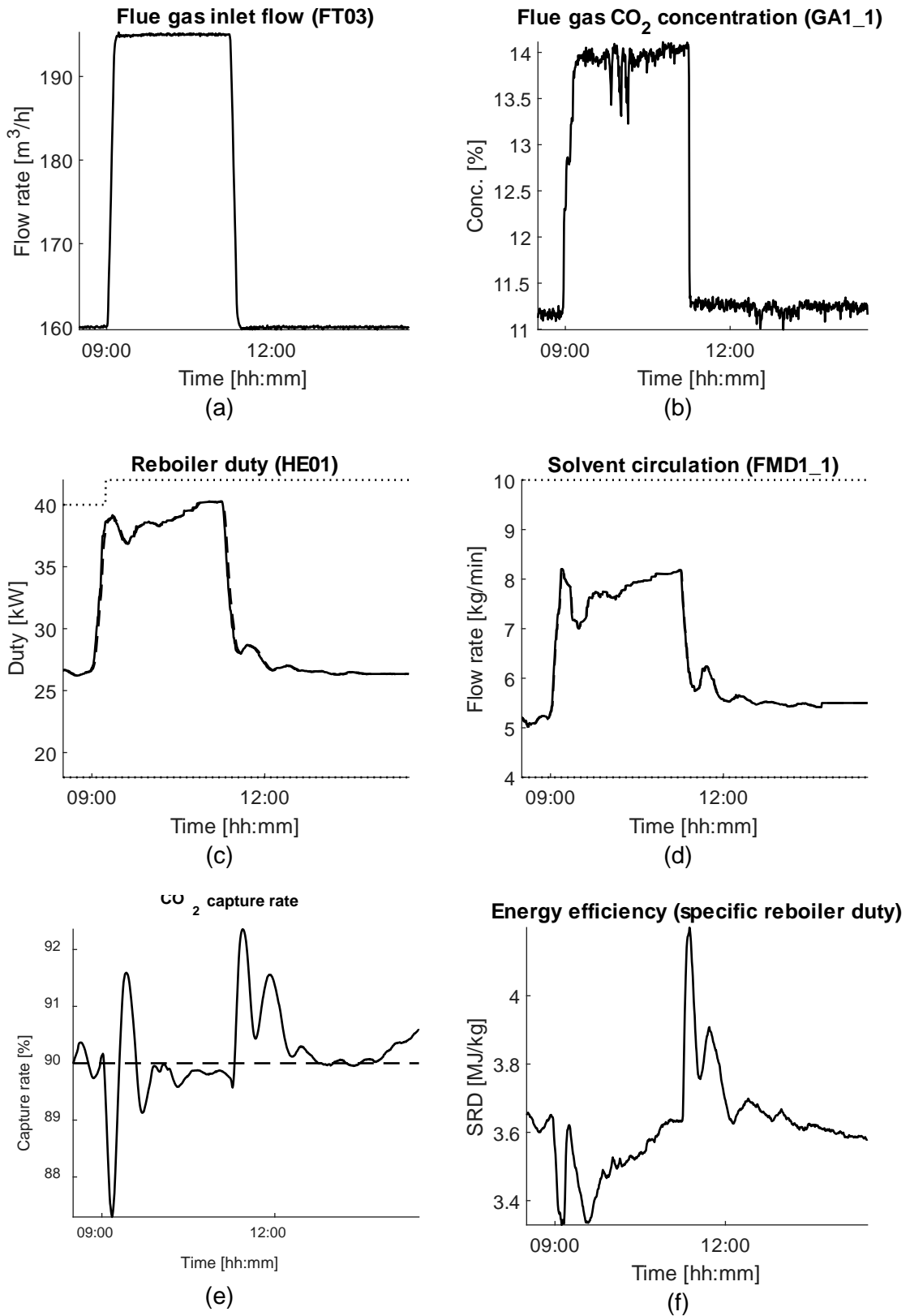
Figure 4.7 Control test (run 46) with combined disturbance in both flue gas flow rate and CO2 concentration. The subfigures show the flue gas flow rate (a) and the flue gas CO2 concentration (b), together with how the NMPC govern the reboiler duty (c) and the solvent circulation rate (d) to obey the capture rate setpoint (e) and minimize the SRD (f). Dashed lines are setpoints, while dotted lines are constraints.
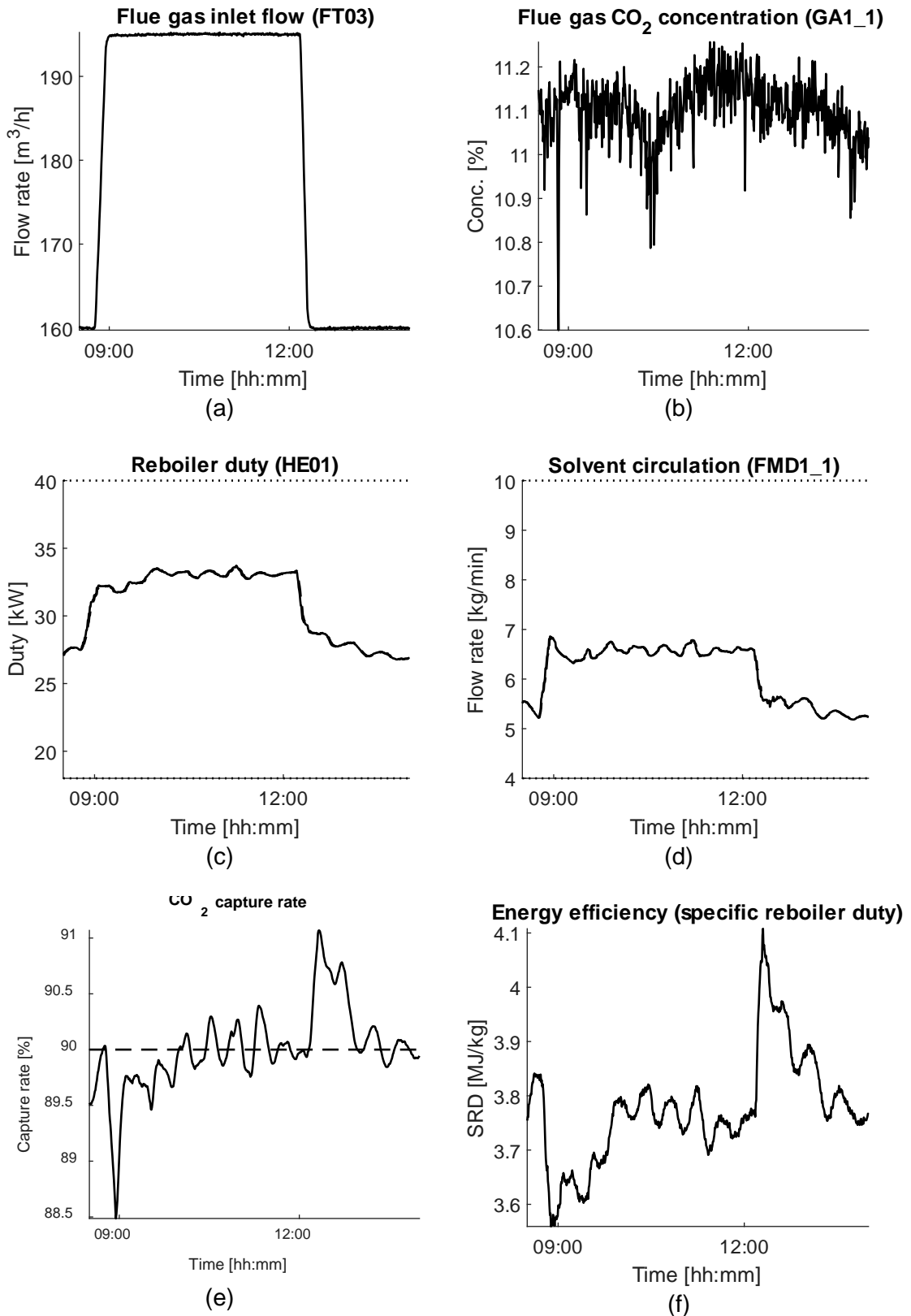
Figure 4.8 Control test (run 43) with changing inlet flow rate of flue gas. The subfigures show the flue gas flow rate (a) and the flue gas CO2 concentration (b), together with how the NMPC govern the reboiler duty (c) and the solvent circulation rate (d) to obey the capture rate setpoint (e) and minimize the SRD (f). Dashed lines are setpoints, while dotted lines are constraints.

4.4.2   Predictable flue gas changes

If the plant personnel, typically the operator, holds information about an upcoming change in the flue gas due to events in an upstream process, it is expected that the NMPC will benefit from knowing this information to improve the predictions. Ideally, such information would automatically be forwarded to the NMPC.

In these experiments, during run 44, the plant deploys ramps in the flue gas flow rate. Typically, this would simulate a power plant that needs to increase or decrease production to satisfy some grid controller, but it applies to a wide variety of scenarios and upstream processes. The idea is sketched in Figure 4.9, where the difference is shown between "the default way" to predict the flue gas inlet flow and "the advanced, knowledgeable way", for a scheduled, ongoing ramp-up[3]. Essentially, it means using a feedforward strategy for flue gas flow. The effect of this feature becomes more evident if the ramps are large (i.e., large absolute change) and long (i.e., relatively low ramp rate). Conversely, this feature does not make a difference during step changes, for instance.
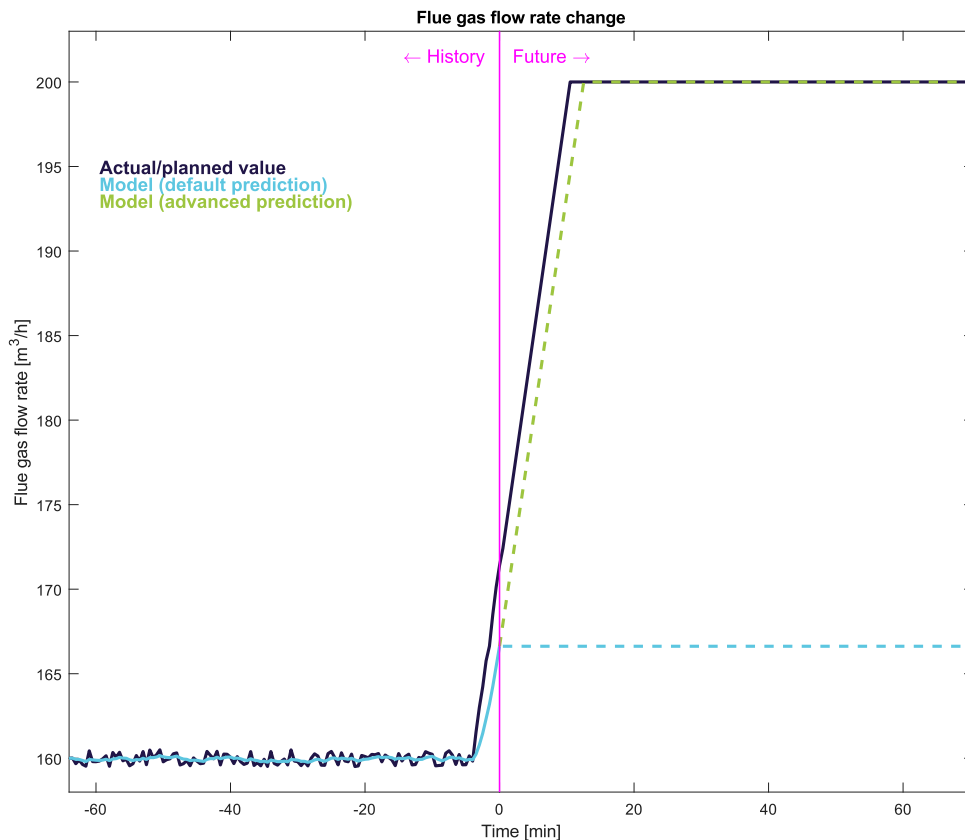

Figure 4.9 Conceptual sketch with comparison between default prediction ("feedback") of flue gas flow rate, in light blue, versus advanced prediction ("feedforward") in green and the actual ramp-up in black.

---

[3] It is also shown that the model has a filter on the measured input, to level out measurement noise. This is balanced so that the model tracks the process carefully without taking in too much noise.
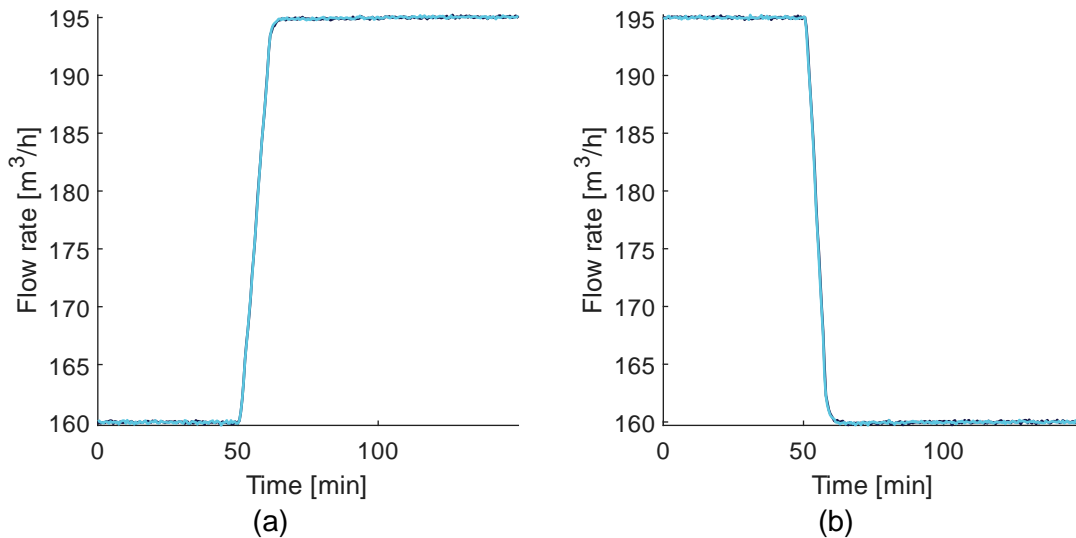
Figure 4.10 Logged data showing flue gas ramps for 4 different experiments (two in each subfigure, which are similar in nature and virtually coincide) from run 43 and run 44, back and forth between 160 m³/h and 195 m³/h. Subfigure (a) shows two identical ramp-ups while subfigure (b) shows two identical ramp-downs of flue gas inlet flow. Two similar ramps were conducted in each direction to demonstrate how additional knowledge in the predictions can aid the controller. These are four separate experiments in time, which are compared with each other, two-by-two, due to their similarity.

The resulting control of the CO_2 capture rate (with a setpoint at 90%), for the flue gas ramps shown in Figure 4.10, is shown in Figure 4.11. The ramps were the same as described in section 4.4.1 for run 43. These investigations involve four separate experiments, with two ramp-ups and two ramp-downs that are compared against each other, respectively.

The deviation from capture rate setpoint is less when the ramping is in the prediction, which was the case during run 44, as expected. These results tend to indicate that if upcoming changes in the flue gas are scheduled, or at least if they are predictable, the NMPC will benefit from knowing about them, as this gives slightly tighter control than in the default strategy, as discussed in the previous subsection.

It is emphasized that the default solution, with no heads-up about the upcoming flue gas change, is considered to give a tight and efficient disturbance rejection in these tests, as well. These are the tests that were presented in Figure 4.8, for run 43.

CO₂ capture rate (a)
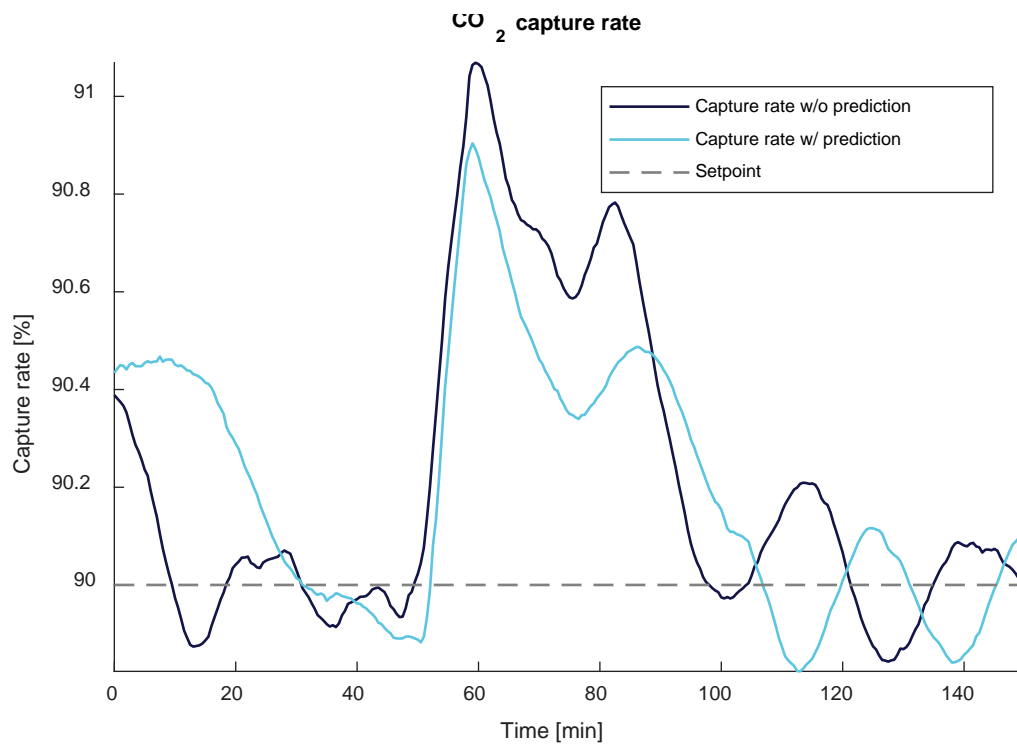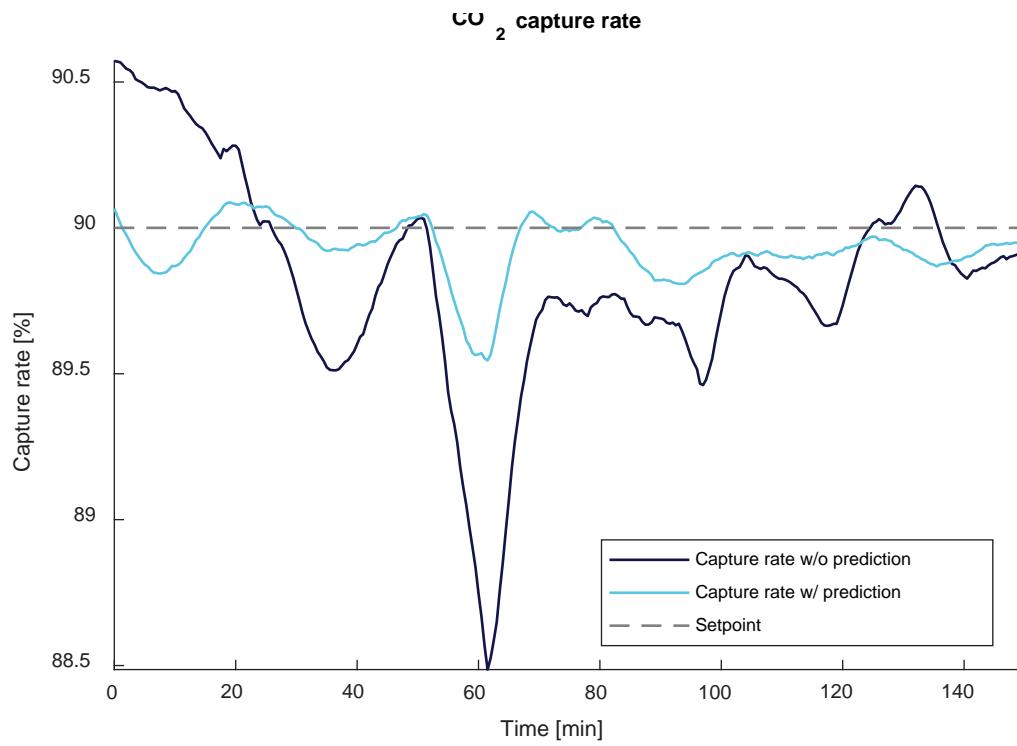

CO₂ capture rate (b)

Figure 4.11 CO₂ capture rate control during significant flue gas flow changes, as indicated in Figure 4.10, with and without extra predictive capabilities in the NMPC, as tested in run 43 and run 44, respectively. Subfigure (a) shows the ramp-ups while subfigure (b) shows the ramp-downs of flue gas inlet flow. The experiments were conducted on separate occasions but compared against each other.

4.4.3 Load following

The final experiment category for disturbance rejection, for the flue gas conditions, is a so-called load following scenario, with significant changes in flue gas inlet flow and flue gas CO_2 concentration. The purpose of the experiment is to place large variations on the inlet flue gas of the capture plant and push the plant towards the operational limits and verify that the NMPC is able to keep up and fulfil the control goals, as before.

The results from the load following controller test (run 48) are shown in Figure 4.12.

The overall conclusion is that the NMPC can detect and effectively counteract *large* variations in the flue gas, like in a typical load following scenario. The demonstration tends to indicate that the capture plant can follow "dramatic" changes in the upstream process, which is an important indicator for the capture plants flexibility. It means that if the capture plant is retrofitted to an existing point-source emitter, the existing process must not alter its operation to accommodate the capture plant.

An alternative strategy, to spare the capture plant from some of the flexing, would be to exhaust a portion of the flue gas directly, in a by-pass fashion, without sending it through the absorber column. This is expected to be a simpler solution if the flue gas is very rapidly changing all the time, but it would imply load *ignoring* rather than load *following*, obviously, which is below the point of this experiment, and the capture rate would be significantly lower, potentially. Additionally, it would mainly be effective for exceptionally large flue gas flows, whereas it would not help much if the total flue gas flow was very low. It is only mentioned here because the control of the by-pass split fraction would pose an interesting control problem, possibly to be handled by an NMPC.
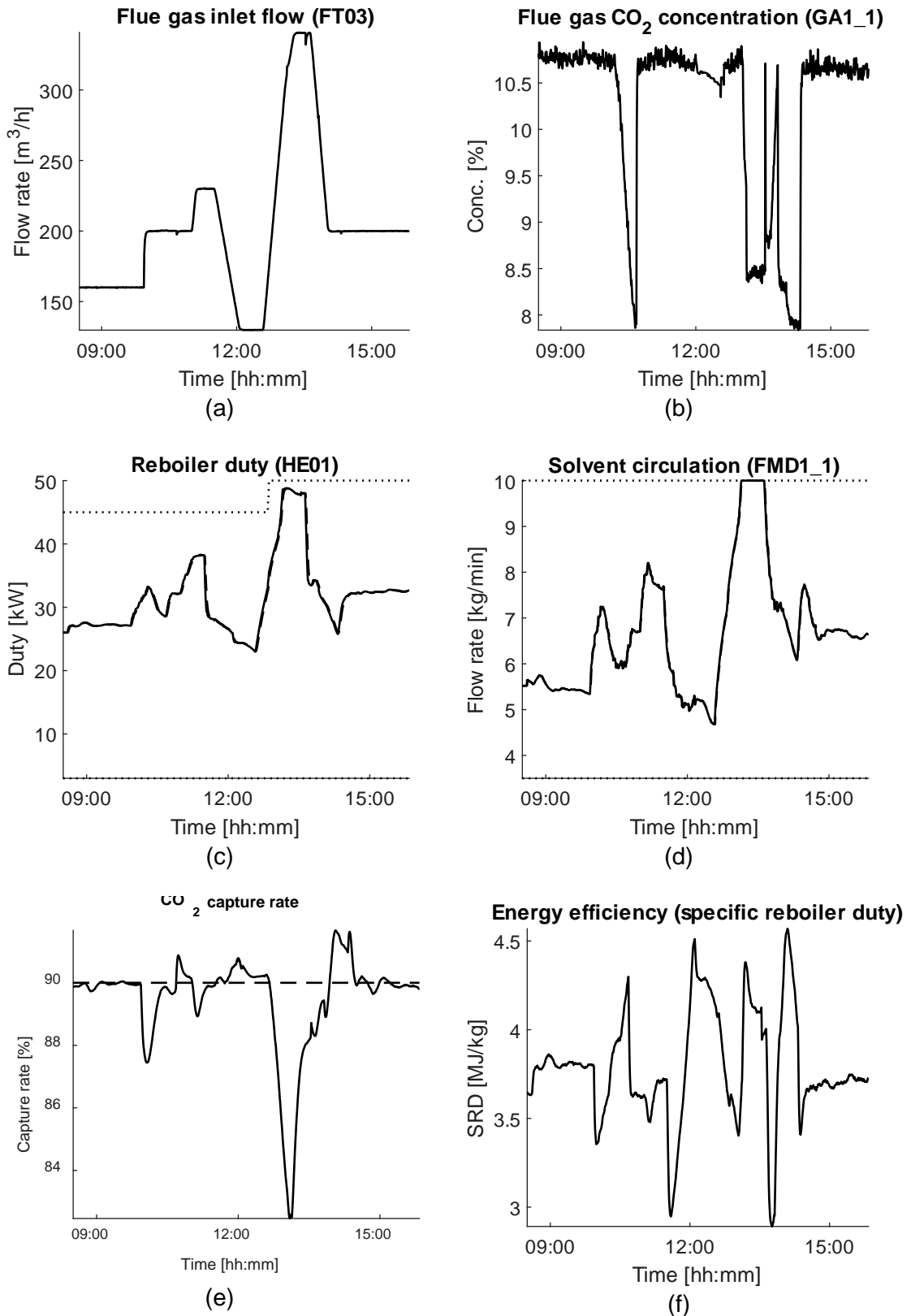
Figure 4.12 Control test (run 48) with load following scenario, where the flue gas conditions are changed significantly towards the boundaries of the plant. The subfigures show the flue gas flow rate (a) and the flue gas CO2 concentration (b), together with how the NMPC govern the reboiler duty (c) and the solvent circulation rate (d) to obey the capture rate setpoint (e) and minimize the SRD (f). Dashed lines are setpoints, while dotted lines are constraints.

4.5 Closed-loop CENIT tests: Steam limitations

The CENIT NMPC will strive to capture the prescribed amount of CO_2, *at minimum energy usage*. In some cases, however, the energy availability is lower than what CENIT would require to maintain a sufficient capture rate. This could be due to external events, for instance changes in an upstream process, or due to limitations set by plant operators. A motivation for deploying NMPC is to efficiently work around such scenarios in the optimal way.

In this section, a demonstration is made to show how the NMPC behaves when the reboiler duty is limited. The tests explore both using moderate constraints that can persist over time (section 4.5.1), and more dramatic limitations for a shorter time (so-called reboiler stops, section 4.5.2). In any case, it is necessary to design the NMPC such that it behaves in a *sustainable* way when energy is not abundant.

At the Tiller pilot plant, the reboiler uses electrical power, but the analogy to steam usage is made on several occasions, as this is more usual in larger scale. The NMPC (i.e., the optimisation criterion) is flexible and indifferent[4] to the *source* of the reboiler power.

4.5.1 Steam availability limitations

Steam limitations could occur in power plants where the need to satisfy the grids demand for electrical power is rising rapidly. It could occur in waste-to-energy combustion plants when the district heating service has peak demand. It could happen in any capture plant using excess heat from a neighbouring or upstream process to power the reboiler. It could happen if (parts of) the steam system is down for maintenance, and the list goes on. In any case, it means that the carbon capture plant has its priority reduced (at least instantaneously, during certain periods) and has to adapt to that.

At first glance, it could seem intuitive for a controller to increase solvent circulation in the event of a steam limitation, to obey the capture rate setpoint. This is only a temporary solution, however, amplifying the problems down the line, and some conventional control structures fall into this trap, indeed. A better response, rather than to obey the capture rate setpoint "at all costs", would be to disregard the capture rate setpoint (to some extent) and focus on maintaining the appropriate lean solvent loading throughout the period of steam limitation.

An experiment with steam availability limitations is shown in Figure 4.13, where the plant operates close to 90% capture with a reboiler duty around 27 kW when the max. available power drops to 24 kW, and then to 20 kW. It shows that the NMPC immediately disregards the capture rate setpoint, indeed, by *reducing* the solvent circulation when reboiler power is lacking. This is thanks to the predictive capabilities of the NMPC, as it can foresee how damaging the lack of reboiler duty is for the lean loading, over time.

---

[4] The optimisation is handled by the generic parts of the CENIT software, using the common parts of the Model and Application Component, while the intricate details of the reboiler are handled by the plant specific parts, as indicated in Figure 4.3.
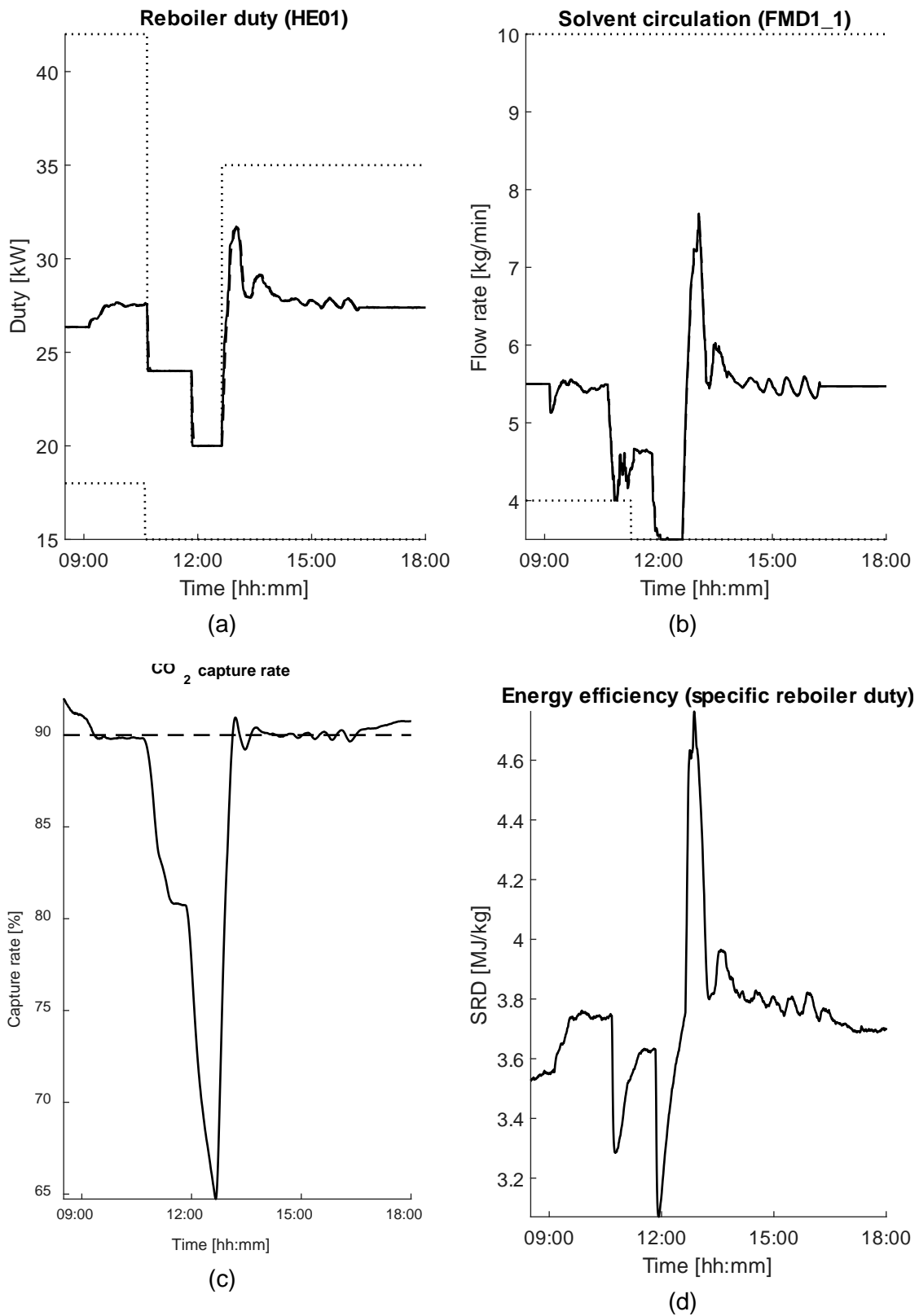
Figure 4.13 Control test (run 46) with reboiler constraints, with 90% capture ration setpoint. The reboiler energy availability is limited in two separate steps. The subfigures show how the NMPC govern the reboiler duty (a) and the solvent circulation rate (b) to obey the capture rate setpoint (c) together with the SRD (d). Dashed lines are setpoints, while dotted lines are constraints.

4.5.2 Grid stabilization with reboiler shut-downs

A more drastic type of reboiler limitation is the scenario where the demand for power delivery on the grid[5] is so large that the CO_2 capture plant must reduce its energy consumption significantly, for a brief period, to prioritize grid stabilization. This scenario was inspired by Haines and Davidson [9], who introduced the term "stripper stop". In practice, it means reducing the reboiler duty by 75%, typically for 1-2 minutes. After the stop, the reboiler regains steam availability gradually, leading to a ramp-up of reboiler duty before the plant is back at normal operation again. The available reboiler duty is restored by 0.8 kW/min, meaning that if the reboiler stop is initiated at a nominal reboiler duty of 25-30 kW, the restoration time of the reboiler duty would be in the range of half an hour. It would be premature to claim that the *system* is *restored* at this point, though, as the build-up of lean loading can be problematic. During the ramp-up of reboiler duty, the flue gas inlet flow to the capture plant also increases, due to increased delivery from the power plant, further complicating the restoration of lean loading. A flashback of this scenario from a different project (ALIGN-CCUS H2020[6]) is shown for the reboiler duty, and the accompanying solvent circulation, in Figure 4.14. The latter shows how the solvent circulation stays at a higher value after each consecutive reboiler event, eventually escalating out of control.
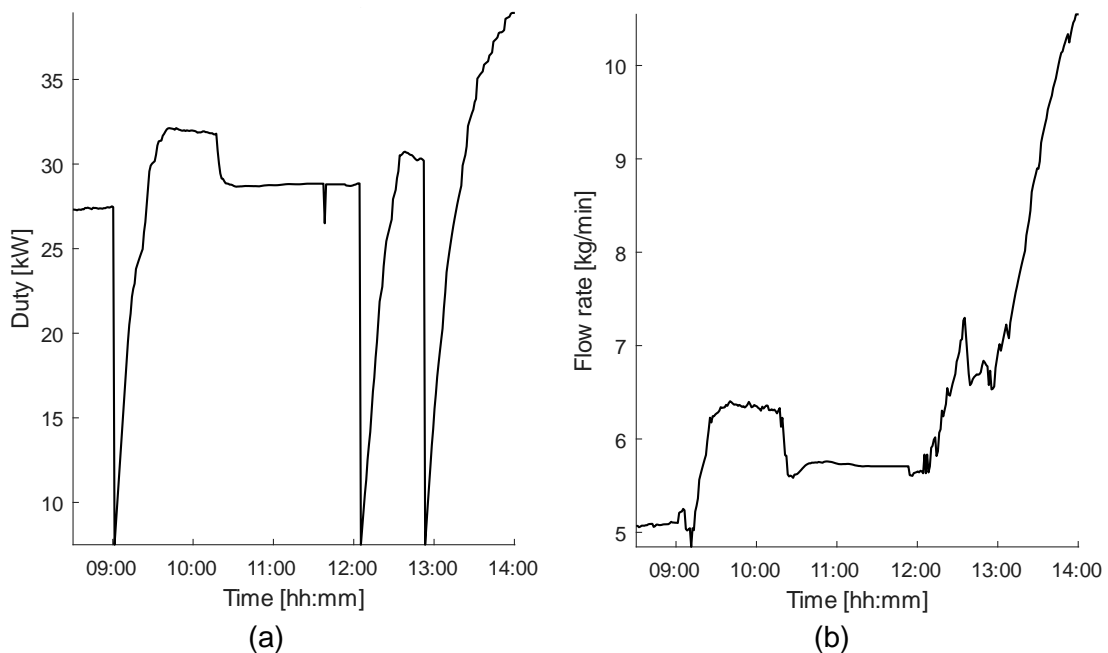

(a)   (b)

Figure 4.14 Flashback to an earlier project (ALIGN-CCUS H2020 [7]), where subsequent reboiler stops caused problems with escalating lean loading.

It is emphasized that the flue gas was unchanged throughout this experiment, but the plant drifted away from the point of steady operation where it started. The underlying

---

[5] This case study is mainly intended for power plants, operating according to the demands of grid controllers, but it also applies for processes where the reboiler is powered by excess heat with very limited supply during events in the upstream process.

[6] The ALIGN-CCUS test campaign was conducted in 2019, using the CESAR-1 solvent. Several other closed-loop control tests with Cybernetica CENIT were made during the project, as well.

reason for this was that the lean solvent loading grew after each reboiler stop, and that the NMPC *was* unable[7] to completely recover from this state before the next reboiler stop occurred.

Efforts were made to conduct a similar experiment during the REALISE campaign, where three consecutive reboiler stops would be forced upon the capture facility, to observe the response of the NMPC, with improved performance. Building on experience from ALIGN-CCUS, it was suggested to include lean loading in the NMPC criterion *explicitly* for a better and more direct control of this property, since escalating lean loading was concluded to be the root cause of the problematic operation (shown in Figure 4.14).

The results from the tests, which were made during run 47, are shown in Figure 4.15.

Compared to controlling the capture rate alone (while minimizing energy usage), the controller becomes more robust to events such as reboiler stops if the lean solvent loading is part of the optimization. Lean loading control also proves to be a useful feature during less severe reboiler limitations. The importance of controlling lean loading is further elaborated in section 4.6.

For the REALISE campaign, several consecutive reboiler stops were conducted without escalation of the lean loading and the associated process parameters. A temporary increase in lean loading in the wake of a reboiler stop will be inevitable (as observed in Figure 4.15d), but the amplitude can be limited through efficient control, and the recovery back to normal operation must be as rapid and efficient as possible. In conclusion, this demonstrates an improvement from ALIGN-CCUS.

---

[7] During ALIGN-CCUS, this behavior was by design, and this was a motivation for redoing the experiments in REALISE, aiming for improvement.
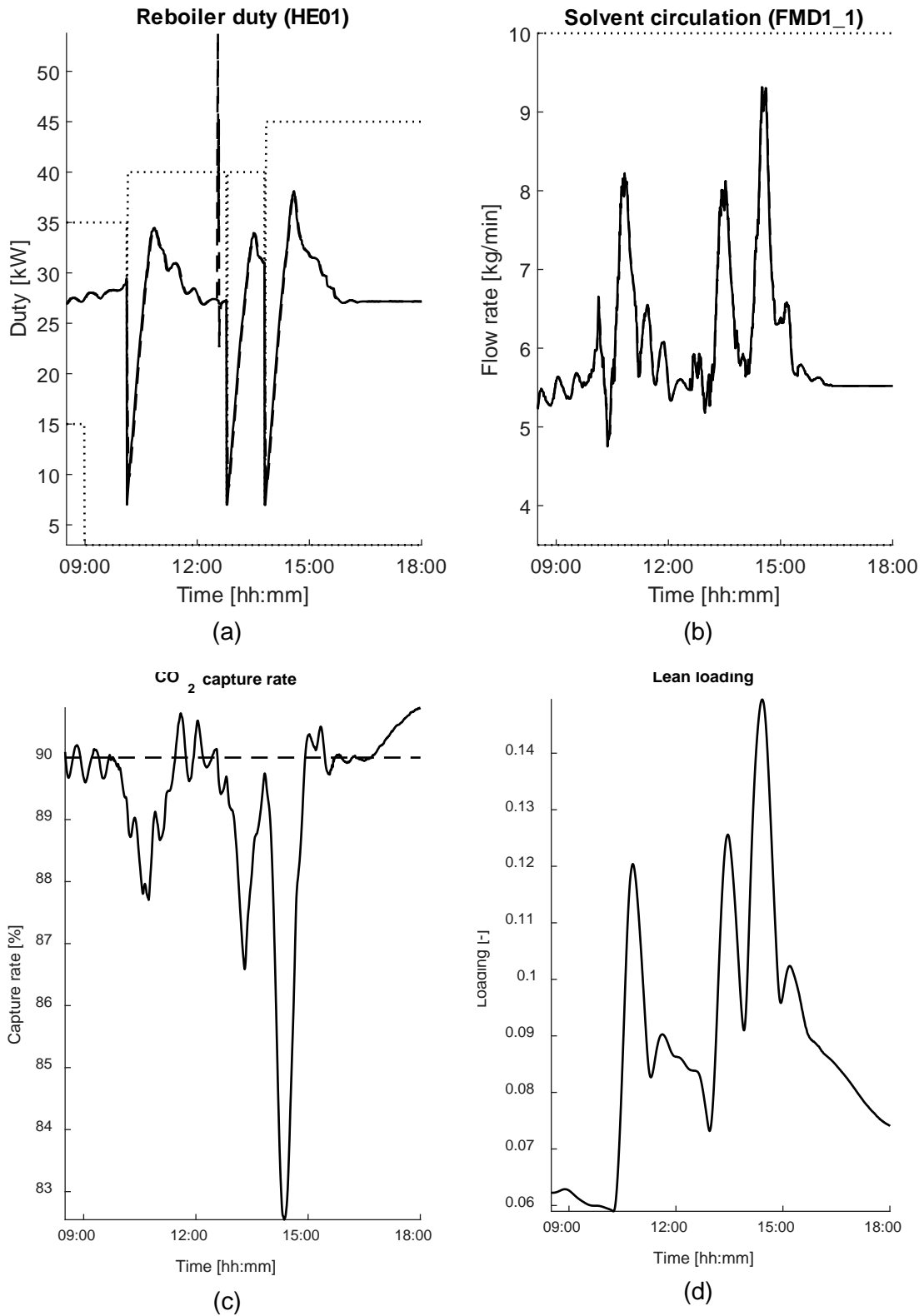
(a)

(b)

(c)

(d)

Figure 4.15 Control test (run 47) with three consecutive reboiler stop events, where the reboiler duty is limited and then ramped back up. The subfigures show how the NMPC govern the reboiler duty (a) and the solvent circulation rate (b) to obey the capture rate setpoint (c) while preventing the lean loading (d) from escalating completely.

4.6 Solvent loading during closed-loop NMPC campaign

Figure 4.16 shows the solvent loading (i.e., the concentration of CO_2), for both lean and rich solvent, throughout the part of the campaign with closed-loop NMPC testing. The black lines are calculated using an empirical correlation made from experimental data (see section 6.3), using grab samples for lab analysis (shown by red markers), while the light blue lines are the CENIT model estimates for loading during the campaign. In some cases, there are dynamic mismatches or even steady-state deviations, but the general impression is that they match reasonably well.

It is observed that after introduction of CENIT NMPC in the campaign, the lean loading decreases significantly, indicating that the *optimal* lean loading could be slightly lower than what it was during earlier parts of the campaign.

Throughout the closed-loop testing period, the lean loading has been controlled around 0.2 mol/kg, even if lean loading is not an explicitly controlled variable of the optimization criterion, but rather an implicit variable to achieve the control objectives. As described in section 4.5.2, experiments were made where the lean loading was directly constrained in the optimization criterion to prevent it from escalating in scenarios where the steam availability is limited, and the results from these experiments were promising.

A potential improvement to the optimal controller is to extend the online estimator, as introduced in section 4.1 and shown in Figure 4.1, to deploy solvent measurements and column measurements more closely, to match the lean loading of the model with the measured lean loading. At this point it must be emphasized, in defence of the NMPC, that the empirical correlation for CO_2 loading (shown in Figure 4.16) was fitted in retrospect after the campaign, and the results from the grab samples are unavailable to the automatic control system in real time.

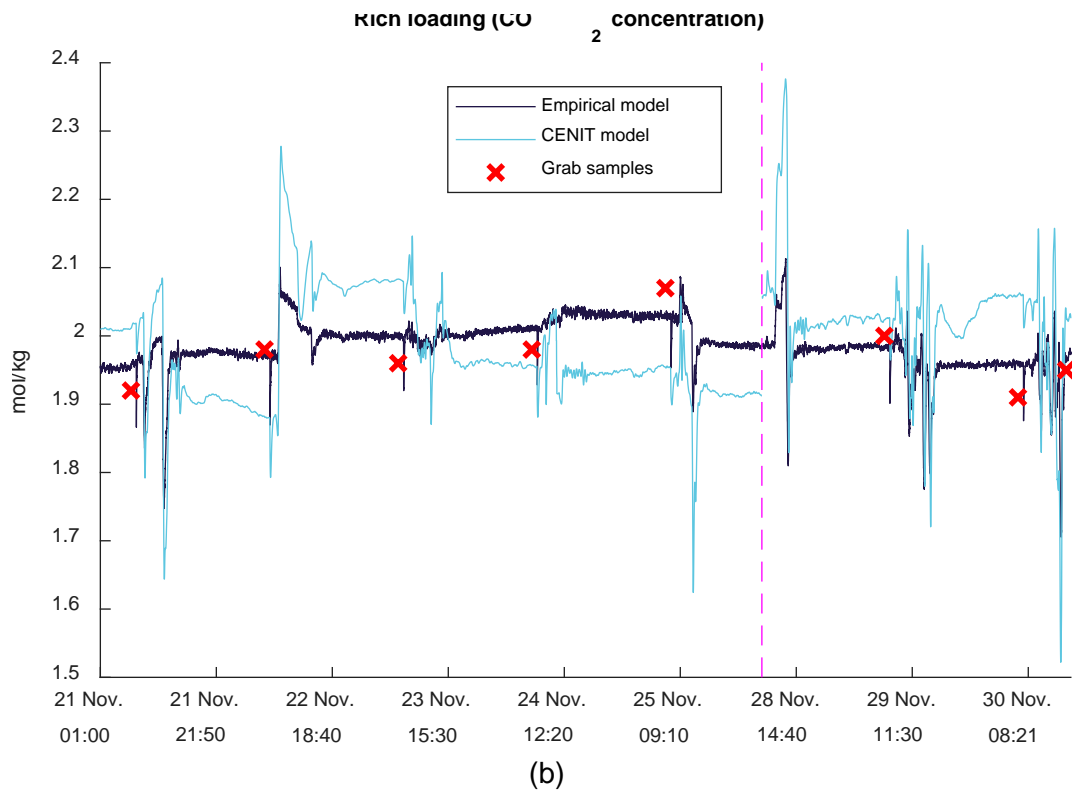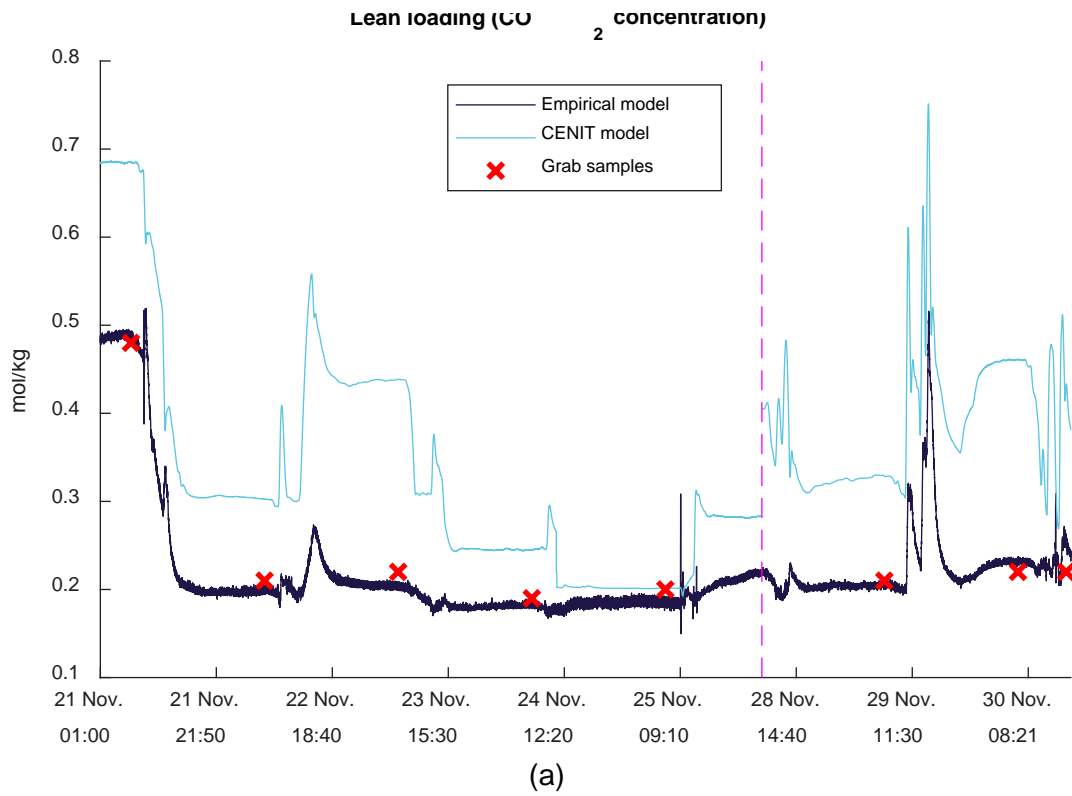*Figure 4.16 CO₂ loading throughout the period of closed-loop control with NMPC. The pink, vertical line indicates a gap in time, where the CENIT application (and the plant DCS) was offline. Subfigure (a) shows lean solvent loading while subfigure (b) shows the rich loading, comparing the CENIT model with and empirical data-driven model and the grab samples (to which the empirical model was fitted).*

5 Solvent analysis and degradation

5.1 Analysis methods

The main technique for analysing solvent and degradation compounds in liquid samples was Liquid Chromatography with a Triple Quadrupole Mass Spectrometry detector (LC-MSMS). Using these techniques quantification is based on fulfilment of four criteria:

- chromatographic separation with specific retention time (of certified reference material)

- molecular-ion formation related to molecular weight (e.g. M-H+, M-NH4+)

- specific fragment-ion formation (collision-induced dissociation in collision cell at a specific set of voltages)

- ratio between formed fragments

Totally methodology for 42 components were developed or modified for the HS-3 solvent, and the compounds were combined into seven methods. For several of the compounds an internal isotope-labelled standard was used, which yields improved precision. Some more details of the instrumental setting for these seven methods are given in Table 5-1. An even more detailed description is given in the paper by Vevelstad et. al [10] as well as in Realise deliverable D1.1, *Solvent optimization*.

Table 5-1 Ion source, chromatographic column, mobile phase used in the different LC-MS methods. Also indicated if and which derivatization was used for the methods.

Component	Ion source	Column	Mobile phase	Derivatization
Amine	APCI	Ascentis® Express Phenyl-Hexyl, 2.7 µm HPLC column	0.1% trifluoroacetic acid (A), methanol (B), gradient	No
Degradation mix	ESI	Discovery® HS F5 HPLC column	0.1% formic acid (A), methanol (B), gradient	No
Ammonia & alkylamine	ESI	Ascentis Express C18 column	0.1% formic acid (A), acetonitrile (B), gradient	Dansyl chloride
Aldehyde & acetone	ESI	Ascentis Express C8 column	0.1% ammonium acetate (A), acetonitrile (B), isocratic	Dinitrophenylhydrazine (DNPH)
Organic acids	ESI	Waters aquity HSS-T3 (15x2.1mm)	0.05% acetic acid (A), acetonitrile (B), gradient	3-nitrophenylhydrazine (3-NPH)
Nitrosamine	APCI	Ascentis® Express Phenyl-Hexyl, 2.7 µm HPLC column	0.1% formic acid (A), acetonitrile (B), gradient	No
Nitramine	ESI	Agilent Eclipse plus C18 RRHD 1.8um (2.1x50mm)	0.1% ammonium acetate (A), isocratic	No

In addition to the LC-MS analysis some more generic/standard methods were used. Total amine concentration (alkalinity) was determined by acid/base titration (0.1 M H_2SO_4), CO_2 was determined with a total inorganic carbon/total organic carbon (TIC/TOC) analyzer, H_2O with Karl Fischer titration and total nitrogen by oxidative catalytic combustion and chemiluminescence detection (Shimadzu TOC-L CPH TNM-L). Total heat-stable salts (HSS) were measured using a wet chemistry method based on ion exchange followed by titration with NaOH, and elements/metals by inductively coupled plasma mass spectrometry (ICP-MS).

An overview over the specific degradation compounds with name and abbreviation used in this chapter is given in Table 5-2.

Table 5-2 Name, CAS and Abbreviation for degradation products used in this report as well as which analytical instrument used for the analysis

Functional group	CAS	Name	Abb	Analytical instrument
Ammonia	7664-41-7	Ammonia	NH$_3$	LC-MS (derivatization)
Alkylamine	74-89-5	Methylamine	MA	
	75-04-7	Ethylamine	EA	
	107-10-8	Propylamine	Propyl-amine	
	124-40-3	Dimethylamine	DMA	
	624-78-2	Ethylmethylamine	Ethylmethyl-amine	
	109-89-7	Diethylamine	DiEA	
	142-84-7	Dipropylamine	Dipropyl-amine	
Aldehyde	50-00-0	Formaldehyde	Formaldehyde	LC-MS (derivatization)
	75-07-0	Acetaldehyde	Acetaldehyde	
Ketone	67-64-1	Acetone	Acetone	
	930-55-2	1-nitroso-pyrrolidine	NPYR	
	70415-59-7	3-(methylnitrosoamino)-1-Propanol	Nitroso-N-Methyl-AP	
Acid	79-14-1	Glycolic Acid	GA	LC-MS (derivatization)
	64-19-7	Acetic Acid	AA	
	79-09-4	Propionic Acid	PA	
	79-31-2	Isobutyric Acid	iBA	
	107-92-6	N-Butyric Acid	BA	
	50-21-5	Lactic Acid	LA	
	298-12-4	Glyoxylic Acid	GlyA	
Amine (secondary)	42055-15-2	3-(methylamino)-1-Propanol	Methyl-AP	LC-MS
	40226-15-1	3-[(3-aminopropyl)amino]-1-Propanol	APAP	
Amide	49807-74-1	N-(3-hydroxypropyl)-Formamide	HPF	
Urea	71466-11-0	N,N'-bis(3-hydroxypropyl)-urea	AP-urea	
Ring structure	5259-97-2	tetrahydro-2H-1,3-Oxazin-2-one/1,3-oxazinan-2-one	OZN	
	123-75-1	Pyrrolidine	Pyrrolidine	
	670227-88-0	tetrahydro-1-(3-hydroxypropyl)-2(1H)-Pyrimidinone	tHHPP	
Aminoacid	55937-35-4	N-(3-hydroxypropyl)-β-Alanine	HPAla	

5.2 Solvent amines

In this campaign total amine by acid/base titration as well as CO$_2$ by TIC/TOC Analyzer were determined for all lean and rich samples. The results are given in Appendix A. Among the lean samples there were selected 9 samples that were analysed in more depth. The selected samples are listed in Table 5-3, where also the results for the solvent amines, water, CO$_2$ and total nitrogen are given.

Table 5-3 Selected lean samples (VSL1) for a wider range of anakysis. Results for solvent amines, total amine, total nitrogen, CO₂ and water.

Journal no	Sample name	RUN No	TOS Hrs	Titration Alkalinity [mol/kg]	TIC/TOC-analyzator CO₂ [mol CO₂/kg]	Karl Fischer H₂O [wt%]	Shimadzu Total N [mg/kg]	LC-MS 1-(2HE)PRLD [g/kg]	3A1P (AP) [g/kg]
P22892	Start solvent unload 22/9-22 10:15		0	5.080		49.3	69 184	368	136
P22834	VSL1 24/9-22 12:55	1	49	5.318	0.807	43.3	76 964	385	145
P22905	VSL1 10/10-22 06:55	13	420	5.391	0.309	42.8	74 716	383	145
P221026	VSL 1 25/10-22 07:10	24	775	5.273	0.254	43.4	76 250	373	138
P221045	VSL1 2/11-22 07:05	27	900	5.282	0.324	43.1	76 697	373	136
P221063	VSL1 10/11-22 07:05	33	1092	5.001	0.497	44.4	71 728	344	126
P221365	VSL1 21/11-22 07:05	41	1356	5.472	0.491	39.9	74 106	369	132
P221444	VSL1 28/11-22 07:10	46	1524	5.279	0.226	40.5	76 810	370	126
P221579	VSL1 9/12-22 10:00	55	1791	5.091	0.294	41.8	74 749	341	120

This includes the solvent amines as well as total nitrogen. These results are compared on mmol N/kg in Figure 5.1. There can be seen that there is good agreement for the trend between the total amine and the sum of the solvent amines determined by LC-MS. As can be seen the total amine are slightly higher than the sum of the two solvent amines by LC-MS, which is reasonable as there is also contribution from degradation products with amine functionality (like pyrrolidine) to the total amine. The total nitrogen is mainly equal or somewhat higher than the total amine.
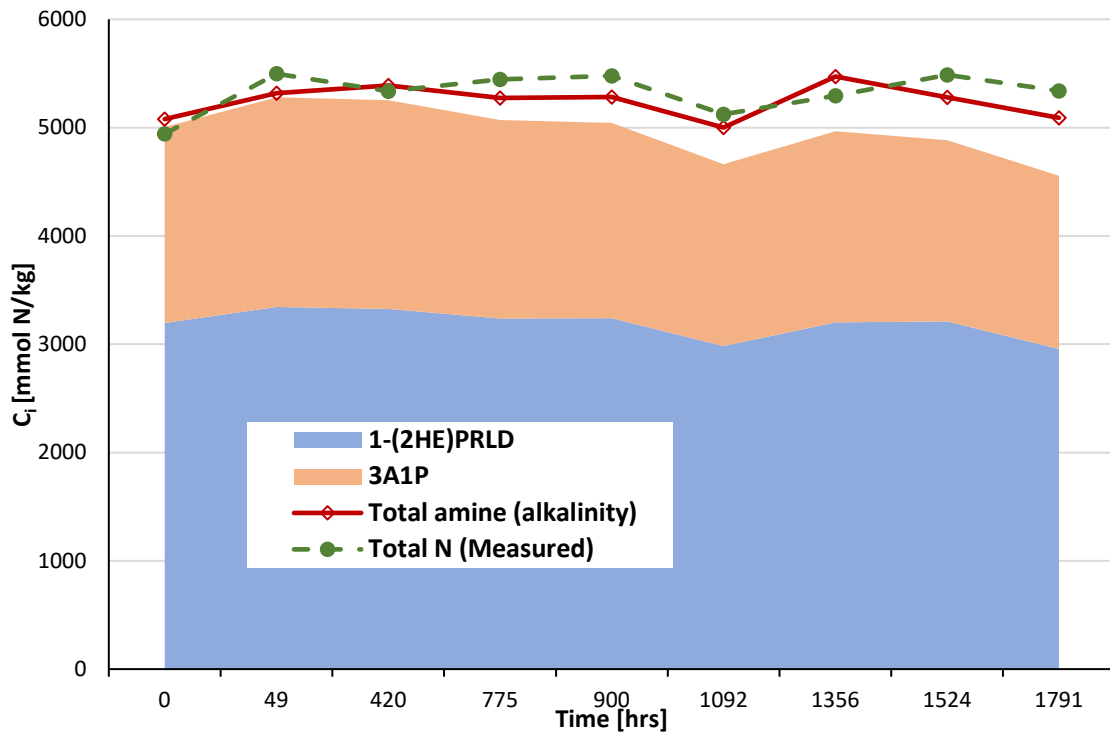

Figure 5.1 Comparison of total amine determined by acid/base titration, solvent amines by LC-MS and Total N determined by Shimadzu TOC-L CPH TNM-L (chemiluminescence detector).

An important factor during the campaign is the mol ratio of the two solvent amines. Here the mol ratio of 3A1P over 3A1P+1-(2HE)PRLD is plotted versus time in Figure 5.2. From this plot it can be observed that the ratio is relatively stable around 0.36 (with a max of 0.367 and a min of 0.342) though with a tendency of slight decrease towards the end.
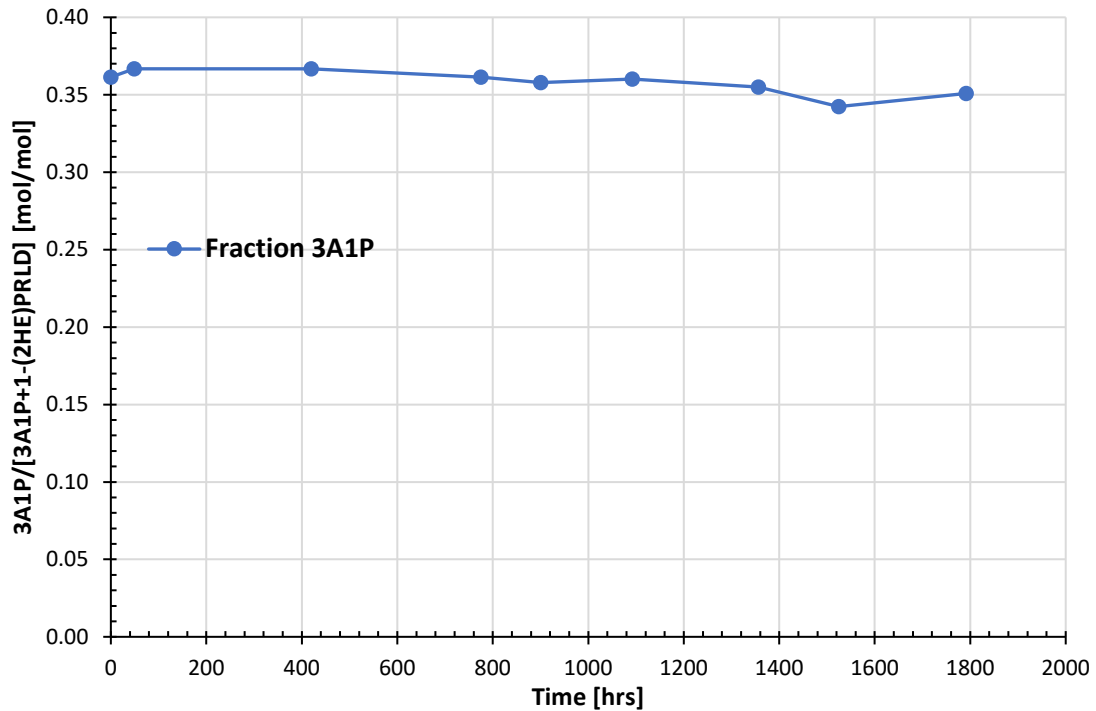

Figure 5.2 Molar fraction of 3A1P with respect to the sum of the two solvent amines in lean samples

5.3 Solvent degradation

The set of selected lean samples were analysed by LC-MS for a range of degradation compounds (totally 34 degradation compounds were included here). Additionally, they samples were also analysed for total nitrogen, metals by ICP-MS, and some of them also for total heat stabile salts (HSS) by a wet chemistry method.

In Table 5-4 determined results for secondary degradation compounds are summarized, and determined ammonia and alkylamines is summarized in Table 5-5.

Table 5-4 Results for secondary degrdation products determined by LC-MS in the selected lean samples

Sample name	TOS Hrs	Methyl-AP mg/kg	OZN mg/kg	AP-Urea mg/kg	Pyrro-lidine mg/kg	HPGly mg/kg	HPF mg/kg	tHHPP mg/kg	APAP mg/kg	HPAla mg/kg
Start solvent unload 22/9-22 10:15	0	47.0	1.9	0.2	1100	< 10	55.4	< 1	< 1	< 1
VSL1 24/9-22 12:55	49	70.3	10.2	291	1172	17.1	157	< 1	3.8	2.0
VSL1 10/10-22 06:55	420	261	16.4	1848	1345	315	165	< 1	62.0	8.1
VSL 1 25/10-22 07:10	775	402	18.5	2529	1506	683	165	6.7	164	19.5
VSL1 2/11-22 07:05	900	453	21.1	2556	1876	784	172	10.4	201	25.6
VSL1 10/11-22 07:05	1092	569	28.0	2830	2374	934	181	16.2	245	36.7
VSL1 21/11-22 07:05	1356	748	29.0	3507	3287	1233	244	31.3	338	50.9
VSL1 28/11-22 07:10	1524	796	20.6	3491	3252	1403	231	41.1	416	58.0
VSL1 9/12-22 10:00	1791	912	21.2	3161	3445	1674	226	61.3	497	77.9

Table 5-5 Results for ammonia and alkylamines determined by LC-MS in the selected lean samples

Sample name	TOS Hrs	NH₃ mg/kg	MA mg/kg	EA mg/kg	Propyl-amine mg/kg	DMA mg/kg	Ethylmethyl-amine mg/kg	DiEA mg/kg	Dipropyl-amine mg/kg
Start solvent unload 22/9-22 10:15	0	< 50	0.19	0.12	0.31	< 0.01	< 0.01	< 0.1	< 0.1
VSL1 24/9-22 12:55	49	96.2	< 0.1	0.09	< 0.1	< 0.01	< 0.01	< 0.1	< 0.1
VSL1 10/10-22 06:55	420	155	< 0.1	0.12	< 0.1	< 0.01	< 0.01	< 0.1	< 0.1
VSL 1 25/10-22 07:10	775	137	0.55	0.15	< 0.1	< 0.01	< 0.01	< 0.1	< 0.1
VSL1 2/11-22 07:05	900	126	0.57	0.23	< 0.1	0.01	< 0.01	< 0.1	< 0.1
VSL1 10/11-22 07:05	1092	140	0.97	0.26	< 0.1	0.04	< 0.01	< 0.1	< 0.1
VSL1 21/11-22 07:05	1356	143	1.44	0.31	< 0.1	0.06	< 0.01	< 0.1	< 0.1
VSL1 28/11-22 07:10	1524	146	1.74	0.35	< 0.1	0.09	< 0.01	< 0.1	< 0.1
VSL1 9/12-22 10:00	1791	154	1.92	0.38	< 0.1	0.09	< 0.01	< 0.1	< 0.1

The distribution of the major and minor degradation products on mol N basis are given in Figure 5.3. We can see that pyrrolidine, AP-urea, ammonia, HPGly and Methyl-AP are the major components, in agreement with the observations at the Irving campaign reported in D2.3 as well as the SDR campaign reported in D1.1. The sum of the determined nitrogen containing degradation compound in the last lean samples is around 2.6% relative to the start composition of 5 mol/kg.

To easier observe the development of the different degradation products, these are also plotted versus time in Figure 5.4 (major & minor) and Figure 5.5 (trace). For the major and minor compounds, it is seen that pyrrolidine and AP-Urea has the largest increase AP-Urea shows an increase until around 1400 hrs, followed by a decrease for the last part of the campaign, pyrolidine has a somewhat different development, with a relatively constant concentration until around 800 hours, followed by fairly linear increase until

around 1400 hrs, were is seems to be relatively constant for the rest of the campaign. It should be noted that around 20 L of used HS-3 (from the campaign at the Irving Oil Whitegate refinery) was added to the plant the 28 of October which is just about 800 hrs TOS. This may have speeded up the degradation of pyrrolidine event if the added volume of the used is relatively small compared to the total solvent inventory of the Tiller plant (around 600 kg). For the other major or minor, except for ammonia, shows a slightly increasing trend.
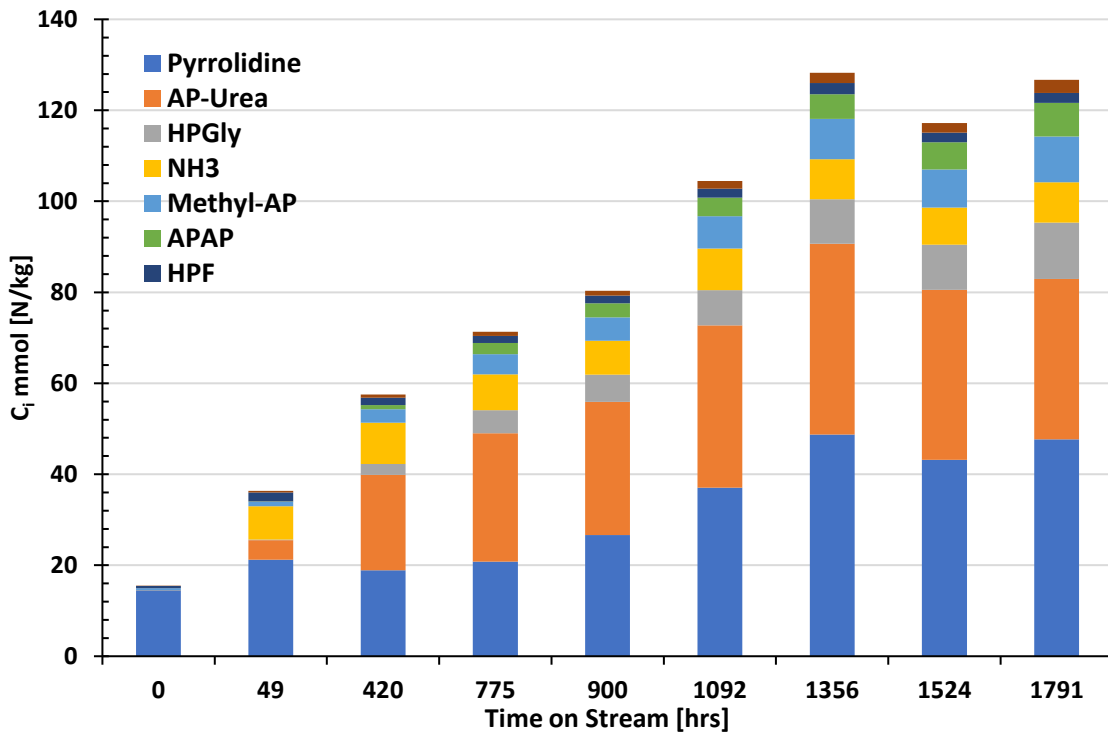

Figure 5.3 Distribution of major and minor degradation products (AP-urea, Pyrrolidine, HPGly, Methyl-AP, HPF, APAP, and NH$_3$) in lean HS-3 during the campaign
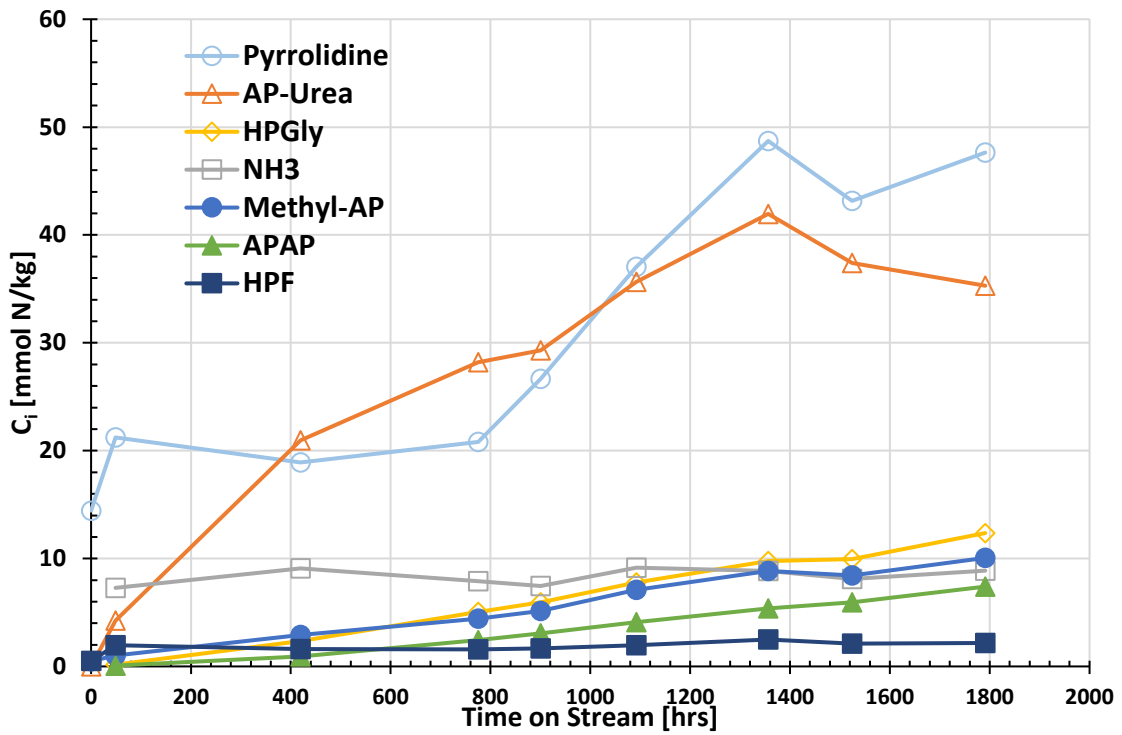
Figure 5.4 Development of major and minor degradation products (AP-urea, Pyrrolidine, HPGly, Methyl-AP, HPF, APAP, and NH$_3$) in lean HS-3 during the campaign

Amongst the trace degradation compounds (Figure 5.5), tHHP and HPAla shows the largest increase. However, all these trace compounds are at low concentrations (<1 mmol N/kg) at the end of the campaign.
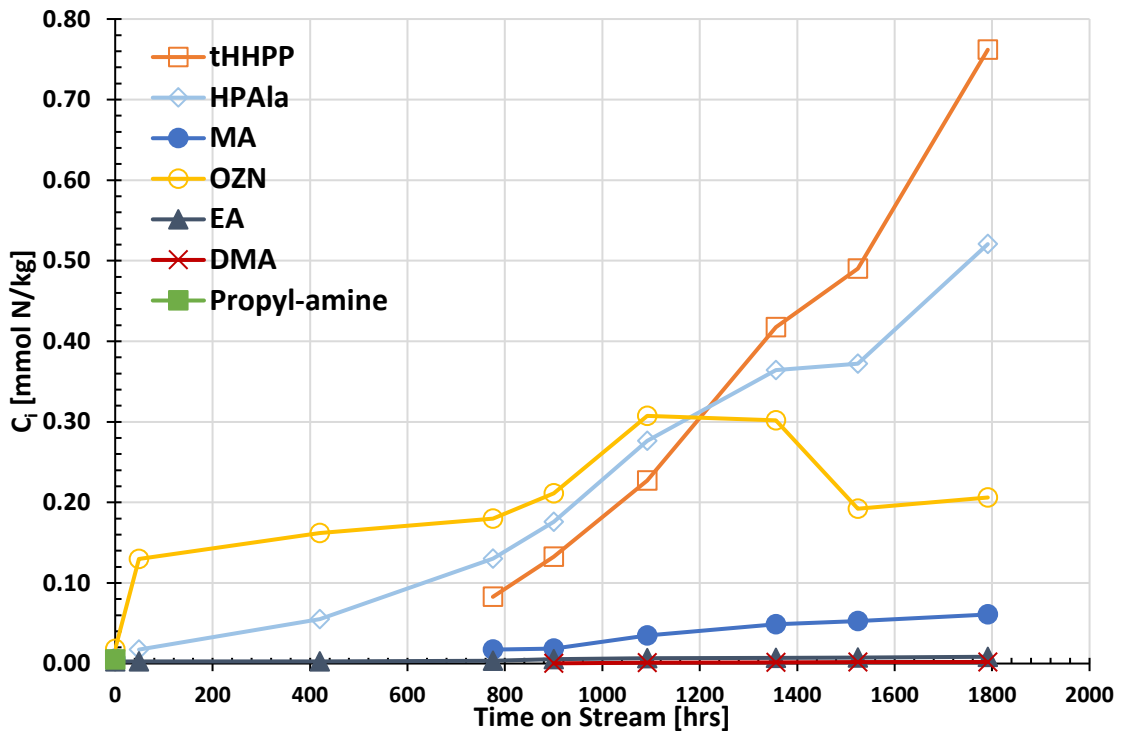

Figure 5.5 Development of trace degradation products (HPAla, tHHPP, OZN, EA, MA, DMA, 3-Mpy, Ethylmethyl-amine and Propyl-amine) in lean HS-3 during the campaign

The selected lean samples were also analyzed for the two nitrosamines NPYR and Nitroso-N-Methyl-AP, which are the nitrosamines from the two degradation products pyrrolidine and N-Methyl-AP, respectively. The results of these two are summarized in Table 5-6.

Table 5-6 Results for solvent specific nitroseamines determined by LC-MS in the selected lean samples

Sample name	TOS Hrs	NPYR mg/kg	Nitroso-N-Methyl-AP mg/kg
Start solvent unload 22/9-22 10:15	0	0.3	< 0.1
VSL1 24/9-22 12:55	49	7.4	0.3
VSL1 10/10-22 06:55	420	20.6	4.2
VSL 1 25/10-22 07:10	775	18.6	9.3
VSL1 2/11-22 07:05	900	18.5	11.9
VSL1 10/11-22 07:05	1092	23.8	16.2
VSL1 21/11-22 07:05	1356	30.6	23.9
VSL1 28/11-22 07:10	1524	27.9	29.2
VSL1 9/12-22 10:00	1791	29.2	45.4

The development of these two are shown in Figure 5.6, where an increase can be observed for Nitroso-N-Methyl-AP during the whole campaign, while NPYR shows a relatively increase for the first part, followed by relatively constant level until around 800 hrs, where it increases again until around 1400 hrs. The pattern for NPYR shows a somewhat correlated development as with pyrrolidine.
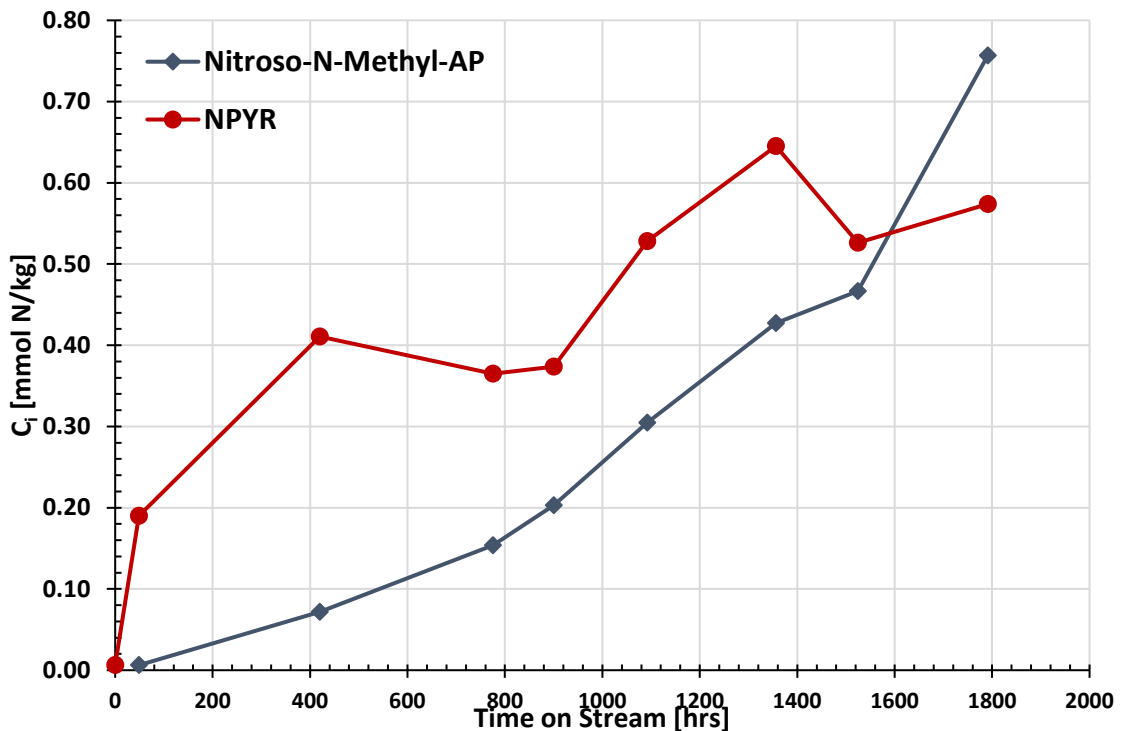

Figure 5.6 Concentration of NPYR and Nitroso-N-Methyl-AP in selected lean samples

As mentioned earlier, the selected lean samples were also analyzed for total nitrogen, which is then used for check of the nitrogen balance in the samples. The nitrogen balance is the sum of nitrogen of all analyzed nitrogen containing compounds relative to the determined total nitrogen. The results of the nitrogen balances are summarized in Figure 5.7. Taking into account analytical uncertainties, the nitrogen balance is mainly closed. There may be some question for the last samples as in that case the nitrogen balance is just below 90%.

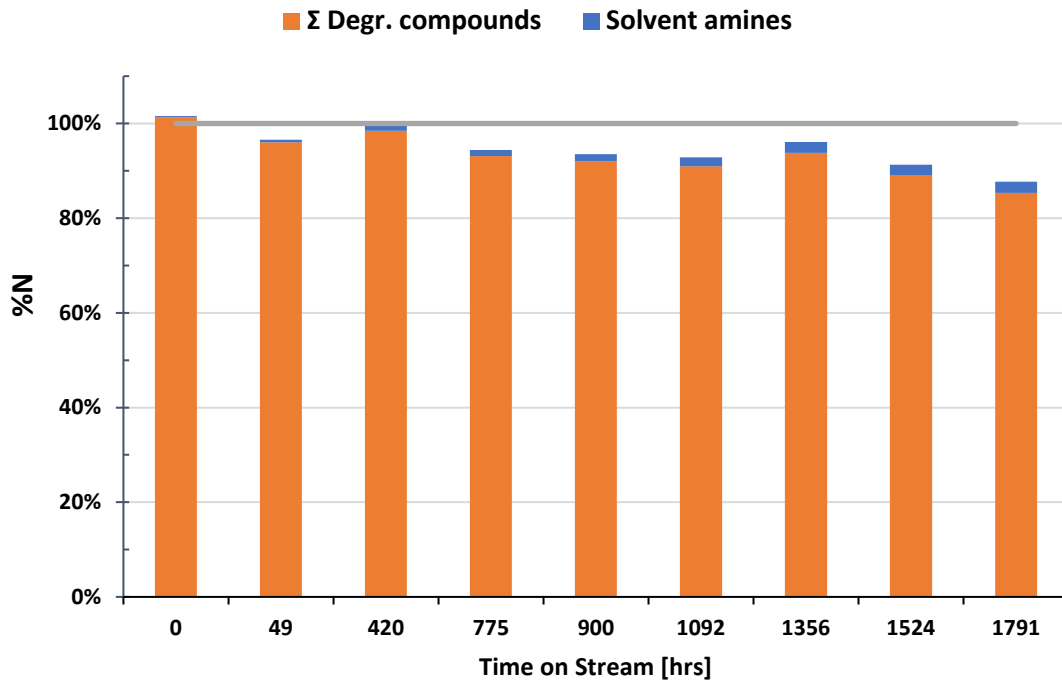*Figure 5.7 Nitrogen balance over the lean samples*

The selected lean samples were also analysed for 9 carboxylic acids (by LC-MS) which could be assigned as specific heat stable salts, the determined concentrations are given in Table 5-7. Additionally, also total heat stabile salts (HSS) were determined by an inhouse wet chemistry method for 4 of the lean samples and the results are given in Table 5-8.

Table 5-7 Results for carbocylic acids determined by LC-MS in the selected lean samples

Sample name	TOS Hrs	Glycolic Acid mg/kg	3-OH Propionic Acid mg/kg	Lactic Acid mg/kg	Formic Acid mg/kg	Acetic Acid mg/kg	Propionic Acid mg/kg	Isobutyric Acid mg/kg	N-Butyric Acid mg/kg	Glyoxylic Acid mg/kg
Start solvent unload 22/9-22 10:15	0	2.2	< 1	< 5	236	< 5	1.7	< 1	< 1	< 1
VSL1 24/9-22 12:55	49	3.2	1.4	< 5	204	9.6	4.7	< 1	< 1	< 1
VSL1 10/10-22 06:55	420	71.2	4.2	5.6	250	57.8	17.5	1.3	< 1	< 1
VSL 1 25/10-22 07:10	775	124	9.5	26.2	263	72.1	23.4	1.5	< 1	< 1
VSL1 2/11-22 07:05	900	151	12.1	36.1	278	94.2	25.7	1.5	< 1	< 1
VSL1 10/11-22 07:05	1092	167	12.9	48.5	260	89.0	24.8	1.6	< 1	< 1
VSL1 21/11-22 07:05	1356	214	21.0	69.8	313	107	28.4	2.1	< 1	< 1
VSL1 28/11-22 07:10	1524	274	24.1	96.9	352	123	28.6	2.1	< 1	< 1
VSL1 9/12-22 10:00	1791	310	30.2	129.3	379	133	31.3	6.2	< 1	< 1

Amongst the carboxylic acids, formic, glycolic, lactic acid and acetic were the major observed, which all exceed 100 mg/kg at the end of the campaign. All shows an increasing trend during the campaign, and especially for Glycolic the trend seems to be linear, see Figure 5.8. For the determined total HSS, a fairly linear increase during the campaign could be observed, as shown in Figure 5.9. For the last sample the sum of the determined carboxylic acids corresponds to 0.02 eq/kg which is less than the results obtained by the total HSS method (0.05 eq/kg). This may indicate that there are other anions present like sulphate or other inorganic anions or even more organic acids, however the level of HSS is relatively low.

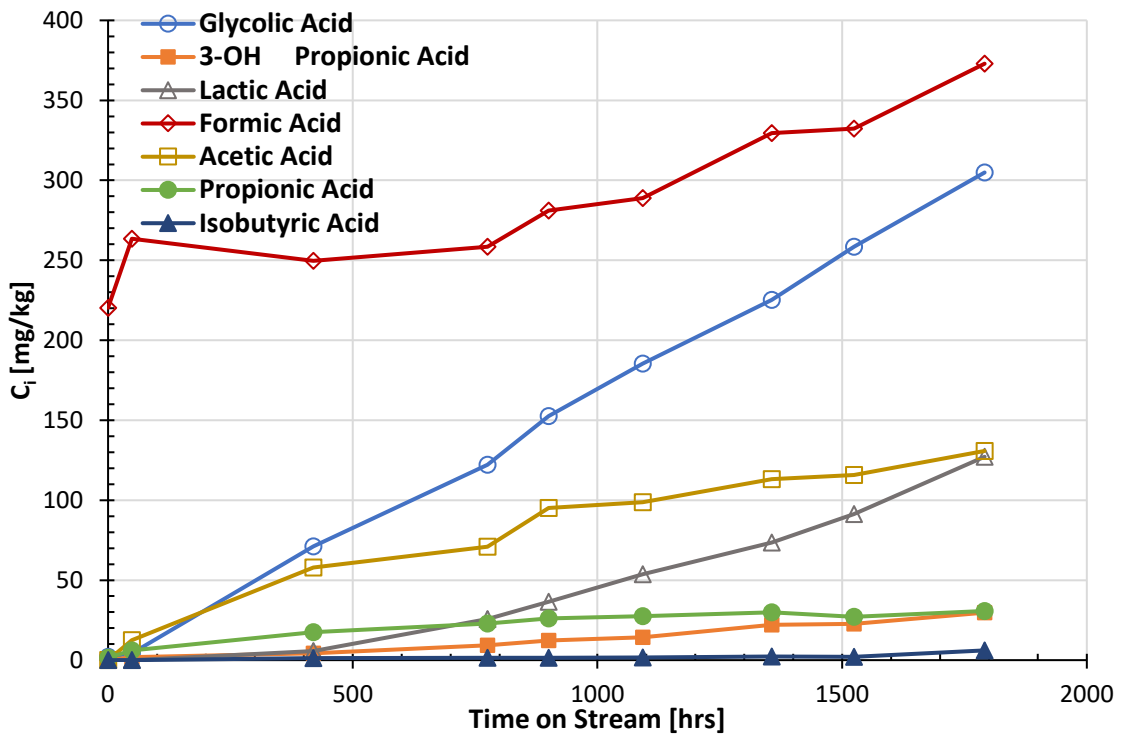*Figure 5.8 Concentration of carboxylic acids in selected lean samples*

Table 5-8 Results for total heat stable salts (HSS) determined by wet chemistry method in the selected lean samples

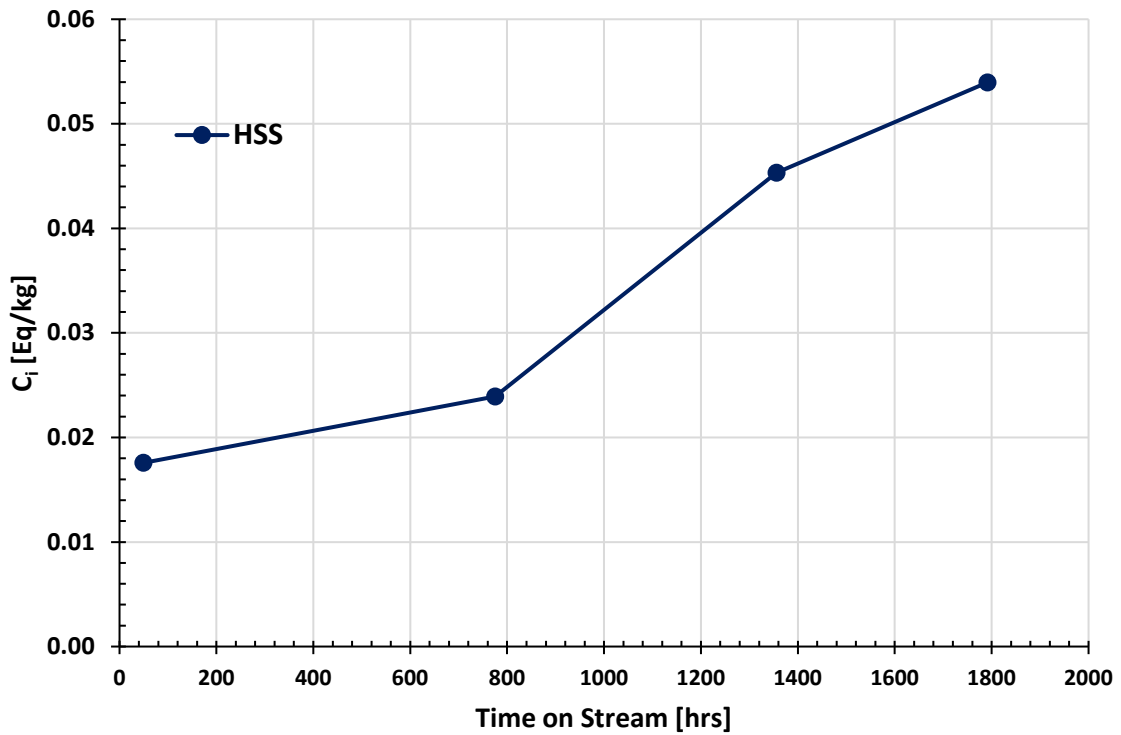| Sample name	TOS Hrs	HSS [eq/kg]
VSL1 24/9-22 12:55	49	0.018
VSL 1 25/10-22 07:10	775	0.024
VSL1 21/11-22 07:05	1356	0.045
VSL1 9/12-22 10:00	1791	0.054

Figure 5.9 Determined total HSS by wet chemistry method in 4 of the lean samples

Additionally, acetaldehyde, formaldehyde and acetone were analysed in the selected lean samples, the results are given in Table 5-9.

Table 5-9 Results acetone and alkylamines determined by LC-MS in the selected lean samples

Sample name	TOS Hrs	Formaldehyde mg/kg	Acetaldehyde mg/kg	Acetone mg/kg
Start solvent unload 22/9-22 10:15	0	16.3	28.2	< 10
VSL1 24/9-22 12:55	49	7.1	17.5	< 10
VSL1 10/10-22 06:55	420	18.6	27.6	< 10
VSL 1 25/10-22 07:10	775	23.1	27.7	< 10
VSL1 2/11-22 07:05	900	24.8	27.6	< 10
VSL1 10/11-22 07:05	1092	26.6	26.1	< 10
VSL1 21/11-22 07:05	1356	33.6	30.1	< 10
VSL1 28/11-22 07:10	1524	46.4	33.0	< 10
VSL1 9/12-22 10:00	1791	54.0	36.9	< 10

Acetone were below the LOQ (10 mg/kg) and the development of the two aldehydes are plotted versus time in Figure 5.10.
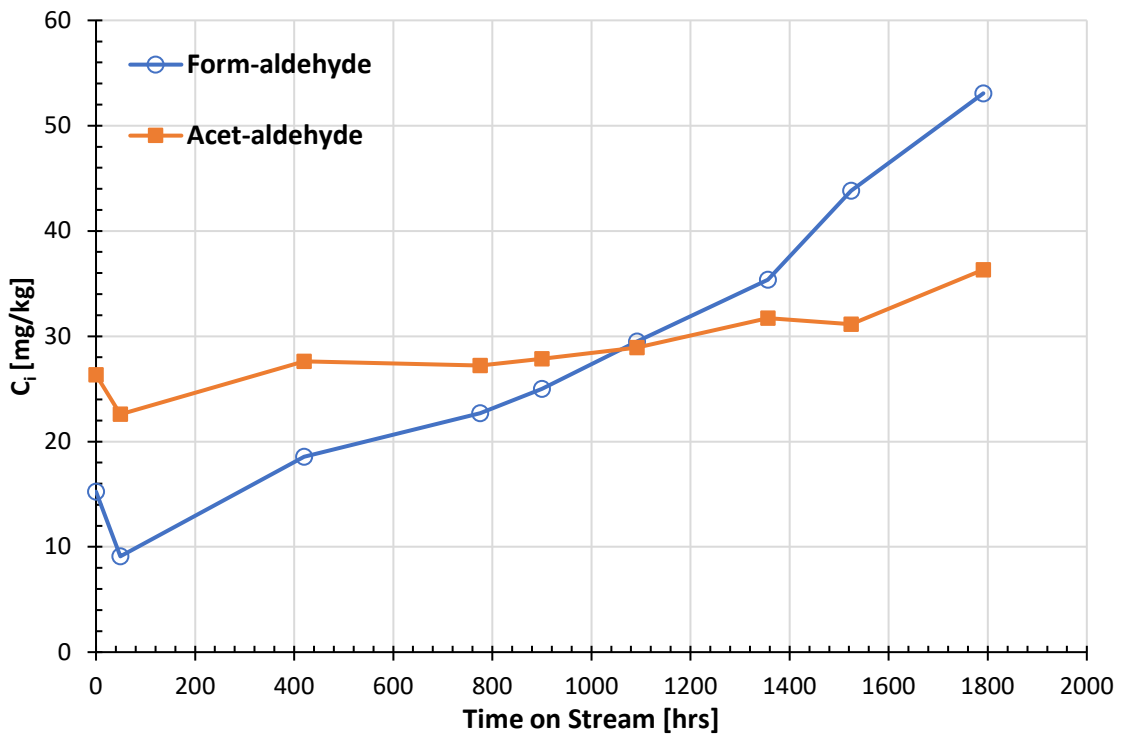
Figure 5.10 Determined concentration of acet- and form-aldehydes by LC-MS in the selected lean samples

5.4 Metal concentration/corrosion

The selected number of lean solvent samples has been analysed for metal (Fe, Cr, Ni, Cu, Zn and Mn) content by ICP-MS. The obtained results given in Table 5-10 and are plotted versus TOS in Figure 5.11.

Table 5-10 Results for metal elements determined by ICP-MS in the selected lean samples

Sample name	TOS Hrs	Fe [mg/l]	Ni [mg/l]	Cr [mg/l]	Cu [mg/l]	Zn [mg/l]	Mn [mg/l]	Na [mg/l]
Start solvent unload 22/9-22 10:15	0	< 0.02	< 0.01	< 0.1	0.24	0.17	< 0.001	< 0.1
VSL1 24/9-22 12:55	49	0.46	0.24	0.12	0.26	0.55	0.007	< 0.1
VSL1 10/10-22 06:55	420	0.39	0.83	0.13	0.18	0.77	< 0.001	< 0.1
VSL 1 25/10-22 07:10	775	0.52	1.04	0.16	0.09	0.74	< 0.001	0.6
VSL1 2/11-22 07:05	900	1.13	2.13	0.26	0.13	0.93	0.002	16.1
VSL1 10/11-22 07:05	1092	1.38	1.98	0.31	0.08	0.88	0.004	11.8
VSL1 21/11-22 07:05	1356	1.68	2.41	0.39	0.05	1.12	0.093	13.3
VSL1 28/11-22 07:10	1524	1.39	2.41	0.34	0.02	1.06	0.020	12.5
VSL1 9/12-22 10:00	1791	1.92	2.39	0.41	< 0.002	1.11	0.096	11.0

The measured concentrations are below 2.5 mg/L for all the determined metal elements. Except for Fe and Ni, there appears to be relatively little increase during the campaign. For Ni and Fe there seems to be a little jump in concentration after around 800 hr For Ni, this is expected to be caused by the addition of some (20L) used solvent from campaign at Irving to the Tiller plant.
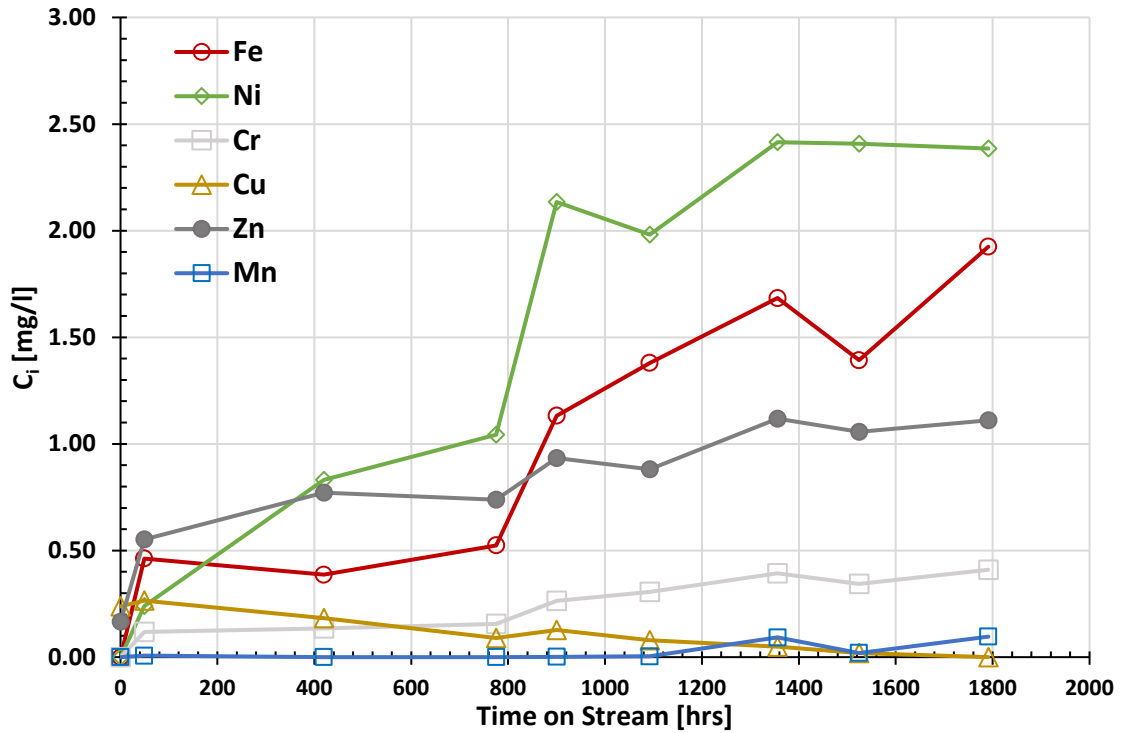

Figure 5.11 Metal concentration in lean solvent during the test campaign at Tiller

6 Discussion

6.1 Quality of data

The CO_2 mass balances around the four independent sampling points, two gas- and to liquid areas, showed low errors and the overall balances were deemed as of very high quality. For the specific analysis regarding solvent performance, the CO_2 flow meter out of the condenser "FT14" was used as the primary measurement sensor, due to its reliability and simple measurement procedure. The dataset created during this campaign is very complete, which enables rigorous validation of models for simulation as well as analysis for scientific research and understanding.

6.2 Approach to equilibrium

A soft model of the liquid loading to partial pressure of CO_2 has been made based on the experimental equilibrium data provided in Realise. One can then calculate the approach to equilibrium at the bottom of the column. The equilibrium loading $\alpha^*_{CO_2}$ for the partial pressure conditions P_{CO_2} in the incoming gas in the bottom is then compared to the measured loading α_{CO_2} as a percentage. In Figure 6.1 the approach to equilibrium is shown for all the runs.
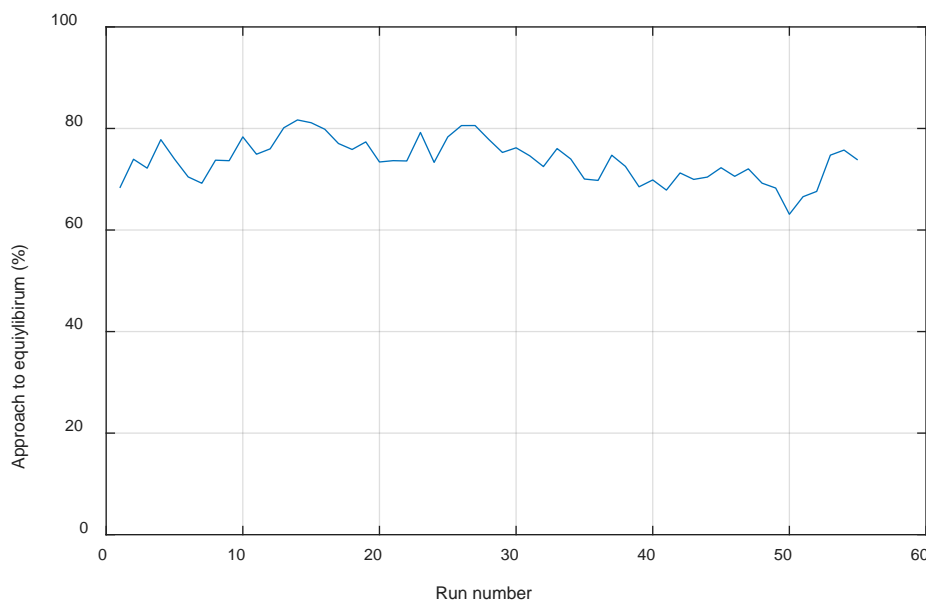
Figure 6.1 Approach to equilibrium for the varia

The variation is quite small during the campaign. The average value was 73.7 % and the standard deviation 4 %. It is remarkable that it doesn't seem that the runs 20-22 which used only 3 sections are significantly lower than the others, although the capture rate is reduced, as earlier discussed, indicating that also the lean loading is increased at equilibrium. The approach is also dependent on other parameters like the liquid rate
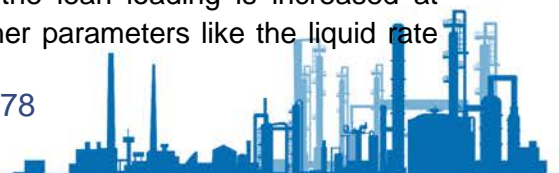
(and thus the liquid hold-up). In Figure 6.2 the approach to equilibrium is plotted as a function of liquid rate.

Figure 6.2 Approach to equilibrium as a function of liquid circulation rate (FMD1_1) The attached numbers are the run number. Red stars are runs with only 3 absorber sections,

Even if there is a large spread in the data the figure shows that approach to equilibrium generally decreases with increasing liquid rate. The figure also shows that the run 20-22 with reduced absorber height are substantial lower compared with other runs with similar liquid rates.

6.3 Density - CO$_2$ concentration correlation

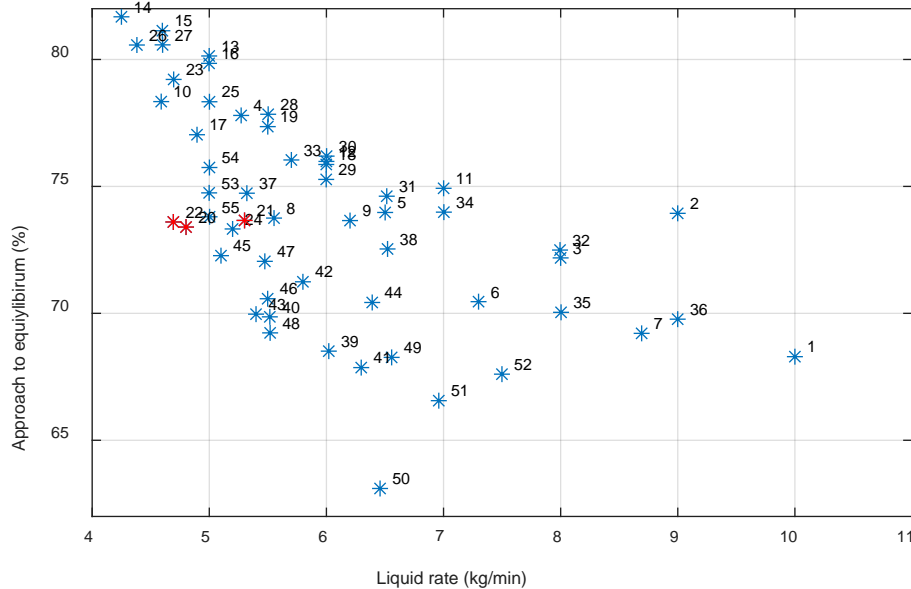A model that correlates the density measured by the Coriolis sensors (FMD1, FMD2 and FMD3) with the CO$_2$ concentrations analysed in the lab has been developed and used during the dynamic tests. The model also uses the temperature measured close to the sensors. In Figure 6.3 the model and the concentration for the runs 35 to 40 are shown. The same model was used both for lean and rich samples. The standard deviation between the model and the data is only 5%.

Using the correlation for all the runs gives not so good fit. In Figure 6.4 the same model was tested on the lean L1 for all runs. We see that the model the model underpredicts fin the beginning of the campaign and overpredicts in the end. This implies that the density for a specific loading is changing during the campaign and that some kind of degradation affects the density of the liquid.
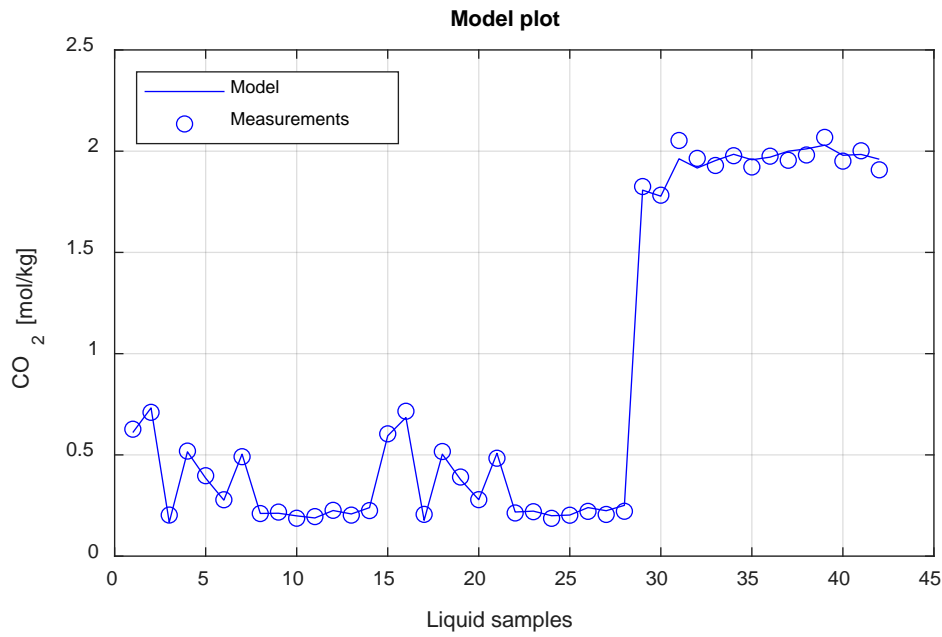
Figure 6.3 Fit of CO_2 concentration model using the runs 35 to 40.
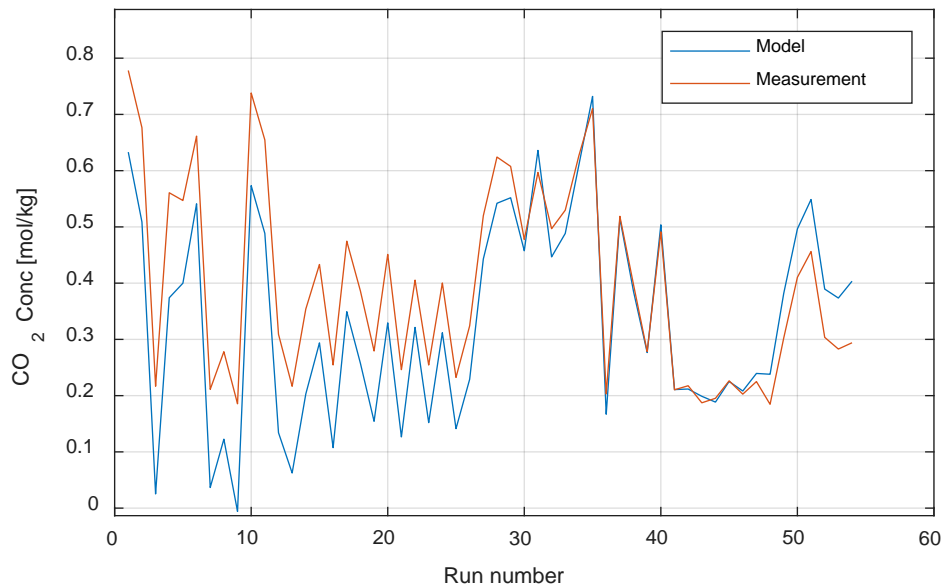
Figure 6.4 Comparison of lean concentration analysed with the model calibrated with the runs 35 to 40.

6.4 Estimated SRD when heat loss is considered.

All the SRD values shown in the report are the measured values, using heat tracing. However, there is some heat loss not compensated for. A good estimate has been a heat loss of 1.5 kW.

Using this heat loss, we can estimate what the SRD would be in a large industrial column where the surface to volume is very small and thus almost adiabatic.

Table 6-1 SRD corrected for heat loss.

CO2 in flue gas	Capture rate	Run nr	SRD measured	SRD without heat loss	Difference
11 %	90 %	5	3.36	3.16	0.20
11 %	95 %	6	3.41	3.22	0.18
5 %	90 %	15	3.72	3.45	0.28
5 %	95 %	13	3.75	3.50	0.26

The figures shows that this solvent has quite low energy requirements and is deemed as an effective solvent for CO_2 capture based on energetic analysis.

6.5 Solvent degradation

The degradation of the solvents seems to be fairly linear during the campaign, as illustrated in Figure 6.5 where sum of the nitrogen containing degradation compounds is plotted versus time on stream (TOS). By using 600 kg as the total inventory the slope of the curve corresponds to a degradation of 40 mmol N per hour on stream. As this is based on nitrogen containing degradation compounds in the solvent, this will be lower than the total degradation, due to that some volatile nitrogen contain degradation compounds will be lost through emission (e.g.NH_3 and pyrrolidine).

Figure 6.5 Sum of nitrogen containing degradation compounds in lean solvent versus time on stream (TOS)

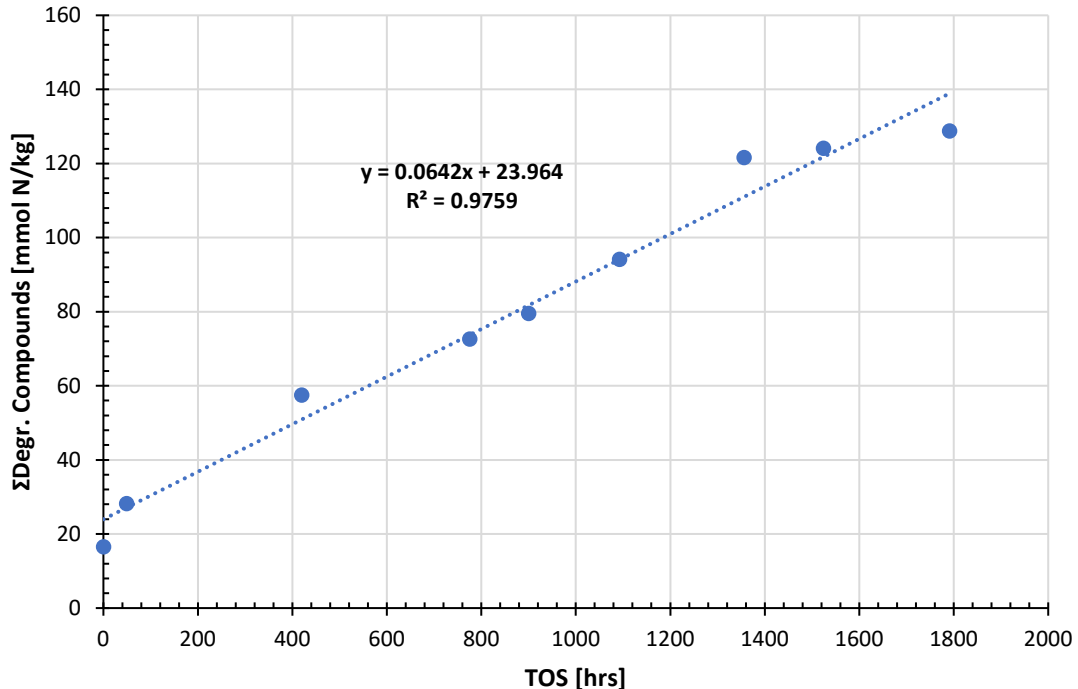In this campaign pyrrolidine and AP-urea, ammonia, HPGly and Methyl-AP were the major degradation compounds observed. Amongst these pyrrolidine and AP-urea where the two in highest amounts. This observation agrees well with the observations at the Irving campaign reported in D2.3 as well as the SDR campaign reported in D1.1

The total heat stable salt (HSS) was observed to be 0.05 eq/kg at the end of the campaign. Based on the specific carboxylic acid analysis, glycolic acid and formic acid are the major contributors to the total HSS. The total HSS at the end of the Irving campaign (0.03 eq/kg) was slightly lower than the one observed in this campaign.

There were determined two nitrosamines during the campaign, these were Nitroso-N-Methyl-AP during and NPYR, both showing an increasing trend during time on stream. At the end of the campaign the total concentration of these were 1.35 mmol/kg). These two nitrosamines are formed from degradation products that are secondary amines, in this case from N-Methyl-AP and pyrrolidine. These two nitrosamines where also observed in the campaign at Irving as well as in the bench scale SDR campaign.

The determined metal concentration (Fe, Cr, Ni, Cu, Zn and Mn) in the lean solvent were low (all below 2.5 mg/l)t, which indicate that the solvent seems not to cause problem with corrosion.

6.6 Dynamic tests

Some properties of the CENIT model show different dynamic behaviour than what is observed from the plant measurements. The CENIT model is fit to match the production rate of CO2 from the condenser atop the desorber (which is a key variable of the process), as described in section 4.2 and shown in Figure 4.4, where the dynamic fit is very promising. An example of a slight dynamic mismatch, however, is revealed when comparing the model to the measured CO_2 concentration in the clean outlet gas from the absorber. This quantity is of particular interest, both dynamically and stationary, because it is closely connected to the capture rate, which is a central controlled variable in the plant. In conclusion, the dynamic mismatch means that the *actual* capture rate will be slightly different from what the NMPC *believes* during short transients, and the controlled variable is the latter. In any case, this indicates a potential for improvement and the NMPC should have its estimator improved such that the dynamics of the outlet gas composition fits the plant measurements better, for this specific property. It is emphasized that the stationary match between the measurement and the model is good, as described in section 4.2 (and shown in Figure 4.4).

CO₂ capture ratio

Clean gas CO₂ concentration

(a)

(b)
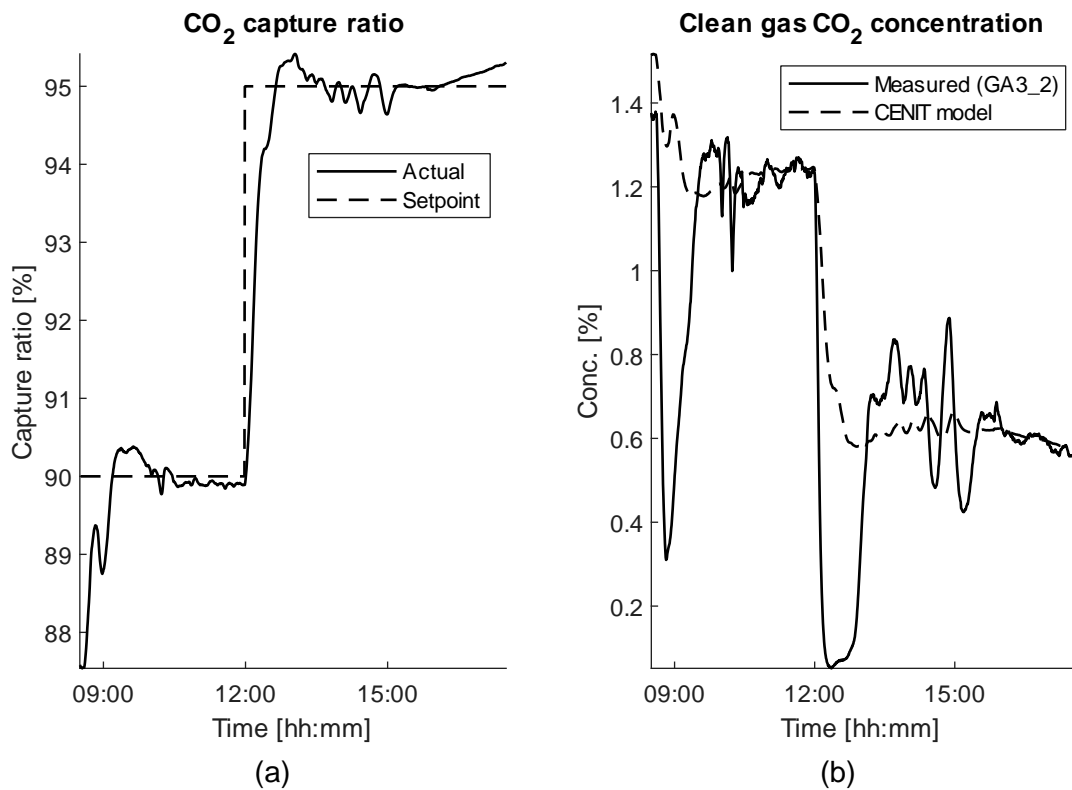
Figure 6.6 Flashback to closed-loop control with setpoint changes, as described in section 4.2 and shown in Figure 4.5. Subfigure (a) shows the capture rate itself while subfigure (b) shows a comparison between the modelled and the measured outlet concentration of CO₂.

6.7 Emissions to air by FTIR.

The emissions were measured on-line by an FTIR right before the gas leaves the building. The measurements were in D2.5 found to be in quite close to the manual sampled results.

In Figure 6.7 the emissions of the amine 1-(2HE)PRLD I shown. The emissions are generally between 5 and 15 ppm. The exception is when only 3 sections in the absorber was used (runs 20-22) and the two last runs where additional water washes was used. Then they show about 1.5 ppm. In runs 20-22 the upper section in the absorber became a dry bed, a configuration that is known to reduce the emissions.
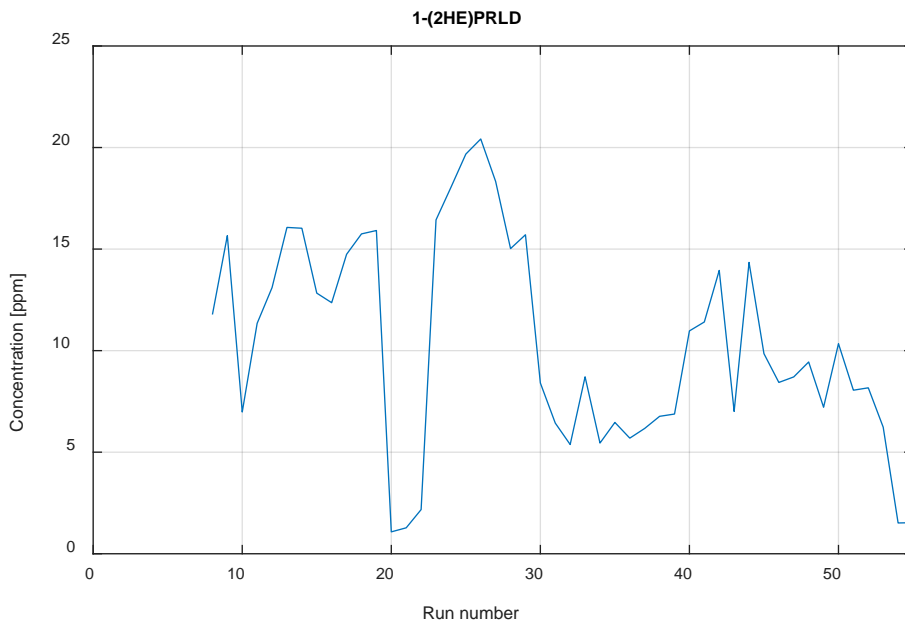
Figure 6.7 1-(2HE)PRLD measured by FTIR.

The aminopropanol 3A1P emissions are shown in Figure 6.8.
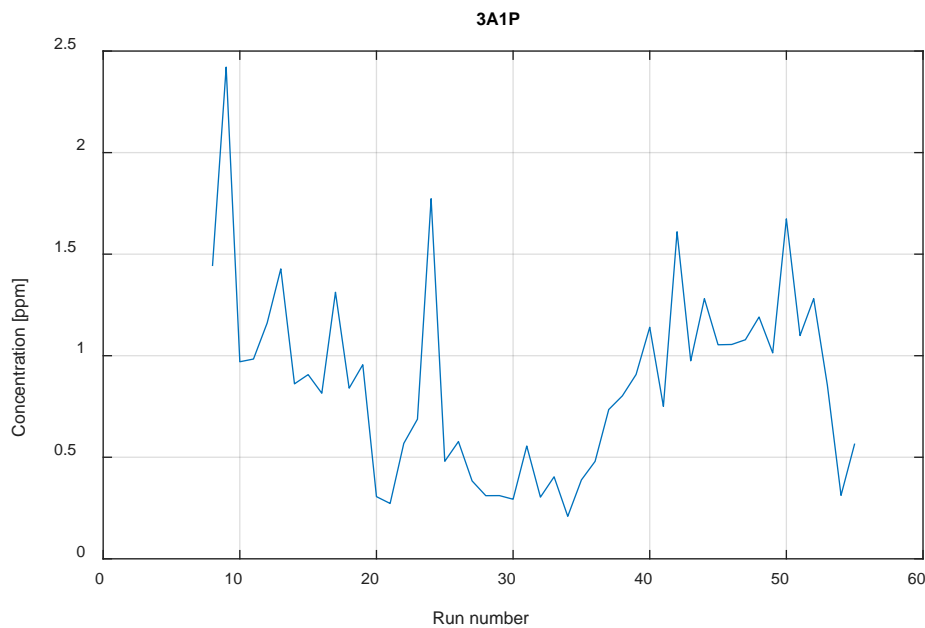
Figure 6.8: 3A1PI measured by FTIR

The emissions are from 0.5 -1.5 ppm. The ammonia emissions are shown in Figure 6.9.

NH$_3$

Concentration [ppm] vs Run number
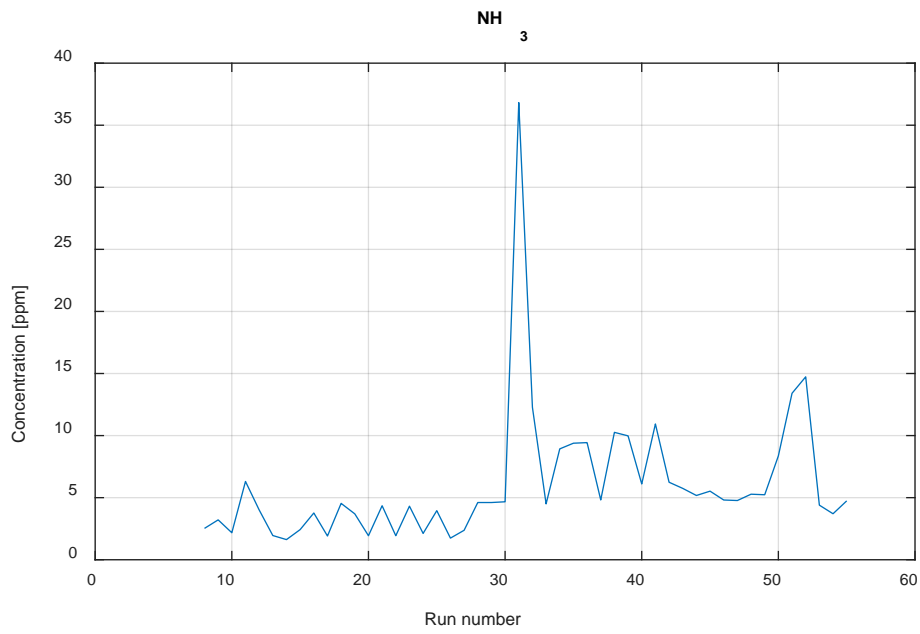
Figure 6.9 Ammonia emissions measured by FTIR .

Except for Run 31 they are acceptable and shows that no acid wash is needed for ammonia.

7 Conclusions

- Operationally the REALISE HS-3 solvent was easy to run in the pilot plant. The plant was up running more than 90% of the time. No precipitation was observed and no other major operational problems.

- The CO_2 mass balance was very good with a standard deviation from 4 independent measurements of only 1.5%.

- For 11% CO_2 gas the SRD was observed to be almost constant for various capture rates up to 98%. The optimal point is close to 2.0 in L/G and an SRD of about 3.35 MJ/kg CO_2 was measured for a fresh solvent.

- For 5.5% CO_2 the optimal L/G was around 1.0 for 90% capture rate and slightly higher for 95% capture rate. The SRD was around 3.72 MJ/kg CO_2 for 90% capture rate and only slightly higher for 95% capturer rate.

- Assuming no heat loss from the plant the SRD was estimated to be around 3.1 MJ/kg CO_2 for 11 mol% CO_2 in the flue gas, and 3.5 MJ/kg CO_2, for 5.5 mol% CO_2.

- Degraded solvent shows a higher need for energy. In the campaign the increase in SRD was about 0.1 - 0.2 MJ/kg CO_2.

- Runs with 15m absorber packing instead of 20m showed a substantially increase in SRD.

- All the dynamic closed loop tests with NMPC showed satisfactory results including the very fast "stripper stop scenario" with limitation in the reboiler duty.

- The degradation rate appears to be nearly constant during the campaign, where pyrrolidine and AP-Urea where the two largest degradation products in the solvent.

- Two nitrosamines (Nitroso-N-Methyl-AP during and NPYR) was observed in the solvent during the campaign, both showing an increasing trend with time.

- The solvent seems to be little corrosive as the determined metal concentration (Fe, Cr, Ni, Cu, Zn and Mn) where low (<2.5 mg/l).

- The campaign created a multitude of data for further scientific analysis, both regarding steady state and dynamic model development.

References

[1] Qin & Badgwell, "A survey of industrial model predictive control technology", Control Engineering Practice 11 (2003), pp. 733-764

[2] Emhemed & Mamat, "Model Predictive Control: A summary of Industrial Challenges and Tuning Techniques", Int. J. Mechatronics, Electrical and Computer Technology (2020), Vol. 10, Iss. 35, pp. 4441-4459

[3] Schei, T.S., Applications of NMPC to industrial batch processes. Keynote lecture at Workshop on Nonlinear Model Based Control - Software and Applications (NMPC-SOFAP), Loughborough, United Kingdom, April 19-20, 2007

[4] Singstad, P., Industrial Batch Control Applications using Nonlinear Model Predictive Control Technology based on Mechanistic Models. Presentation held at the KoMSO Challenge Workshop – Challenges for Mathematical Modeling, Simulation and Optimization for Advanced Process Control of Batch Processes, Heidelberg, 9-10 February 2017

[5] Kolås, S. and Wasbø, S.O., A nonlinear model based control strategy for the Aluminium Electrolysis Process, Light Metals, TMS (The Minerals, Metals & Materials Society), Seattle WA, February 14-18, 2010

[6] Hauger et. al., "Demonstration of non-linear model predictive control of post-combustion CO_2 capture processes"; Computers and Chemical Engineering 123 (2019), pp. 184-195

[7] Mejdell et. al., "Demonstration of non-linear model predictive control for optimal flexible operation of a CO_2 capture plant", International Journal of Greenhouse Gas Control 117 (2022) 103645, 2022

[8] Kvamsdal et. al., "Demonstration of two-level nonlinear model predictive control of CO_2 capture plants", 14th International Conference on Greenhouse Gas Control Technologies, GHGT-14, 21st – 25th October 2018, Melbourne, Australia

[9] Haines & Davison, "Enhancing dynamic response of power plant with post combustion capture using 'Stripper stop'", International Journal of Greenhouse Gas Control 20 (2014)

[10] Vevelstad et. al., "Chemical Stability and Characterization of Degradation Products of Blends of 1-(2-Hydroxyethyl)pyrrolidine and 3-Amino-1-propanol", Ind. Eng. Chem. Res. 62 (2023), pp 610-626

Appendix A D2.4

Jornalnr	Sample name	Rekv. nr.	RUN Nr	Titration Alkalinity [mol/kg]	TOC-analyzator (Shimadzu) CO$_2$ [mol CO$_2$/kg]	LC-MS 1-(2HE)PRLD g/kg	LC-MS 3A1P (AP) g/kg
P22834	VSL1 24/9-22 12:55	20220093	1	5.318	0.807	402	145
P22835	VSL2 24/9-22 13:00	20220093	1	5.398	0.894		
P22836	Rich 24/9-22 12:55	20220093	1	4.738	1.630		
P22837	VSL1 26/9-22 08:10	20220093	2	5.247	0.778		
P22838	VSL2 26/9-22 08:10	20220093	2	5.221	0.785		
P22839	Rich 26/9-22 08:10	20220093	2	4.950	1.878		
P22840	VSL1 27/9-22 08:10	20220093	3	5.130	0.676		
P22841	VSL2 27/9-22 08:10	20220093	3	5.058	0.667		
P22842	Rich 27/9-22 08:10	20220093	3	4.876	1.878		
P22853	VSL1 28/9-22 08:15	20220095	4	5.274	0.217		
P22854	VSL2 28/9-22 08:15	20220095	4	5.071	0.220		
P22855	Rich 28/9-22 08:15	20220095	4	4.844	2.123		
P22856	VSL1 29/9-22 08:08	20220095	5	5.442	0.561		
P22857	VSL2 29/9-22 08:08	20220095	5	5.289	0.523		
P22858	Rich 29/9-22 08:08	20220095	5	5.047	2.052		
P22859	VSL1 30/9-22 08:10	20220095	6	5.471	0.547		
P22860	VSL2 30/9-22 08:10	20220095	6	5.371	0.539		
P22861	Rich 30/9-22 08:10	20220095	6	5.185	1.963		
P22862	VSL1 03/10-22 08:08	20220096	7	5.243	0.661		
P22863	VSL2 03/10-22 08:08	20220096	7	5.219	0.637		
P22864	Rich 03/10-22 08:08	20220096	7	5.016	1.816		
P22865	VSL1 04/10-22 07:10	20220096	8	5.500	0.211		
P22866	VSL2 04/10-22 07:10	20220096	8	5.395	0.207		
P22867	Rich 04/10-22 07:10	20220096	8	5.100	2.100		
P22892	Utgangsblanding, uten CO2, 22.09.22	20220099		5.080			
P22893	VSL1 05/10-22 06:50	20220099	9	5.622	0.278		
P22894	VSL2 05/10-22 06:50	20220099	9	5.407	0.276		
P22895	Rich 05/10-22 06:50	20220099	9	5.180	2.092		
P22896	VSL1 05/10-22 14:40	20220099	10	5.569	0.186		
P22897	VSL2 05/10-22 14:40	20220099	10	5.394	0.191		
P22898	Rich 05/10-22 14:40	20220099	10	5.143	2.252		
P22899	VSL1 06/10-22 07:10	20220099	11	5.325	0.738		
P22900	VSL2 06/10-22 07:10	20220099	11	5.283	0.723		
P22901	Rich 06/10-22 07:10	20220099	11	5.044	2.047		
P22902	VSL1 07/10-22 07:05	20220099	12	5.350	0.655		
P22903	VSL2 07/10-22 07:05	20220099	12	5.267	0.644		
P22904	Rich 07/10-22 07:05	20220099	12	5.085	1.790		
P22905	VSL1 10/10-22 06:55	20220100	13	5.391	0.309		
P22906	VSL2 10/10-22 06:55	20220100	13	5.277	0.306		
P22907	Rich 10/10-22 06:55	20220100	13	5.072	1.887		
P22908	VSL1 11/10-22 07:05	20220100	14	5.359	0.217		
P22909	VSL2 11/10-22 07:05	20220100	14	5.219	0.217		
P22910	Rich 11/10-22 07:05	20220100	14	4.972	1.896		
P22911	VSL1 12/10-22 07:00	20220100	15	5.407	0.354		
P22912	VSL2 12/10-22 07:00	20220100	15	5.248	0.353		
P22913	Rich 12/10-22 07:00	20220100	15	5.024	1.906		
P22914	VSL1 13/10-22 07:10	20220101	16	5.402	0.433		
P22915	VSL2 13/10-22 07:10	20220101	16	5.317	0.433		
P22916	Rich 13/10-22 07:10	20220101	16	5.033	1.871		
P22917	VSL1 14/10-22 07:10	20220101	17	5.361	0.255		
P22918	VSL2 14/10-22 07:10	20220101	17	5.207	0.253		
P22919	Rich 14/10-22 07:10	20220101	17	5.059	1.820		
P22920	VSL1 17/10-22 07:15	20220101	18	5.223	0.475		
P22921	VSL2 17/10-22 07:15	20220101	18	5.118	0.467		
P22922	Rich 17/10-22 07:15	20220101	18	4.959	1.756		
P22945	VSL1 18/10-22 07:05	20220104	19	5.230	0.386		

Appendix A D2.4

Jornalnr	Sample name	Rekv. nr.	RUN Nr	Titration Alkalinity [mol/kg]	TOC-analyzator (Shimadzu) CO₂ [mol CO₂/kg]	LC-MS 1-(2HE)PRLD g/kg	LC-MS 3A1P (AP) g/kg
P22946	VSL2 18/10-22 07:05	20220104	19	5.080	0.381		
P22947	Rich 18/10-22 07:05	20220104	19	4.934	1.784		
P221017	VSL1 19/10-22 07:05	20220111	20	5.399	0.279		
P221018	Rich 19/10-22 07:05	20220111	20	5.089	1.748		
P221019	VSL1 20/10-22 07:05	20220111	21	5.395	0.451		
P221020	Rich 20/10-22 07:05	20220111	21	5.099	1.754		
P221021	VSL1 21/10-22 07:10	20220111	22	5.396	0.246		
P221022	Rich 21/10-22 07:10	20220111	22	5.059	1.745		
P221023	VSL1 24/10-22 07:10	20220112	23	5.194	0.405		
P221024	VSL 2 24/10-22 07:10	20220112	23	5.148	0.413		
P221025	Rich 24/10-22 07:10	20220112	23	4.865	1.807		
P221026	VSL 1 25/10-22 07:10	20220112	24	5.273	0.254	404	137
P221027	VSL 2 25/10-22 07:10	20220112	24	5.249	0.255		
P221028	Rich 25/10-22 07:10	20220112	24	4.946	1.689		
P221029	VSL 1 31/10-22 07:05	20220112	25	5.218	0.400		
P221030	VSL 2 31/10-22 07:05	20220112	25	5.099	0.405		
P221031	Rich 31/10-22 07:05	20220112	25	4.910	1.795		
P221032	VSL 1 1/11-22 07:10	20220112	26	5.313	0.232		
P221033	VSL 2 1/11-22 07:10	20220112	26	5.216	0.233		
P221034	Rich 1/11-22 07:10	20220112	26	4.934	1.861		
P221045	VSL1 2/11-22 07:05	20220114	27	5.282	0.324	401	133
P221046	VSL2 2/11-22 07:05	20220114	27	5.215	0.325		
P221047	Rich 2/11/22 07:05	20220114	27	4.888	1.835		
P221048	VSL1 3/11-22 07:10	20220114	28	5.175	0.520		
P221049	VSL2 3/11-22 07:10	20220114	28	5.113	0.519		
P221050	Rich 3/11-22 07:10	20220114	28	4.875	1.771		
P221051	VSL1 4/11-22 07:05	20220114	29	5.155	0.624		
P221052	VSL2 4/11-22 07:05	20220114	29	5.063	0.617		
P221053	Rich 4/11-22 07:05	20220114	29	4.873	1.707		
P221054	VSL1 7/11-22 07:05	20220115	30	5.054	0.608		
P221055	VSL2 7/11-22 07:05	20220115	30	5.059	0.596		
P221056	Rich 7/11/22 07:05	20220115	30	4.815	1.716		
P221057	VSL1 8/11-22 07:05	20220115	31	5.038	0.478		
P221058	VSL2 8/11-22 07:05	20220115	31	4.963	0.473		
P221059	Rich 8/11-22 07:05	20220115	31	4.701	1.947		
P221060	VSL1 9/11-22 07:05	20220115	32	5.007	0.597		
P221061	VSL2 9/11-22 07:05	20220115	32	4.927	0.630		
P221062	Rich 9/11-22 07:05	20220115	32	4.688	1.821		
P221063	VSL1 10/11-22 07:05	20220115	33	5.001	0.497	374	119
P221064	VSL2 10/11-22 07:05	20220115	33	4.936	0.494		
P221065	Rich 10/11-22 07:05	20220115	33	4.751	1.695		
P221066	VSL1 11/11-22 07:10	20220115	34	5.029	0.530		
P221067	VSL2 11/11-22 07:10	20220115	34	5.012	0.536		
P221068	Rich 11/11-22 07:10	20220115	34	4.693	1.903		
P221165	VSL1 14/11-22 07:10	20220126	35	5.062	0.627		
P221166	VSL2 14/11-22 07:10	20220126	35	5.092	0.604		
P221167	Rich 14/11-22 07:10	20220126	35	4.822	1.825		
P221241	VSL1 15/11-22 07:10	20220133	36	5.138	0.710		
P221242	VSL2 15/11-22 07:10	20220133	36	5.106	0.716		
P221243	Rich 15/11-22 07:10	20220133	36	4.862	1.783		
P221353	VSL1 16/11-22 07:10	20220143	37	5.298	0.203		
P221354	VSL2 16/11-22 07:10	20220143	37	5.202	0.206		
P221355	Rich 16/11-22 07:10	20220143	37	4.861	2.053		
P221356	VSL1 17/11-22 07:10	20220143	38	5.297	0.519		
P221357	VSL2 17/11-22 07:10	20220143	38	5.246	0.517		
P221358	Rich 17/11-22 07:10	20220143	38	4.893	1.965		

Jornalnr	Sample name	Rekv. nr.	RUN Nr	Titration Alkalinity [mol/kg]	TOC-analyzator (Shimadzu) CO₂ [mol CO₂/kg]	LC-MS 1-(2HE)PRLD g/kg	LC-MS 3A1P (AP) g/kg
P221359	VSL1 18/11-22 07:10	20220143	39	5.417	0.397		
P221360	VSL2 18/11-22 07:10	20220143	39	5.342	0.391		
P221361	Rich 18/11-22 07:10	20220143	39	5.039	1.929		
P221362	VSL1 18/11-22 14:30	20220143	40	5.483	0.278		
P221363	VSL2 18/11-22 14:30	20220143	40	5.366	0.279		
P221364	Rich 18/11-22 14:30	20220143	40	5.048	1.978		
P221365	VSL1 21/11-22 07:05	20220143	41	5.472	0.491	375	125
P221366	VSL2 21/11-22 07:05	20220143	41	5.353	0.484		
P221367	Rich 21/11-22 07:05	20220143	41	5.062	1.922		
P221425	VSL1 22/11-22 07:05	20220150	42	5.445	0.210		
P221426	VSL2 22/11-22 07:05	20220150	42	5.387	0.213		
P221427	Rich 22/11-22 07:05	20220150	42	4.995	1.975		
P221428	VSL1 23/11-22 07:05	20220150	43	5.446	0.218		
P221429	VSL2 23/11-22 07:05	20220150	43	5.363	0.219		
P221430	Rich 23/11-22 07:05	20220150	43	5.007	1.955		
P221438	VSL1 24/11-22 07:05	20220153	44	5.624	0.187		
P221439	VSL2 24/11-22 07:05	20220153	44	5.498	0.187		
P221440	Rich 24/11-22 07:05	20220153	44	5.151	1.981		
P221441	VSL1 25/11-22 07:05	20220153	45	5.493	0.195		
P221442	VSL2 25/11-22 07:05	20220153	45	5.438	0.202		
P221443	Rich 25/11-22 07:05	20220153	45	5.130	2.068		
P221444	VSL1 28/11-22 07:10	20220153	46	5.279	0.226		
P221445	VSL2 28/11-22 07:10	20220153	46	5.287	0.221		
P221446	Rich 28/11-22 07:10	20220153	46	4.954	1.951		
P221447	VSL1 29/11-22 07:10	20220153	47	5.304	0.203		
P221448	VSL2 29/11-22 07:10	20220153	47	5.302	0.206		
P221449	Rich 29/11-22 07:10	20220153	47	4.963	2.002		
P221450	VSL1 30/11-22 07:05	20220153	48	5.360	0.225		
P221451	VSL2 30/11-22 07:05	20220153	48	5.255	0.222		
P221452	Rich 30/11-22 07:05	20220153	48	4.951	1.908		
P221508	VSL1 1/12-22 07:05	20220159	49	5.506	0.185		
P221509	VSL2 1/12-22 07:05	20220159	49	5.395	0.188		
P221510	Rich 1/12-22 07:05	20220159	49	5.094	1.911		
P221511	VSL1 2/12-22 07:05	20220159	50	5.446	0.303		
P221512	VSL2 2/12-22 07:05	20220159	50	5.342	0.298		
P221513	Rich 2/12-22 07:05	20220159	50	5.075	1.779		
P221567	VSL1 5/12-22 07:25	20220164	51	5.266	0.410		
P221568	VSL2 5/12-22 07:25	20220164	51	5.200	0.406		
P221569	Rich 5/12-22 07:25	20220164	51	4.934	1.825		
P221570	VSL1 6/12-22 11:20	20220164	52	5.167	0.456		
P221571	VSL2 6/12-22 11:20	20220164	52	5.182	0.453		
P221572	Rich 6/12-22 11:20	20220164	52	4.912	1.791		
P221573	VSL1 7/12-22 09:35	20220164	53	5.193	0.304		
P221574	VSL2 7/12-22 09:35	20220164	53	5.098	0.299		
P221575	Rich 7/12-22 09:35	20220164	53	4.881	1.712		
P221576	VSL1 8/12-22 07:15	20220164	54	5.092	0.283		
P221577	VSL2 8/12-22 07:15	20220164	54	5.010	0.285		
P221578	Rich 8/12-22 07:15	20220164	54	4.769	1.685		
P221579	VSL1 9/12-22 10:00	20220164	55	5.091	0.294		
P221580	VSL2 9/12-22 10:00	20220164	55	5.020	0.289		
P221581	Rich 9/12-22 10:00	20220164	55	4.774	1.670		